UNIVERSITY OF CATANIA

DEPARTMENT OF CHEMICAL SCIENCES

International PhD in Chemical Sciences, XXIX cycle

Angela Margherita Aura

SURFACE PLASMON RESONANCE IMAGING BIOSENSORS FOR THE DETECTION OF PATHOGENS AND TOXINS IN FOOD

PhD Coordinator:
Prof. S. Sortino

Tutor:
Prof. G. Spoto

Accademic Years 2013- 2016

CONTENTS

ABSTRACT

The detection of pathogens and toxins in food represents an essential requirement for food quality control. Standard methods for pathogen detection rely on laborious and time-consuming growth of pathogens in different culture media followed by biochemical or serological identification. Such methods often operate with poor sensitivity and selectivity. In recent years, efforts have been made to provide rapid, reliable and sensitive detection platforms for foodborne pathogens detection. The demand for more rapid, sensitive and accurate methods has been push forward by the implementation of the Hazard Analysis and Critical Control Points (HACCP) protocols. In this context, biosensing platforms provide promising alternatives for the detection of pathogens and toxins with good selectivity and sensitivity. In particular, optical biosensors based on Surface Plasmon Resonance Imaging (SPRI) are attractive because they allow the sensitive detection of analytes from food matrices in real-time. SPRI can assays crude samples without purification and can exploits antibodies or single-stranded DNA (ssDNA) probes for the specific detection of pathogens and toxins with high sensitivity.

My research activity has been aimed at developing SPRI biosensors able to detect pathogens and toxins in food matrices in a rapid, specific and sensitive way. In this perspective, specific oligonucleotide sequences and antibodies have been used for the detection of DNA and bacterial toxins, respectively. SPRI biosensor sensitivity benefited of the use of properly functionalized gold nanoparticles (AuNPs). The combination of the SPRI sensing apparatus with microfluidics devices reduces the amount of sample needed for the analysis and provides an efficient environment for the detection.

1. INTRODUCTION

"Food safety is a hidden, and often overlooked, problem."[1]

The detection of pathogens and toxins in food represents a challenging task with implications in food safety and quality control. Pathogens, which include viruses, toxins, parasites, bacteria and bacterial toxins, can contaminate food at any point of the food chain: through the production site, at the slaughterhouse or packing plant, in manufacturing, processing and retailing of food, domestic preparation and storage.[2] According to World Health Organization (WHO), foodborne illnesses are diseases caused by agents that enter the body through the ingestion of food.[3]

The occurrence of foodborne diseases has increased over years and represents a worldwide public health significant issue. Foodborne pathogens responsible for the majority of disease out-breaks are: *Listeria monocytogenes* (*Listeria m.*), *Escherichia coli* O157:H7, *Staphylococcus aureus* (*S. aureus*), *Salmonella enterica, Bacillus cereus, Vibrio* spp., *Campylobacter jejuni, Clostridium perfringens,* and Shiga toxin-producing *Escherichia coli* (STEC).[4] Some foods, such as milk, cream or meat must be pathogen-free, with a specific attention to *Listeria m.* and *S. aureus*.[5] As stated by Commission Regulation (EC) No 2073/2005 of 15 November 2005, "Foodstuffs should not contain microorganisms or their toxins or metabolites in quantities that present an unacceptable risk for human health".[6] Unfortunately, according to estimates provided by the Centers for Disease, Control and Prevention (CDC) for foodborne illnesses, every year 48 million U.S. citizens gets sick, 128,000 are hospitalized and 3,000 die as a consequence of foodborne diseases. The top five pathogens causing domestically acquired foodborne illnesses and deaths are listed in **Table 1** and **Table 2**.[7]

Table 1. Top five pathogens contributing to domestically acquired foodborne illnesses (**Ref. 7**).

Pathogen	Estimated number of illnesses	90% Credible Interval	%
Norovirus	5,461,731	3,227,078–8,309,480	58
Salmonella, nontyphoidal	1,027,561	644,786–1,679,667	11
Clostridium perfigens	965,958	192,316–2,483,309	10
Campylobacter spp	845,024	337,031–1,611,083	9
Staphylococcus aureus	241,148	72,341–529,417	3
Subtotal			91

Table 2. Top five pathogens contributing to domestically acquired foodborne illnesses resulting in death (**Ref. 7**).

Pathogen	Estimated number of deaths	90% Credible Interval	%
Salmonella, nontyphoidal	378	0–1,011	28
Toxoplasma gondii	327	200–482	24
Listeria monocytogenes	255	0–733	19
Norovirus	149	84–237	11
Campylobacter spp.	76	0–332	6
Subtotal			88

Progress in microbiological safety of food have been extensively driven by public demand due to disease outbreaks. Nevertheless, despite efforts paid from scientists, governments and industry, foodborne disease will continue to be a major issue in public health, with implications for both the social welfare of populations and for national economies.[8] Consequently, there is a need for new methods for the efficient and rapid detection of pathogens in food in order to minimize their spread and outbreaks.

2. CONVENTIONAL METHODS FOR THE DETECTION OF FOODBORNE PATHOGENS AND TOXINS

Conventional methods for detecting foodborne bacterial pathogens rely on microbiological analysis, followed by biochemical, serological, or molecular tests for the pathogen identification. Such methods include colony counting, polymerase chain reaction (PCR) and immunological methods.[9]

Colony counting method is considered as the “gold standard” for pathogen detection.[10] It is labor-intensive and time-consuming (typically more than 7 days)

because it is linked to the ability of microorganisms to grown in different culture media.[11] In addition, contamination from fast growing microorganisms may interfere with the detection.[12,13]

PCR methods exploit the nucleic acid amplification to enhance the sensitivity of the detection and have been extensively used for the identification of pathogens in food matrices.[14] However, PCR methodologies involve the extraction and purification of the pathogen DNA or RNA with protocols that are depending from the food sample properties. An incorrect amplification of contaminants sequences produces false positive results, while amplification of positive samples produces high concentrations of target molecules that can certainly lead to cross-contamination of negative samples.[15,16] On a large scale basis, routine PCR-based detection of microbes is expensive and is usually performed by skilled personnel only.[17]

Immunological methods are widely used to detect bacterial cells, spores, viruses and toxins[18] and are based on the specific binding of an antibody to an antigen.[12,19,20,21,22] Enzyme-linked immunosorbent assay (ELISA)[23] is among the immunological-based methods used for the detection of pathogens and toxins.[24,25,26,27] Immunological assays are usually reliable, but an enrichment step is needed to increase the bacteria count in the food sample, thus enhancing the sensitivity but also increasing the time required for the analysis.[28]

3. BIOSENSORS FOR THE DETECTION OF FOODBORNE PATHOGENS AND TOXINS

Over the last decade, biosensors have been shown to offer promising alternatives for pathogenic microorganisms detection in food.[29,30,31,32,33]

A biosensor is an analytical device that integrates a biorecognition element (or bioreceptor) with a suitable transducer. The bioreceptor is a crucial element in

biosensing. It defines the selectivity of the biosensor: i.e. its ability to detect only the target biomolecule and not interfering molecules. Antibodies, enzymes, phages, aptamers or single-stranded nucleic acid sequence (ssDNA, RNA) may act as the biorecognition element.

Transducers convert the biorecognition event in a detectable signal. The transduction mechanism may be optical, electrochemical, thermometric, piezoelectric, magnetic, micromechanical or a combination of them.[34,35,36]

Biosensors are classified on the basis of the transduction method or according to the bioreceptor involved (*catalytic biosensors* if an enzyme is used or *affinity-based biosensors* if proteins, nucleic acids, membranes, whole cells are employed for the biomolecular recognition).[37] Antibodies and nucleic acids represents the main biorecognition elements used in biosensing.[38] When antibodies or antibody fragments are used as the recognition element, the device is called *immunosensor*, while biosensors using nucleic acids sequences are named *genosensor* or DNA or RNA sensors.[39]

Antibodies are usually immobilized on a solid surface to obtain an immunosensor.[40] The interaction between an antigen and an antigen-specific antibody can be illustrated as a lock and key fit. An antigen-specific antibody binds its unique antigen, often with high specificity and for this reason antibodies can be used as specific probes for the recognition of specific analytes that are present even at extremely low concentration and in a mixture with other species.[41]

Genosensors identify target nucleic acids by matching the complementary base pairs that are often the genetic components of an organism. Those biosensors can be simple, rapid, and inexpensive[38] and are widely used in pathogen detection.[42,43,44]

Biosensors are used to detect a wide range of targets ranging from small molecules to viruses and bacteria. General characteristics include accuracy, near real-time assay,

sensitivity, specificity, reproducibility, robustness and ease of use. False-positive and false-negative results should be very low, ideally zero, particularly for application in food industry where false-negatives can bring expensive recall and the loss of public confidence, whereas false-positive could increase production costs.[45]

Two different approaches can be implemented for bacterial biosensing. They are based on the detection of bacterial components released after the bacterial lysis or processing-free methods targeting components at the bacteria surface.[37]

Among biosensors developed over the past decade for the detection of foodborne pathogens, optical and electrochemical biosensors are today the most commonly used. Optical biosensors, detecting light absorption, luminescence, reflectance, Raman scattering or changes in media refractive index, are powerful alternatives to conventional analytical techniques and have received attention for bacterial pathogen detection.[46,47,48] In particular, optical biosensors based on SPRI are used for real-time and label-free monitoring interactions between biomolecules, with high sensitivity and selectivity.[49] SPR biosensors have been employed to investigate the presence of pathogens and toxins in food[50], particularly to detect *S. aureus* and Staphylococcal enterotoxins[51,52], *Salmonella*[53,54], *Listeria m.*[55,56], *Escherichia coli* O157:H7[57,58] and tetrodotoxin[59].

4. SURFACE PLASMON RESONANCE IMAGING (SPRI)

4.1. SPRI principles

The surface plasmon resonance physical phenomenon has been observed for the first time by Wood[60] and since then SPR has become one of the fastest-growing biosensing analytical tool.[61]

SPR exploits the evanescent electromagnetic (EM) field generated at the surface of a thin metal layer when properly irradiated with an incident light beam. EM field is

generated by electron charge density fluctuations (surface plasmons[62]) occurring at metal/dielectric interfaces.

Free electrons in metals can be treated as a high density plasma (density about 10^{23} cm^{-3}). Electron density fluctuations propagate through the volume of a metal with a characteristic frequency given by (**eq.1**):

$$\hbar\omega_p = h\sqrt{\frac{4\pi ne^2}{m_e}} \qquad \text{eq.1}$$

where ω_p is the oscillation frequency of the plasmon, n is the free electron density, e and m_e are the electron charge and the effective mass of an electron respectively.

Electron fluctuations are confined at the boundary and vanishes both sides of the metal surface. Surface plasmon waves are *p*-polarized and are described by a wave vector k_x parallel to the metal surface having magnitude (**eq.2**):

$$k_x = \frac{\omega}{c}\sqrt{\frac{\varepsilon_1\varepsilon_2}{\varepsilon_1+\varepsilon_2}} \qquad \text{eq.2}$$

where $\varepsilon_1 = \varepsilon'_1 + i\varepsilon''_1$ is the complex dielectric constant of the metal and ε_2 is the dielectric constant of the medium.

The above mentioned surface charge fluctuations are accompanied by a mixed transversal and longitudinal electromagnetic field (E), which disappears at an infinite distance from the metal surface and has its maximum at the metal surface. The frequency ω_p of the longitudinal oscillations of the surface plasmon is tied to its wave vector k_x by a dispersion relation $\omega_p(k_x)$ (**Figure 1**).[61]

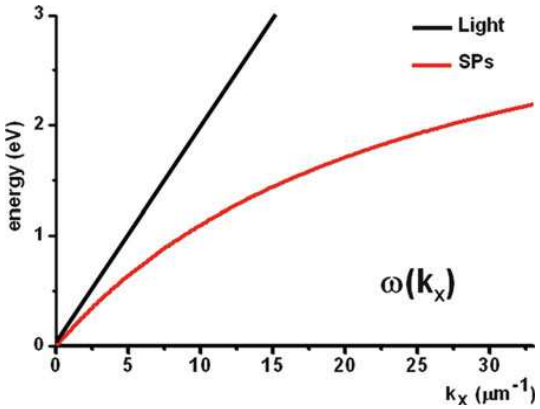

Figure 1. Surface plasmon dispersion ω(kx) on gold surface. The vertical axis is scaled as ω(eV). The straight solid line in figure shows the light line. $k_x = \omega / c\sqrt{\varepsilon_2}$ (**Ref. 61**).

For plasmon excitation by a photon to take place, the energy and the momentum must be conserved during the photon-plasmon coupling. This requirement is met when the wave vector of the electromagnetic radiation k_{light} and the plasmon k_x equal in magnitude and direction. The direction of the wave vector is the direction of the wave propagation, while its magnitude depends on the dielectric constant of medium at the interface. The wave vector (k_x) associated with surface plasmons is always larger than wave vector of light (k_{light}) having the same energy and travelling through the medium ε_2 whereby the surface plasmon dispersion relation never interests the dispersion relation of electromagnetic radiation (**Figure 1**). As a result, surface plasmon cannot couple with freely propagating light beam irradiating the metal surface. In order to couple photons at a given energy with surface plasmons, the wave vector has to be increased by Δk_x (**Figure 1**). A similar increase can be obtained either by passing the light through a medium with a refractive index greater than that of the dielectric medium at the boundary at which the surface plasmon is to be excited or by using diffraction effects. Thus, prism, grating, fiber-optic or waveguide couplers are needed for SPR-based sensors. Prism couplers are the most common setup for excitation of surface plasmons. They exploit the attenuated total reflection effect with the Kretschmann configuration (**Figure 2**) that increases the wave vector of the radiation

travelling through a prism coupler (dielectric constant ε_{pr}) with an incidence angle θ by $\sqrt{\varepsilon_{pr}}$ sin θ. Under similar conditions, the wave vector magnitude matching condition is obtained when (**eq.3**)

$$\frac{\omega}{c}\sqrt{\omega_{pr}}\sin\theta=\frac{\omega}{c}\sqrt{\frac{\varepsilon_1\varepsilon_2}{\varepsilon_1+\varepsilon_2}} \qquad \text{eq.3}$$

and a drop in the intensity of the light reflected by the prism under the attenuated total reflection condition is observed (**Figure 2**). Any change of the value of ε_2 caused by chemical or physical effects modifies the matching condition and a shift in the energy position of the minimum of the reflected light (reflectance dip) is observed.[63]

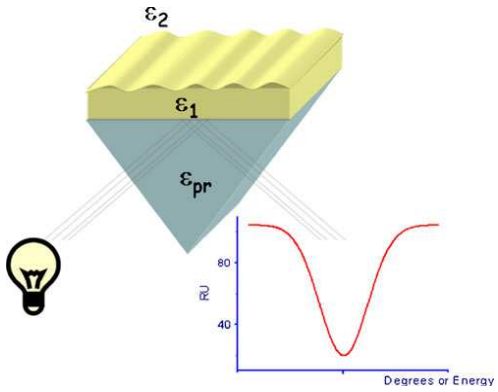

Figure 2. From Ref. 63. Configuration of the Kretschmann geometry.

The surface plasmon wave is therefore highly sensitive to changes of the dielectric constant (simply related to the refractive index) of the medium at the metallic interface.[61] This distinguishing property is the basic principle which makes the surface plasmon resonance useful as biosensor.[64]

Conditions for surface plasmon resonance are obtained in the infrared and visible wavelength region for air/metal and water/metal interfaces.

Many points can be considered for the choice of a metal for SPR:

- The metal should have a low imaginary part of the refractive index to reduce the dissipation and, consequently, to obtain a more narrower reflectance dip. Silver and gold are noble metals that satisfy this condition,

while aluminum has a large imaginary part and exhibits wider dips compared to silver and gold.

- The chemical purity of the surface since oxides and sulfides formed after the metal interaction with the atmosphere can interfere with the SPR phenomenon.
- The compatibility of the metal reactivity with the surface chemistry needed for the SPR experiment.[61]

An SPR biosensor is able to measure the binding between target analyte molecules and receptor molecules immobilized on the gold surface. During the receptor/analyte binding event, the shift of the dip in the spectrum of the reflected light is monitored over time and information on kinetics of biomolecules interactions is gathered.[65]

SPR allows to investigate interactions between antigens and antibodies, nucleic acid sequences and their complementary strands, and substrates and enzymes with no need for labeling of the interacting components. The kinetic events at the metal surface, displayed as a sensorgram, can be investigated by monitoring the SPR signal change as a function of time. The time interval during which the analyte interacts with the surface bound receptor defines the "association phase" while the time interval following the analyte interaction is termed "dissociation phase". In the association phase there is a simultaneous association and dissociation equilibrium. A steady-state condition is reached when the association rate equals the dissociation rate. Under ideal experimental conditions, only dissociation should take place during the dissociation phase. In order to perform replicate SPR experiments any bound analyte molecule should be removed with no disruption of the receptor structure and activity. So, a typical SPR experiment involves several steps displayed in **Figure 3**.[61]

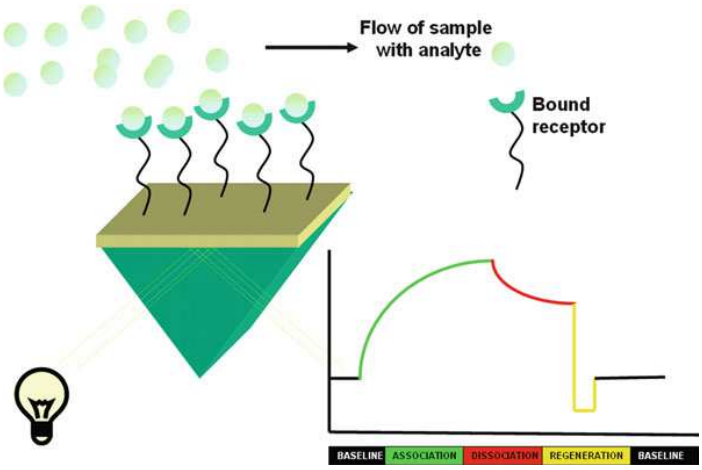

Figure 3. From Ref. 61. Pictorial description for the receptor-analyte interaction: the analyt is captured by receptors immobilized on the sensor surface. A sensorgram with the steps of an analysis cycle is also shown.

Different configurations are used to carry out SPR experiments: angle modulation[66], wavelength modulation[67] and intensity modulation also known as SPRI, or SPR microscopy.[68]

SPRI was first introduced by Rothenhäusler and Knoll in the 1988[69]. It combines typical advantages of the traditional SPR in terms of real time analysis, no label requirements and high sensitivity, with those associated to an imaging system such as the easy coupling with microfluidic devices, the high spatial resolution and the possibility to adopt an array-compatible detection approach.[61]

SPRI uses optical detectors to measure differences in the intensity of the reflected light (expressed as percent reflectivity %R) at a fixed angle and wavelength.[70] In particular, SPRI platforms based on a Kretschmann geometry use a p-polarized light beam to illuminate a prism/thin gold film assembly and the intensity of the reflected light is detected with a 2D detector (CCD) to obtain an SPR image. The spatially resolved surface functionalization of the metallic SPRI surface permits the detection in real time of parallel interaction events.[49] In this case the spatial contrast comes from the heterogeneity of the dielectric constant owing to differences in the refractive index

or film thickness near the surface at different positions across the surface. Difference images obtained by the subtraction of a reference image from a post binding image provide visual confirmation of the binding events. The SPRI system allows to make simultaneous and independent measurements on different locations of the same sensor surface.[63] Moreover, the strength of SPRI is the possibility to observe visually the sensor surface in real time, along with other advantages related to optical sensitivity and instrumentation simplicity.[61]

In recent years, the coupling of microfluidic devices, often made in poly(dimethylsiloxane) (PDMS), with SPRI have been show to constitute a powerful tool for the simultaneous monitoring of interactions of arrayed biomolecules. The use of microfluidic devices allows to overcome mass-transport rate limitation thanks to the reduced sample volume involved. In addition, microscale conditions induce the laminar flow of fluids and optimize the way in which liquids are put in contact to the SPRI sensor surface.[71]

4.2. SPR biosensing formats

Various detection formats have been used in SPR biosensing.[72] The format is chosen according to the size of target analyte molecules, the binding characteristics of biomolecular recognition elements investigated, the range of concentration of the analyte to be measured, and sample matrix.[73]

The most frequently employed formats are the direct, sandwich or binding inhibition formats (**Figure 4**).

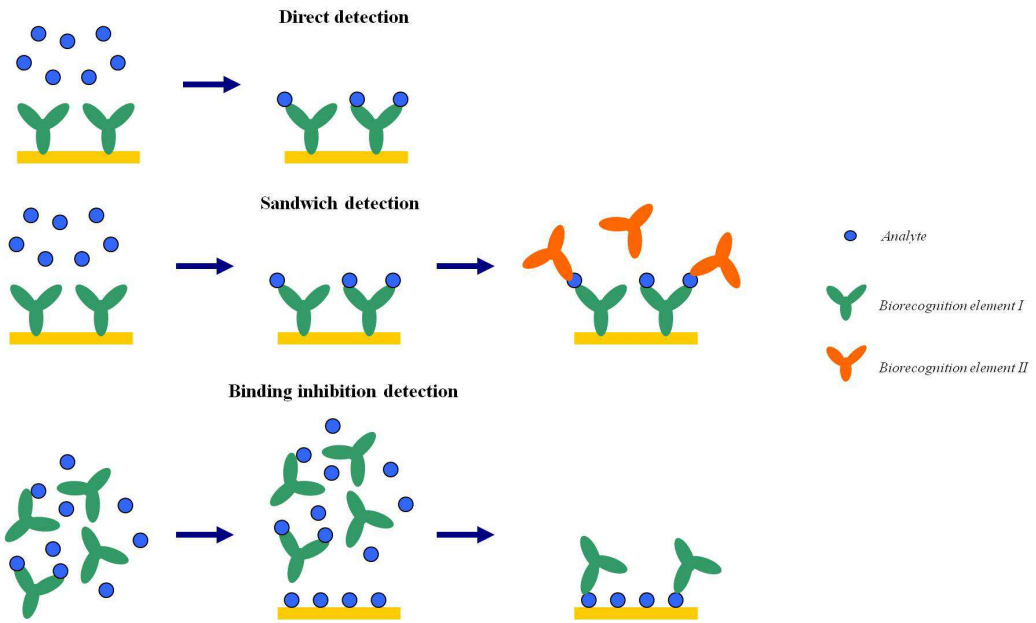

Figure 4. Modified from Ref. 74. Main detection formats used in SPR biosensors: direct, sandwich and binding inhibition detection format.

The direct detection format is based on a direct interaction between the analyte and the biomolecular recognition element (e.g., antibody or oligonucleotide) immobilized on the SPRI sensor surface. The interaction causes a change in the local refractive index which is directly proportional to the concentration of analyte. The sandwich assay format involves two steps. Firstly, the sample is put in contact with the sensor and analyte molecules bind the biomolecular recognition element (e.g., antibody or oligonucleotide) immobilized on the sensor surface. Then a labeled secondary biorecognition element is bound to the previously captured analyte further increasing the number of bound biomolecules and thus also the sensor response. The binding inhibition detection format involves a competitive reaction of analyte in solution and analyte immobilized on the sensor surface with free antibodies. In particular, a sample is mixed with respective antibodies and analyte in the sample bind to antibodies thus blocking their binding sites. Then the mixture of analyte with antibodies is brought in contact with the sensor surface coated with analyte molecules, so that the unoccupied antibodies can bind to analyte molecules immobilized on the sensor surface. In this

format, the SPR biosensors determine the concentration of target analyte from the concentration of unbound antibodies.[74]

4.3. Functionalized gold nanoparticles (AuNPs) for biosensing

AuNPs have gained remarkable interest thanks to their optical properties which can be exploited in innovative applications in sensing[75,76] or imaging.[77,78]

AuNPs can be produced in a range of shapes, such as nanospheres, nanorods, nanobelts, nanocages, nanoprisms, nanostars. The final size and shape of AuNPs affects the nanoparticles chemical, optical, and electromagnetic properties. For instance, metallic gold is golden yellow, whilst gold nanoparticles dispersions are red.[79] The intense red color of AuNPs is consequence of the resonant interaction between incident light and localized collective oscillations of free electrons in the particles, known as localized SPR (LSPR). AuNPs with diameters of about 10-100 nm or aggregated AuNPs generate color changes of the colloidal dispersion from red to blue.[80]

Various synthetic approaches can be used to obtain AuNPs, such as chemical reduction[81], photochemistry,[82] sonochemistry,[83] seeding growth[84], radiolysis[85], but the most widely employed method is the Turkevich-Frens method.[86,87,88] In this case, citrate ions are used as both reducing and capping agents, in order to electrostatically stabilize nanoparticles against aggregation by exploiting the negative surface charge of the citrate layer.[89,90] The formation of stable colloidal suspensions having precise particles size and shape is obtained if the right synthetic strategy in conjunction with an appropriate awareness of the close correlation between the surface of the particles and the stabilizing agent are combined.[91] Production volume, temperature, stirring rate and citrate concentration affect the physical properties of the nanoparticles, namely size, size distribution, zeta potential and optical characteristics. In particular, AuNPs

with average diameters from 20 to 80 nm can be synthesized by modulating the amount of citrate added.[92]

AuNPs are widely employed in the developing of DNA-based biosensors, precisely because the nanoparticles can be obtained with definite size, shapes, and optical properties. In addition AuNPs dispersions have extremely high extinction coefficients ($2.7 \times 108\ M^{-1}\ cm^{-1}$ at ~ 520 nm for 13 nm spherical AuNPs), while their large surface area enables to load hundreds of capture probe whereas the three-dimensional architecture of the probe reduces steric hindrance and encourage target-probe hybridization.

Basic approaches used to functionalize AuNPs with biomolecular systems for DNA detection rely on ligand-like binding to AuNPs surface, electrostatic interactions between positively charged biological molecules and negatively charged AuNPs, covalent binding between the biological molecule and the stabilizing shell around the AuNPs and affinity-based binding.[80]

AuNPs surface modification with biomolecules must not affect the AuNPs properties and the biorecognition activity of the immobilized biomolecular system, which in turn is employed for the detection of specific target analytes.[93,94]

DNA-functionalized AuNPs fulfill a significant role in biosensing and nanobiotechnology[95] and they are used in different molecular diagnostic and therapeutic applications, such as gene regulation,[96,97] drug delivery,[98,99] cell imaging,[100,101] array-based electrical detection,[102] atomic force microscopy based detection,[103] ion colorimetric detection,[104,105] nucleic acids detection.[106,107,108,80]

Recently, the use of properly DNA-functionalized AuNPs in sandwich detection formats has been exploited to obtain an ultrasensitive SPRI detection of genomic DNA (gDNA).[80,109] The enhancement of the SPRI detected signal is due to:

- an increase of the absolute mass of species associated to the binding event;

- an increase in the intensity of the local electromagnetic field, obtained as a consequence of the interaction between electromagnetic fields associated to LSPR and propagating SPR;
- the bulk refractive index of the AuNPs that is significantly higher than that of the biomolecules.[110]

AuNPs have been used in the sensing of bacteria[111,112] including *S. aureus*[113,114,115,116], *Escherichia coli*[117,118,119,120], *Campylobacter jejuni*[121], *Listeria m.*[122,123,124]. Recently, new gene-independent amplification detection methods have been developed by modify the surface of AuNPs with antibodies.[125] Such systems have been used to detect *Listeria m.*,[126] *Escherichia coli* O157:H7,[127] *S. aureus*,[128] *Salmonella.*[129]

5. *STAPHYLOCOCCUS AUREUS*

S. aureus is responsible for a wide range of infections in humans and different other animal species.[130] The name of the organism is derived from Greek words *staphyle* (a bunch of grapes) and *coccus* (grain or berry).[131]

S. aureus is a Gram-positive, facultative anaerobic, catalase-positive, oxidase-negative, non-motile microorganism, which creates smooth, convex, lustrous, circular colonies reaching a size of 0.5-1.5 μm in diameter and growing in an irregular three-dimensional bunch of grapes-like clusters of cells.[132]

Pathogenicity of *S. aureus* is related to its ability to produce staphylococcal enterotoxins (SEs) and other virulence factors that cause gastroenteritis in humans.[133] While the microorganism can be inactivated through heat treatment of the food, enterotoxins survive the heat treatment and can cause staphylococcal food poisoning.[134] SEs belongs to the superantigene protein family, which induces a polyclonal response by direct binding to class II major histocompatibility complex

proteins and T-cell without being internalized and processed like a normal antigen. Such toxins may be involved in modulating the host immune response and may contribute to evasion of hosts defenses and bacterial persistence.[135] SEs are single-chain proteins with weights ranging from 26 to 30 kilo Dalton. They are highly resistant to heat, freezing and drying. They are also resistant to proteolytic enzymes, such as pepsin or trypsin. For this reason they are able to transit the gastrointestinal tract after ingestion.[136]

There are five classical enterotoxin serotypes: SEA, SEB, SEC1,2,3, SED, and SEE. More recently SEG, SEH, and SEI have been also described. All of them exhibit emetic activity. There are also SE-like enterotoxin serotypes, SElJ-SElU that have not been confirmed to exhibit emetic activity. SE serotypes are similar in composition and biological activity, but are different in antigenicity and are identified serologically as separate proteins.[137]

SEs are considered the main causative agents of staphylococcal food poisoning. The detection of SEs in food matrices, such as milk, cheese and meat represents a challenging analytical task for the low concentrations of the toxin together with high concentrations of other possibly interfering proteins in the sample that may produce false results.[138] SEA, SEB, SEC and SED are the most frequent toxins in foods, and SEA is the most commonly recovered from food poisoning outbreaks[139] because of its high thermal and proteolytic stability.[140] The minimum level of enterotoxin that causes gastroenteritis in humans is approximately 1 ng/g or ng/mL of food.[141] SEA is a single-chain protein having 233 amino acid residues with a molecular weight of 27 078 Da. It is responsible for animal (mastitis) and human (emesis, diarrhea, atopic dermatitis, arthritis, and toxic shock) syndromes.[142]

Origins of staphylococcal food poisoning differ widely among countries due to differences in food consumption and eating habits.[143] The main source of

contamination are humans, mostly food handlers carrying enterotoxin-producing *S. aureus* in their noses or on their hands. In fact, *S. aureus* is commonly found in nasal passages, throat, hair and skin of carriers.[144] Three categories of *S. aureus* carriers have been recognized: persistent, intermittent (occasional) and never-carriers. Persistent carriers are infected with the same staphylococcal strain for months or even years and are estimated to be 20%-35% of humans. Intermittent carriers represent 40%-70%, whilst never-carriers are uninfected and represent 10%-40% of the population.[145] Contamination is largely associated with inappropriate handling of cooked or processed foods, followed by storage under conditions that permit growth of *S. aureus* and production of the enterotoxins. Air, dust, and food contact surfaces can also serve as vehicles in the transfer of S. aureus to foods.[139] Furthermore, in food such as raw meat, sausages, raw milk, and raw milk cheese, contaminations from animal origins are more frequent and due to animal carriage or to infections (e.g., mastitis).[137]

Foods that have been frequently incriminated for staphylococcal poisoning comprise meat and meat products, poultry and egg products, milk and dairy products, salads, bakery products, particularly cream-filled pastries and cakes, and sandwich fillings.[139] In particular, milk and dairy products can contain *S. aureus* due to direct contact with contaminated sources in the dairy farm environment, excretion from the mammary gland of a cow with mastitis and poor sanitation, such as coughing or sneezing and not washing hands when handling milk storage equipment, during or after milking.[146]

For dairy industry, the microbial quality of milk is an important challenge because:

- outbreaks of disease in human beings have been attributed to the consumption of unpasteurized and pasteurized milk;
- unpasteurized milk is consumed directly by dairy producers, farm employees, and their families, neighbors, and raw milk supporters;

- several types of cheeses are manufactured from unpasteurized milk and consumed by a large segment of the population;
- pasteurization may not destroy all foodborne pathogens in milk.[147]

In particular, the presence of *S. aureus* above 10^3 UFC in milk increases the risk of staphylococcal toxin production more resistant to heat processes of pasteurization.[148] The growth of *S. aureus* and the production of enterotoxins in dairy products is affected by different conditions, such as temperature, pH, salt and water activity and competitive microorganisms.[149,150]

Many instances of staphylococcal diseases or food poisoning outbreaks due to ingestion of contaminated dairy products or milk have been reported.[151,152,153] For example, in 1985, chocolate milk was the origin of a staphylococcal food poisoning in the Kentucky, USA. The chocolate milk was contaminated and stored at too high temperature for 4-5 hours before pasteurization. Pasteurization killed the staphylococci but had no effect on the SEs.[154] In June 2000, in Japan, consumption of low-fat milk produced from skim milk powder contaminated with SEA caused a large scale outbreak.[155] At the end of 2009, soft cheese made from unpasteurized milk was found to be the common source of the outbreaks in France.[156]

S. aureus ability to form biofilms can cause enduring contamination of food processing.[157] Biofilms are very ordered bacterial cellular structures due to irreversible attachment, proliferation, and production of an extracellular polymeric substance (EPS) on solid surfaces. EPS, made of polysaccharides, proteins, extracellular DNA (eDNA) and phospholipids, enables the bacterial adhesion to surfaces, thus protecting the microorganism from antimicrobial agents.[158] As a result, biofilms lower the efficacy of sanitizers, cause economic losses to industry, contaminate food and can enhance the level of antimicrobial resistance.[159] Antimicrobial resistance is a complex, many-sided, critical global problem.[160] Recently, the European Food Safety Authority

has underlined the increasing concern for public health caused by the presence of *Methicillin Resistant Staphylococcus Aureus* (MRSA) in food producing animals, whereby has recommended the importance to detect and quantify MRSA.[161] MRSA resistance to antibiotic treatments[162] is due to the presence of the mecA gene, which encodes an altered penicillin binding protein with decreased affinity for betalactam antibiotics.[163]

Animal food products such as meat, meat products and milk may be contaminated by MRSA through slaughter or milking of colonized/infected animal.[164] The MRSA colonization in food has an effect not only on food production but also on health of people that work with animals or that consume contaminated food.[165,166,167]

In the last years, different cases of MRSA in food have been food, such as in meat, [168,169,170,171,172,] milk and dairy products,[168,169,173,174,175,176] chicken and turkey meat,[177,178] pork.[179] This aspect represents an important risk factor for the spread of staphylococcal infections, whereby the tuning of new methods for detecting *S. Aureus*, especially MRSA, became essential.[180]

6. *LISTERIA MONOCYTOGENES*

Listeria m. is the only species of the genus *Listeria* to be pathogenic to humans.[181] It is a ubiquitous Gram positive, facultative anaerobic, motile, non-spore forming bacteria, typically 0.5-2μm in length and 0.5μm in diameter, present frequently in food, environment and animals.[182,183] The microorganism can grow and survive at low temperature (4°C) and pH (4.4) values and at salt concentrations of up to 14%. As a result, low temperature, extreme pH and high salt concentration conditions could be unsuccessful for food preservation.[184] The consumption of food contaminated with *Listeria m.* causes listeriosis[185], a serious infection that may cause sepsis, meningitis and encephalitis.[186,187] In particular, non-invasive gastrointestinal illness affects

immunocompetent people, while invasive listeriosis infections leading to septicemia, meningitis, and abortion is usually observed in immunocompromised individuals or pregnant women.[182] However, also healthy individuals could be affected by gastroenteritis when they consume large amounts of the bacteria.[181] The pathogenesis is due to the capacity of *Listeria m.* to cross the intestinal barrier, the blood brain barrier and the materno-fetal barrier.[188]

Infection by *Listeria m.* is mediated by virulence factors, among which the most important is listeriolysin O (LLO). It is found only in virulent strains of the species and it is a secreted protein. Its detection is indicative for the presence of *Listeria m.* in a food sample.[189] LLO is a pore-forming toxin and it is one of the 20 pore-forming toxins of cholesterol-dependent cytolysins (CDCs). CDCs are secreted as water-soluble monomers, which bind to the cholesterol of host membranes, oligomerize and form large pores.[190] Oligomerization of CDCs seems to depend on the sequential addition of monomers or multimers. Sometimes oligomerization is not complete, generating arc-like structures that have been suggested to still be active pores.[191]

The *Listeria m.* intracellular lifecycle starts with the entry of the pathogen into a host cell. Then, it is internalized by multiple phagocytic receptors, such as complements, immunoglobulins and scavenger receptors, in phagocytic cells and by several virulence factors in non-phagocytic cells. After internalization, the bacteria is located into an endosome, called the primary vacuole. This vacuole is quickly disrupted by the LLO, encoded by the hly gene. At an early stage of infection, wild type bacteria were located within a vacuole, and then they proliferate in the cytosol. Instead, if the hly is interrupted by the insertion of a transposon or deleted, the bacteria remained trapped in the vacuole, unable to divide. LLO-deficient strains were also nonvirulent in vivo, showing the crucial role of this toxin in pathogenesis.[192]

Since the hlyA gene is only present in the pathogenic species, it is a suitable target for the detection of *Listeria m.* using nucleic acid-based methods.[189] The hlyA is 1717 base pairs (bp) long and only a single copy of this gene is present in the genome of the pathogen.[193]

Listeria m. forms biofilm difficult to remove from food processing apparatus and bacteria in biofilms are often more resistant to sanitizers than planktonic cells.[194] The biofilm formation relies on variations in transcriptional regulation, metabolism, and flagellum and peptidoglycan biosynthesis. The formation of the biofilm is based on an irreversible attachment to a surface; then a protective extracellular polymeric substance (EPS) matrix is produced, developing a mature biofilm. The EPS surrounds the cells, helping them to resist environmental stresses.[195]

The occurrence of *Listeria m.* in food has significant economic implications such as food market withdrawal and declining sales.[196] *Listeria m.* is commonly found in processed seafood and meat, ready-to-eat (RTE) food and dairy products.[197] The European Union has notified an increase of human cases of listeriosis of 8.6 % between 2012 and 2013[198] and 30% between 2013 and 2014, confirming a statistically significant increasing trend of listeriosis over 2008-2014.[199] Recent *Listeria m.* outbreaks have involved frozen vegetables,[200] raw milk,[201] packaged salads,[202] soft cheese,[203] creameries products,[204] caramel apples,[205] dairy products.[206] According to the European commission regulation 2073/2005 on microbiological criteria for foodstuffs, the concentration of *Listeria m.* must be kept below 100 cfu/g.[207]

Food contact surfaces, like stainless steel (SS) or polyethylene (PE) are the main ways of cross-contaminations with *Listeria m.* and have been associated with many outbreaks linked to the food industry. Organic residues on these surfaces rise the persistence of the pathogen.[208]

In order to guarantee food-safety and to preserve humans from infections, many efforts have been paid to reduce bacterial aggregation, biofilm formation and persistence of *Listeria m.* on industrial surfaces and food.[209]

Listeria m. is usually susceptible to antimicrobial agents against Gram positive bacteria, but some reports underline antimicrobial resistance originating from food-producing animals, food processing environments, and food (e.g. the food chain). In particular, food chain impacts on antimicrobial resistance through horizontal exchange of genes, induction of antimicrobial resistance-stress responses and frequent exposure to disinfectants in the processing environments.[182] Usually, β-lactam antibiotics, such as penicillin or ampicillin, alone or in combination with an aminoglycoside (e.g. gentamicin) are administrated in case of listeriosis in immunocompromised patients. For patients allergic to β-lactams, trimethoprim and a sulfonamide (e.g. sulfamethoxazole) are used. The diffusion of antibiotic resistance in *Listeria m.* may have noteworthy future clinical repercussions for the treatment of listeriosis. Antimicrobial susceptibility of *Listeria m.* is little known, above all for strains isolated from food and food processing environments, indicating the need of monitoring the spreading and diffusion of antimicrobial resistance.[210]

7. ANTIFOULING MATERIALS FOR SURFACE PLASMON RESONANCE BIOSENSING

The non-specific adsorption of molecules from complex samples (e,g, milk, juice, blood plasma) on the solid surface of biosensors generates responses unrelated to the analyte binding. Such effect is referred to as “fouling”.[211,212]

The Vroman effect helped in describing the adsorption of proteins on a solid surface on the basis of a thermodynamically favored displacement of low molecular

weight proteins already adsorbed on the surface by higher molecular weight proteins.[213]

Proteins adsorption on a surface leads initially the exclusion of water molecules from both the surface and the protein, with a reduction of the free energy barrier due to dehydration entropic effects. The surface hydration depends on physicochemical properties and surface packing of materials.[214] Further water molecules exclusion is triggered by protein-surface interactions involving hydrogen bonding, van der Waals and electrostatic interactions, with a reduction of the Gibbs free energy.[215]

The surface hydration is considered as the main driving factor in the non-specific adsorption of proteins.[216] Water molecules can interact with antifouling molecules through hydrogen bonds, generating a ‘‘hydrated layer” on the surface with antifouling capabilities.[217]

The use of surfactants (e.g. Tween) or additives (e.g. bovine serum albumin, BSA) has only limited effect on the reduction of hydrophobic and/or electrostatic interactions between the sample components and the surface.[211]

Surfaces able to resist to the adsorption of proteins hold the following molecular properties:

- comprise polar functional groups;
- contain hydrogen-bond acceptors;
- do not contain hydrogen-bond donors;
- are electroneutral.[218,219]

Antifouling materials can be generally classified into hydrophilic materials, such as poly(ethylene glycol) (PEG) and zwitterionic compounds. PEG and PEG-derived materials are able to resist protein fouling because favor the formation of a strong hydration layer through hydrogen bonding. Zwitterionic compounds are hopeful

alternatives to PEG reagents thanks to their ability to bind water molecules more strongly than PEG.[220]

Mixed self-assembled monolayers (SAMs) of alkane monothiols ending with tri and hexa ethylene glycol units have been used for SPR biosensing.[221] The length of the PEG chain, the chemical functionality and the concentration of functional groups available for the binding of the receptor can be easily modulated.

Surface monolayers containing a mixture of hydrophobic (methyl-terminated) and hydrophilic [hydroxyl-, maltose-, hexa(ethylene glycol)-terminated] alkanethiols can be used to modulate the degree of adsorption.[222] In the mixture one of alkanethiols forming SAM contains functional groups able to bind the probe molecule while the other carries hydrophilic end groups, such as hydroxyl or PEG, and limit non-specific adsorption of undesired biological entities.[223] SAMs with short ethylene glycol oligomers ($[CH_2CH_2O]n$, n=2-7; OEG, oligo(ethylene glycol)) effectively resist non-specific adsorption of proteins.[224]

Experimental and theoretical studies on OEG- and PEG-terminated SAMs show that the protein adsorption-resistance is due to several factors, such as the packing density and the hydrophilicity of the chains, the nature of the surrounding environment and the temperature.[225] In particular, antifouling capabilities of OEGn SAMs and PEG coatings depend on the correlation between the ability to bind interfacial water molecules and the angular distribution of water dipole moments. Lone pairs of oxygen atoms in the ethylene glycol repeating unit highly interact with the electron-poor regions of water molecules, providing an orientation of the interfacial water molecules with oxygen atoms pointing away from the PEG chain. The enthalpy required to break up the hydrogen bonding of the interfacial hydration layer is high enough to disfavor the adsorption of proteins.[226]

Several grafting approaches have been developed to enhance the antifouling capabilities of PEG. For example, "grafting to" approaches can be used to covalently link PEG to surfaces in order to form linear polymer brushes, while "grafting from" techniques can be used to polymerize PEG methacrylates, by forming linear polymer with PEG side chains.[227] Graft density and molecular weight (MW) of PEG affect the conformation of PEG chains on surfaces. PEG chains are settled in the "brush" or "mushroom" conformation if a high or low graft density is obtained, respectively. High graft density can be obtained with "grafting from" approaches.[228]

The reduced protein adsorption on high molecular weight PEG is due to steric repulsion in the polymer. The adsorption of protein on the polymer generates a compression of the chains and is entropically disfavored. The compression also causes the transfer of water molecules to the bulk, so that the polymer is desolvated and an enthalpic penalty occurs. These factors do not affect monolayer with short oligomers of the ethylene glycol groups, because the short chains probably cannot accommodate a high degree of solvation and conformational dynamics.[229]

Gold surfaces can be functionalized with PEG/OEG-based compounds through a single-step self-assembly, leaving active functional groups on the surface for later immobilization. Thanks to their easy preparation, PEG-based antifouling materials are often used in SPR biosensing. PEG/OEG-based compounds resist protein adsorption in both single-protein systems, such as human serum albumin (HSA) and fibrinogen, as well as complex systems, such as serum and plasma.[217] However, PEG suffers rapid autoxidation, particularly in the presence of oxygen and transition metal ions, which limit its use for long-term stability in antifouling coatings.[230] In order to beat this limitation, several modifications of the PEG/OEG chains (the chain length, side chain morphology, polymerization density, and terminal group features) have been studied.[217]

Zwitterionic molecules have been shown to operate as antifouling coating materials able to provide ultralow protein adsorption (range of <0.3 ng/cm^2).[231] Zwitterionics bring an equivalent fraction of positive and negative charges, retaining thus the overall charge neutrality required for antifouling surfaces.

Zwitterionic molecules are commonly considered substitutes of PEGs in preventing non-specific protein adsorption. From a chemical point of view, while PEG polymers usually show the same repeating unit, zwitterionic polymers exhibit different monomeric units. In particular, the chemical diversity involve:

- type of ionic groups in the structure (e.g. carboxylate, sulfonate or phosphate as anionic moieties, and quaternary ammonium, phosphonium, pyridinium or imidazolium as cationic moieties);
- the nearness of the oppositely charges within the same monomeric unit or the separation of the oppositely charges onto different side chains;
- structures that can switch between zwitterionic and non-zwitterionic forms or that have a charged biologically active molecule as a part of the zwitterionic component.[232]

The stimulus to employ zwitterion materials as antifouling agents derived from the study of the external surface of the mammalian cell membrane with phospholipids bringing zwitterion headgroups.[233]

Similarly to PEG, zwitterionics form a closely bounded water molecules layer, which represents a physical and energetic barrier for protein adsorption on the surface.[231] Zwitterionics can bind with water molecules more strongly than conventional hydrophilic materials, through an electrostatically induced hydration. Moreover, it is believed that the bilayer of plasma lipids formed on the surface of zwitterionic materials represents a further protection against non-specific adsorption. Nevertheless, this explanation do not account for the antifouling properties in fluids

derived from plasma lipids. Then, like PEG, mobility and flexibility of zwitterionic materials provide protein resistance.[215]

Polyzwitterionic materials can be categorized in:

- polybetaines, having a positive and a negative charge on the same monomer unit. Examples are 2-methacryloyloxylethyl phosphorylcholine, sulfobetaine methacrylate and carboxybetaine methacrylate;
- polyampholytes, carrying 1:1 positive and negative charge ratio on two different monomer units. Examples are mixed charge complex and natural amino acids.[214]

The sulfobetaine monomer, having a quaternary ammonium cation and a sulfonate anion on the same side chain is easier to handle than phosphorylcholine. Carboxybetaine methacrylate holds side chains made of cationic quaternary ammonium and anionic carboxylate functional groups. Carboxybetaine differs from sulfobetaine because of the negatively charged carboxylic acid groups. Poly(carboxybetaine) integrates the ultralow fouling with bio-recognition elements.[234]

Surface modification with zwitterionic materials includes several approaches:

- Surface coating: initiated chemical vapor deposition (iCVD), adsorption and SAMs.
- Surface segregation: self-assembly process of amphiphilic block copolymers.
- Surface grafting: inclusion of polymer chains onto a solid surface with good long-term stability through ‘‘grafting to” and ‘‘grafting from” approaches, which involve the direct graft of preformed end-functionalized polymer chains onto surfaces and the graft polymerization of monomers from surfaces, respectively. “Grafting from” techniques include conventional radical polymerization and living radical polymerization (atom transfer

radical polymerization (ATRP) and reversible addition-fragmentation chain-transfer polymerization (RAFT)). [235]

Controlled/living radical polymerization approaches are more advantageous than conventional polymerization for the preparation of brushes and bioconjugates.[236]

SPR specificity is a valuable task for biosensing, particularly in real-sample analysis. In general, two kinds of non-specific adsorption could affect the detection: the binding of non-specific proteins, cells, and bacteria on the sensor surface, due to the great amount of active binding sites, which gives non-specific signals; the specific and non-specific adsorption on sensor surface, which originates a high baseline and scarce immobilization of the bioreceptor. The reference method and antifouling applications are the only approaches able to beat these limitations, even if the reference method is not reliable in complicated real samples.[217]

8. PURPOSE OF THE PERFORMED RESEARCH ACTIVITY

The development of analytical methodologies capable to detect, with high sensitivity and specificity, potentially harmful pathogens and toxins present in food, represents a field of research whose effects have an important and considerable social impact, both for the requirements deriving from the protection of consumers' interests and health, and economic implications of the food industry.

In this context, the purpose of the research activity I performed during my PhD course was to develop SPRI-based biosensors for the ultrasensitive detection of *S. Aureus* and *Listeria m.* in food samples.

In particular, three different aspects have been investigated:

1) the development of SPRI genosensors for the detection of *S. Aureus* and *Listeria m.* genomic DNA (gDNA);
2) the development of SPRI immunosensors for the detection of SEA;
3) the tuning of SPRI sensor surfaces able to resist non-specific adsorptions.

SPRI capabilities for genosensing have been explored through the in situ gDNA hybridation to peptide nucleic acid (PNA) probes immobilized on SPRI sensor surface. An appropriate design of the surface geometry has been taken into account.

At the same time, specific antibodies have been used to produce immonosensors able to detect very low concentrations (pM) of the toxins in complex food matrices (e.g. milk). Different antibody immobilization strategies have been studied in order to immobilize a suitable number of biorecognition elements as well as to minimize non-specific binding events.

Properly functionalized AuNPs have been employed to amplify SPRI signals thus enhancing the biosensors sensitivity.

The development of SPRI surfaces able to resist fouling started from the requirement of detecting pathogens and toxins in real food matrices.

9. MATERIALS AND METHODS

9.1. Materials and reagents

Reagents were obtained from commercial suppliers and used without further purification. Trisodium citrate dihydrate, tetrachloroauric(III) acid, ethanol, dimethyl sulfoxide, sodium hydroxide solutions (10M in water), *11*-mercaptoundecanoic acid (MUA), *N*-Ethyl-*N'*-(3-Dimethylaminopropyl)Carbodiimide (EDC), *N*-Hydroxy-succinimide (NHS), ethanolamine hydrochloride, dithiobis(*N*)succinimidylpropionate (DTSP), *n*-dodecil mercaptano (NDM), graphene oxide (GO), Tween 20, bovine serum albumin (BSA), methoxypolyethylene glycol amine (mPEG 5000), tris(hydroxymethyl)aminomethane hydrochloride (TRIZMA HCl), *11*-mercaptoundecanoic acid (MUA), Staphylococcal enterotoxin A (SEA) from *Staphylococcus aureus* were purchased from Sigma-Aldrich (Italy). Methyl- and carboxy-thiol PEGylation reagents [2,5,8,11-tetraoxatridecane-13-thiol or Methyl-PEG4-Thiol or $MT(PEG)_4$; 1-mercapto-3,6,9,12,15,18,21,24,27,30,33,36-dodecaoxanonatriacontan-39-oic acid or Carboxy-PEG12-Thiol or $CT(PEG)_{12}$] were purchased from Thermo Scientific. Streptavidin was purchased from Invitrogen. Phosphate buffered saline (PBS) solutions at pH 7.4 (137mM NaCl, 2.7mM KCl, phosphate buffered 10mM) were obtained from Amresco (Italy). Anti *Staphylococcus aureus* enterotoxin A 2S7-F12 (Anti-SEA F12), anti *Staphylococcus aureus* enterotoxin A 2S7-H5 (Anti-SEA H5) and anti *Staphylococcus aureus* enterotoxin A 2S7-H5B (Anti-SEA H5B) were purchased from Acris Antibodies. Anti *Staphylococcus Aureus* Monoclonal Antibody (Anti-*S. Aureus*) was purchased from LSBio, LifeSpan BioSciences, Inc. Oligonucleotides were purchased from ThermoFisher Scientific, Inc. PNA probes were purchased from Panagene. *Staphylococcus aureus subsp. Aureus* genomic DNA ATCC-700699D-5 (*S. Aureus* gDNA) and genomic DNA from *Listeria monocytogenes* Strain EGDe ATCC-BAA-

679D-5 (*Listeria m.* gDNA) were purchased from LGC Standards. Bovine Genomic DNA Female was purchased from AMS Biotechnology. SPRI gold chips were purchased from Xantec Bioanalytics. Gold nanoparticles conjugated with streptavidin were purchased from Nanopartz (AuNPs-SA NP). Methoxy PEG disulfide (mPEG) and PEG NHS ester disulfide (NHS PEG disulfide) were purchased from Polypure. Ultra-pure water (Milli-Q Element, Millipore) was used for all the experiments.

9.2. Surface Plasmon Resonance Imaging Apparatus and measurements

SPRI experiments were carried with an SPR imager apparatus (GWC Technologies, USA), equipped with a white light source and an SF-10 prism. A narrow bandpass filter (830 nm) was placed before the CCD camera used as a detector for SPR images. SPR images were analyzed by using the V++ software (version 4.0, Digital Optics Limited, New Zealand).

Data provided by the instrument were expressed as pixel intensity units (PIUs) on a 0-255 scale and were converted to the real change in reflectivity Δ%R, that is an absolute physical unit of measurement. To convert SPR signal change to Δ%R the polarizer adjuster was rotated 90° in order to change the polarization of the light from "p" to "s". There is no SPR response to s-polarized light, so all of the light is reflected off the gold surface, and the CCD image for these regions is white. The light energy reaching the prism was reduced by using a neutral density filter in front of the polarizer to not saturate the detector. After having acquired the s-polarized image, the V++ software generated a text window containing reflectivity data for each ROI on the s-polarized image. These values are used for the adjustment of data to Δ%R using the following formula (**eq.4**):

$$\Delta\%R = 100 \cdot I_p \cdot 0.85 \cdot (1 - d) / I_s \qquad \text{eq.4}$$

where d is the density of the filter used, and I_p and I_s refer to the reflected light intensity detected using p- and s-polarized light, respectively.

Kinetics data were obtained by plotting the difference in percent reflectivity (Δ%R) from selected regions of interest (ROIs) of the SPR images as a function of time.

SPRI experiments were carried by coupling SPR imager apparatus with a microfluidic device: microfluidic channels were fabricated in poly(dimethylsiloxane) (PDMS) polymer as described elsewhere.[237] Briefly, PDMS microchannels were created by replication from a master in polyvinyl chloride (PVC), with a pattern of six (80 μm depth, 1.4 cm length, 400 μm width) parallel channels, featuring circular reservoirs (diameter 400 μm) at both ends of each channel. PEEK tubes (UpChurch Scientific) were inserted in such reservoirs in order to connect the PDMS microfluidic cell to an Ismatec (Ismatec SA, Switzerland) peristaltic pump. The microfluidic device was assembled by fixing the PDMS mold on the SPRI gold chip surface (**Figure 5**). A refractive index (1.7200±0.0005) matching liquid (Cargille Laboratories, Inc.) was used to obtain the optical contact between the gold chip and the prism.

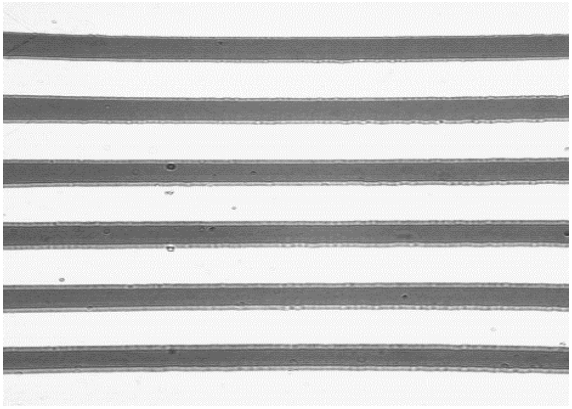

Figura 5. Representative SPRI image. The contrast was generated by the continuous flowing of PBS into the six parallel microchannels.

9.3. PNA probes and synthetic oligonucleotides sequences for the development of SPRI-based genosensors for the detection of *Staphylococcus Aureus* and *Listeria monocytogenes* in food

Sequences of PNA probes and synthetic oligonucleotides (**Table 3**) used for the selective detection of DNA target sequences from *S. Aureus* and *Listeria m.* were selected from sequences of the *S. Aureus* gene encoding the SEA and *Listeria m.* gene encoding the LLO, respectively.

Table 3. PNA and oligonucleotide sequences used for the experiments.

***Staphylococcus Aureus* sequences**	
PNA Sau	5'-$(AEEEA)_2$-TTATGGCTAGACG-3'
PNA Ctr	5'-$(AEEEA)_2$-CTCTACTAATTCC-3'
Target Sau	5'-ACCGTTTCCAAAGGTACTGTATTTTGTTTACCGTCTAGCCATAA-3'
DNA oligo Sau	5'-TACAGTACCTTTGGAAACGGT-Biotin TEG-3'
***Listeria monocytogenes* sequences**	
PNA Lm	5'-$(AEEEA)_2$-CCTAAGACGCCAATCGAA-3'
Target Lm	5'-CGATTTCATCCGCGTGTTTCTTTTCGATTGGCGTCTTAGG-3'
DNA oligo Lm	5'-GCGGATGAAATCG-Biotin TEG-3'
AEEEA={2-[2-(2-amino-ethoxy)-ethoxy]-ethoxy}-acetic acid	

In order to check for the specificity of the DNA target detection, a PNA unrelated sequence (PNA Ctr) was used as the negative control for *S. Aureus* detection, whereas *S. Aureus* gDNA was employed as the negative control for *Listeria m.* detection.

Figure 6 shows the region of *S. Aureus* Strain Mu50 (ATCC 700699D-5) gDNA that includes the Target Sau sequence.

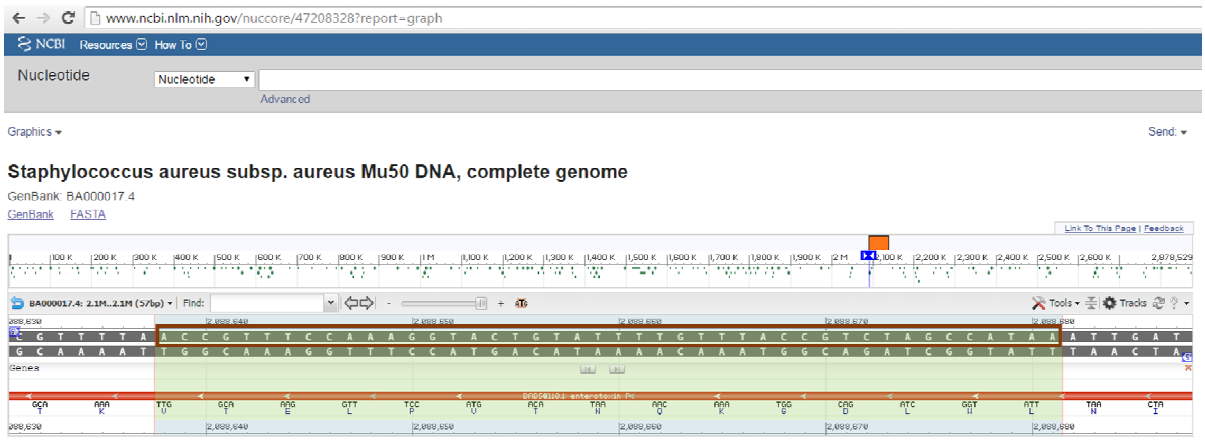

Figure 6. Target Sau sequence within the gDNA of *S. Aureus* Strain Mu50 (**Ref. 238**).

The *S. Aureus* Mu50 is a MRSA strain with vancomycin resistance[239] isolated in 1997.[240]

9.4. SPRI-based genosensors for the detection of *Staphylococcus Aureus* in food

9.4.1. *Staphylococcus Aureus* PNA probe surface immobilization

PNA probes were immobilized on gold sensors modified with DTSP (**Figure 7**), through an amine-coupling reaction between the *N*-hydroxysuccinimidylester ends of DTSP and the *N*-terminal group of the {*2*-[*2*-(*2*-amino-ethoxy)-ethoxy]-ethoxy}-acetic acid (AEEEA) linker of PNA probes. The probe immobilization was performed by using 0.1 μM PNA probes solutions in PBS (flow rate 10μL/min).

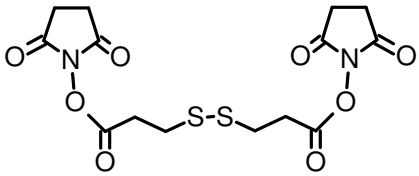

Figure 7. DTSP.

9.4.2. *Staphylococcus Aureus* ssDNA hybridization experiments

The SPRI hybridization experiments were performed at room temperature by using 300 μL of ssDNA solutions at concentrations 1, 50 and 100 fM which were adsorbed (flow rate 10 μL/min) on the PNA probes functionalized surfaces.

9.4.3. *Staphylococcus Aureus* gDNA hybridization experiments

The SPRI hybridization experiments were performed at room temperature by using 300 μL of gDNA solutions at concentrations 1, 50 and 100 fM which were allowed to flow (flow rate 10 μL/min) on the PNA probes functionalized surfaces. Before SPRI analyses gDNA samples were fragmented by sonication (ELMA Transsonic T480/H-2) for 2 minutes and by vortexing (IKA Vortex GENIUS 3) for 1 min and then they were heated to 95°C for 5 minutes to denature the DNA strands into single-stranded state.

9.4.4. *Staphylococcus Aureus* and bovine gDNA hybridization experiments

The SPRI hybridization experiments were performed at room temperature by using mixtures of bacterial and bovine gDNA. The total concentration of bacterial and bovine gDNAs was 5 ng/mL with different ratios between bovine and bacterial gDNA. Before SPRI analyses gDNA mixtures were fragmented by sonication (ELMA Transsonic T480/H-2) for 2 minutes and by vortexing (IKA Vortex GENIUS 3) for 1 min and then they were heated to 95°C for 5 minutes to denature the DNA strands.

9.4.5. Synthesis and functionalization of gold nanoparticles for *Staphylococcus Aureus* genomic DNA detection

AuNPs were synthesized by citrate reduction of $HAuCl_4 \cdot 3H_2O$ according to methods elsewhere described[241] and were functionalized with streptavidin. Streptavidin (like avidin) is a tetrameric protein with a high-affinity biotin-binding site (Kd ~ 10^{-15} M^{-1}) for each subunit.[242] Consequently, AuNPs were conjugated to the biotinylated DNA sequence according to procedures elsewhere described.[110]

Gold nanoparticles were characterized by UV-vis spectroscopy (NanodropTM 1000) and Dynamic Light Scattering (DLS) and Zeta Potential (ζ) measurements (Zetasizer Nano Series, Malvern Instruments).

9.5. SPRI-based genosensors for the detection of *Listeria monocytogenes* in food

9.5.1. *Listeria monocytogenes* PNA probe surface immobilization

PNA probes were immobilized on gold sensors modified with DTSP (**Figure 7**), through the amine-coupling reaction between the *N*-hydroxysuccinimidylester ends of DTSP and the *N*-terminal group present on the AEEEA linker. The probe immobilization was achieved by using 0.1 μM PNA probes solutions in PBS (flow rate 10μL/min).

9.5.2. *Listeria monocytogenes* gDNA hybridization experiments

The SPRI hybridization experiments were performed at room temperature by using 300 μL of gDNA solutions at concentrations 1, 10, 100 aM which were made to flow (flow rate 10 μL/min) on the PNA probes functionalized surfaces. Before SPRI analyses gDNA samples were fragmented by sonication (ELMA Transsonic T480/H-2) for 2 minutes and by vortexing (IKA Vortex GENIUS 3) for 1 min and then they were heated to 95°C for 5 minutes to denature the DNA strands.

9.5.3. Synthesis and functionalization of gold nanoparticles for *Listeria monocytogenes* genomic DNA detection

AuNPs were synthesized by citrate reduction of $HAuCl_4 \cdot 3H_2O$ according to methods elsewhere described[241] and were functionalized with streptavidin. Then, AuNPs were conjugated to the biotinylated oligonucleotide sequence.[110]

Gold nanoparticles were characterized by UV-vis spectroscopy (Expedeon VersaWave) and Dynamic Light Scattering (DLS) and Zeta Potential (ζ) measurements (Zetasizer Nano Series, Malvern Instruments).

9.6. SPRI-based immunosensors for the detection of Staphylococcal enterotoxin A (SEA) in food

9.6.1. SPRI sensor surface functionalization with methyl- and carboxy-thiol PEGylation reagents

The sensor surface was functionalized with Carboxy-PEG12-Thiol and Methyl-PEG4-Thiol (**Figure 8**) (ratio 1/10) by flowing the mixed thiol solution (2 mM total concentration in PBS) on the sensor surface for 30 minutes. Then carboxylic acid groups were activated for 7 minutes by using EDC 0.2 M and NHS 0.05 M.

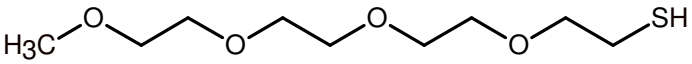

Methyl-PEG4-thiol

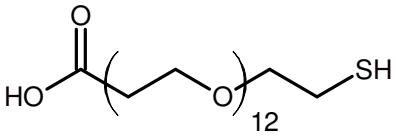

Carboxy-PEG12-thiol

Figure 8. Methyl-PEG4-thiol and Carboxy-PEG12-thiol.

9.6.2. SPRI sensor surface functionalization with *n*-dodecil mercaptano (NDM) and graphene oxide (GO)

The sensor surface was functionalized with SAM of NDM (**Figure 9**) (10 mM in ethanol for 24 hours). Then the substrate was immersed into GO solution (0.150 mg/mL) for 36 hours to favor the formation of GO sheets onto the SAM film. After removal from the GO solution, gold substrates were thoroughly rinsed with ultrapure water to remove GO unstably adsorbed on the film surface and dried with nitrogen gas. At that point, carboxyl groups of GO were activated with EDC 0.2 M and NHS 0.05 M on rocking platform shaker.

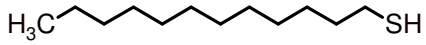

Figure 9. NDM.

9.6.3. SPRI sensor surface functionalization with DTSP

SPRI gold surfaces were functionalized with DTSP (**Figure 7**) by immersing gold substrates for 2 days into 4 mM solutions of DTSP in DMSO. After removal from the ethanolic solution, gold substrates were thoroughly rinsed with ultrapure water and ethanol and dried with nitrogen gas.

9.6.4. SPRI sensor surface immobilization of Anti *Staphylococcus aureus* enterotoxin A 2S7-F12 (Anti-SEA F12)

The SPRI immobilization experiments were carried out at room temperature by using antibody solutions at concentrations ranging from 0.05 to 40 µg/mL in PBS (flow rate 5 µL/min). After the antibody immobilization, reversibly bound species were removed from the surface by washing with buffer solution. Then, the unbound NHS esters were blocked by flowing ethanolamine hydrochloride 1 M pH =8.5 or mPEG 5000 4mM.

9.6.5. SPRI detection of staphylococcal enterotoxin A

Solutions of SEA at concentrations 36 nM, 9 nM, 1.8 nM , 180 pM, 18 pM and 0 pM were prepared in PBS from an aqueous stock solution 36 µM. These solutions were flowed for 30 min on the SPRI sensor surface and then the sensor was washed with PBS for 10 minutes.

Solution of SEA at concentrations 18 pM and 0.9 pM were prepared in PBS from an aqueous stock solution 36 µM. These solutions were flowed for 20 min on the SPRI sensor surface and then the sensing channels were rinsed with PBS for 10 minutes.

Solution of SEA at concentrations 1.8 nM and 180 pM were prepared in aqueous diluted milk solution from an aqueous stock solution 36 µM. These solutions were

flowed for 20 min on the SPRI sensor surface and then the sensor was washed with PBS for 10 minutes. The aqueous diluted milk solution was prepared as following: milk was diluted 20x in ultra-pure water and again 20x in ultra-pure water, and centrifuged for 45 minutes at 14000 rpm at 4◦C and then for 30 minutes at 14000 rpm at 4◦C to discard the fat. SEA-free aqueous diluted milk solutions were prepared in the same conditions, by considering therefore the same dilution ratios.

9.6.6. SPRI sandwich detection with Anti Staphylococcus aureus enterotoxin A 2S7-H5 (Anti-SEA H5)

A solution of detection antibody Anti-SEA H5 at concentration 30 μg/mL in PBS was allowed to flow over the sensor surface for 15 minutes (flow rate 10 μL/min). Then the sensing channels were rinsed with PBS for 10 minutes.

9.6.7. Synthesis and functionalization of gold nanoparticles for Staphylococcal enterotoxin A detection

AuNPs were synthesized by citrate reduction of HAuCl4·3H2O according to methods elsewhere described[238] and were characterized by UV-vis spectroscopy (NanodropTM 1000) and Dynamic Light Scattering (DLS) and Zeta Potential (ζ) measurements as described above.

Detection antibody-AuNPs conjugate was prepared according methods elsewhere described,[243,244] and was characterized by UV-vis spectroscopy (NanodropTM 1000). Briefly, AuNPs solution (125 μL) was added dropwise into the detection antibody solution (250 μL, 100 μg/mL in PBS pH=7.4), with gentle stirring. Then, the mixed solution was incubated at 37°C and centrifuged for 10 min at 6000 rpm and washed with PBS solution containing 1% BSA for 3 times.

The successful conjugation of AuNPs with the detection antibody was confirmed by UV-vis analysis (**Figure 10**). A shift of the band from 520 nm to 532 nm was

observed after conjugation of AuNPs with the detection antibody (AuNPs-Anti-SEA H5). The decrease of peak intensity of the plasmon band is due to nanoparticle concentration change during the workup of Anti-SEA H5/AuNPs conjugation.

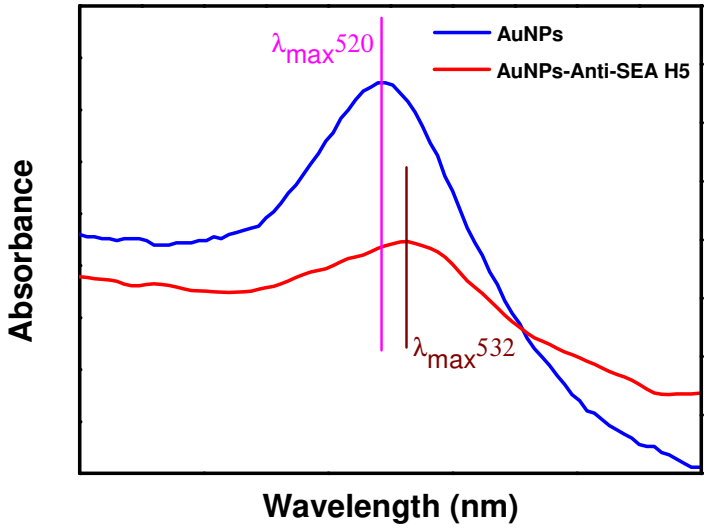

Figure 10. Uv-vis spectra of AuNPs before and after conjugation with the detection antibody (AuNPs and AuNPs-Anti-SEA H5, respectively).

9.6.8. SPRI sandwich detection with Anti Staphylococcus aureus enterotoxin A 2S7-H5 (Anti-SEA H5) and Anti Staphylococcus aureus enterotoxin A 2S7-H5 (Anti-SEA H5B)

Solutions of the detection antibodies Anti-SEA H5 and Anti-SEA H5B at concentration 10 µg/mL in PBS were allowed to flow over the sensor surface for 15 minutes (flow rate 10 µL/min). Then the sensing channels were rinsed with PBS for 10 minutes.

9.6.9. Gold nanoparticles for staphylococcal enterotoxin A detection in milk

AuNPs-SA NP solution at concentration 0.1 nM was prepared in PBS 1%, 0.1% Tween 20 from a stock solution 65.45 nM.

9.7. Antifouling surfaces development for SPRI biosensing

9.7.1. SPRI sensor surface functionalization with *11*-mercaptoundecanoin acid

MUA (**Figure 11**) monolayers on SPRI gold surface were prepared by immersing gold substrates for 24 hours into 40 mM solutions in ethanol. After removal from the ethanolic solution, gold substrates were thoroughly rinsed with ultrapure water and ethanol and dried with nitrogen gas. Then, the carboxyl groups were activated with EDC 0.2 M and NHS 0.05 M on rocking platform shaker. After the activation, the modified substrate was positioned onto the SPRI holder, interfaced with the microfluidic flow cell and used to study the immobilization of the Anti-*S. Aureus* and the subsequent interaction with milk.

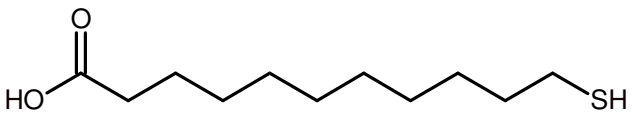

Figure 11. MUA.

9.7.2. SPRI sensor surface functionalization with Methyl- and Carboxy-Thiol PEGylation reagents

The sensor surface was functionalized with Carboxy-PEG12-Thiol and Methyl-PEG4-Thiol (**Figure 8**) (ratio 1/10) by flowing the mixed thiol solution (2 mM total concentration) on the sensor surface for 20 minutes. Then carboxylic acid groups were activated by using EDC 0.2 M and NHS 0.05 M.

9.7.3. SPRI sensor surface immobilization of Anti *Staphylococcus Aureus* Monoclonal Antibody

The SPRI immobilization experiments were carried out at room temperature by using Anti-*S. Aureus* solutions at concentrations 2, 6, 18 μg/mL in PBS (flow rate 10 μL/min).

After the antibody immobilization, reversibly bound species were removed from the surface by washing with buffer solution. Then, the unbound NHS esters were blocked by flowing TIZMA HCl 0.25 M.

9.7.4. SPRI sensor surface functionalization with Methoxy PEG disulfide (mPEG disulfide) and PEG NHS ester disulfide (NHS PEG disulfide)

The SPRI sensor surface was functionalized with mPEG disulfide (**Figure 12**) and NHS PEG disulfide (**Figure 13**) in different ratios (1/1, 10/1, 7/3) with a disulfide total concentration 2 mM in DMSO.

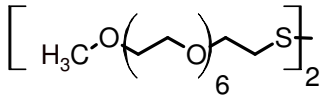

Figure 12. mPEG disulfide

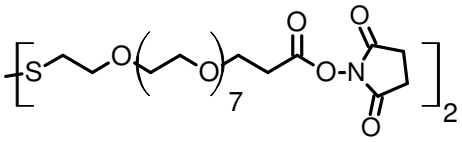

Figure 13. NHS PEG disulfide

9.7.5. SPRI sensor surface functionalization with PEG NHS ester disulfide (NHS PEG disulfide) and backfilling with Methoxy PEG disulfide (mPEG disulfide)

The SPRI sensor surface was functionalized with NHS PEG disulfide and backfilled with mPEG disulfide (0.2 mM in DMSO and 1 mM in DMSO, 1 mM in DMSO and 4 mM in DMSO, 0.5 mM in DMSO and 4.5 mM in DMSO, respectively).

9.7.6. Milk treatment

Milk was used as:

- undiluted;
- diluted 400x in PBS;
- centrifuged for 45 min;

- centrifuged for 45 min and diluted 400x in PBS;
- centrifuged for 45 min and again for 30 min;
- centrifuged for 45 min and again for 30 min and diluted 400x in PBS.

The centrifugation process was performed at 14000 rpm at 4◦C to discard the fat.

Two different types of milk were used: skimmed milk and whole milk.

10. RESULTS AND DISCUSSION

10.1. SPRI-based genosensors for the detection of *Staphylococcus Aureus* and *Listeria monocytogenes* in food

The detection of bacterial gDNA is a quite selective method for the identification of pathogens. Standard protocols used with this purpose involve the amplification of the target nucleic acid sequence in gDNA.[245] SPRI-based genosensors here described and developed to detect *S. Aureus* and *Listeria m.* gDNA allow to overcome limitations introduced by PCR amplification methods because they rely on non-amplified gDNA. SPRI genosensing has been obtained on the basis of a sandwich detection strategy (**Figure 14**).

The sensing method is based on the use of surface immobilized PNA probes. PNAs, introduced by Nielsen et al. in 1991, are DNA mimics in which the negatively charged phosphate deoxyribose backbone of natural nucleic acids is replaced by neutral *N*-(2-aminoethyl)glycine repeating units.[246]

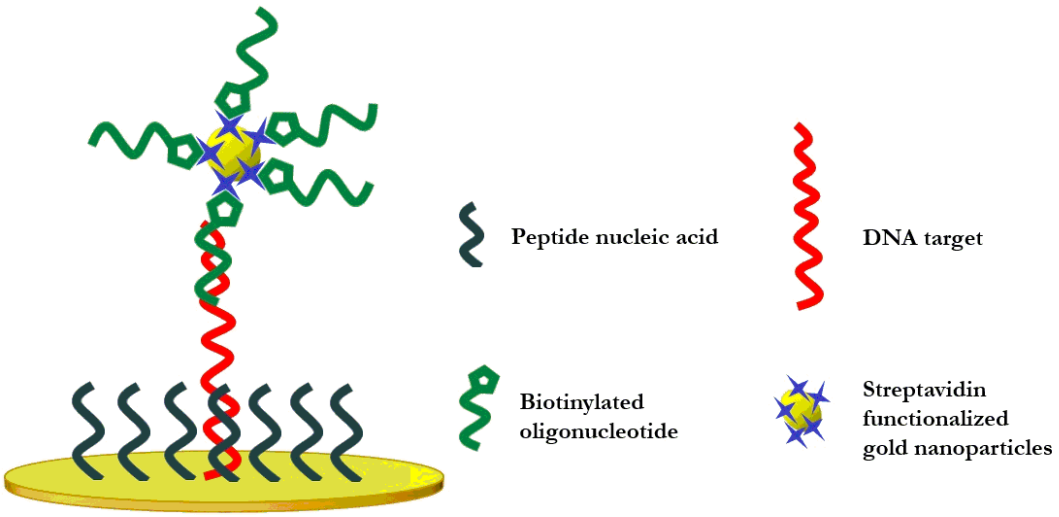

Figure 14. Pictorial description of the sandwich hybridization strategy used for the sensitive nanoparticle-enhanced SPRI detection of *S. Aureus* and *Listeria m.*.

The sandwich assay uses AuNPs conjugated to an oligonucleotide complementary to the final tract of the DNA target not involved in the hybridization with the SPRI sensor surface-immobilized PNA probe.

In order to develop effective genosensors for the detection of *S. Aureus* and *Listeria m.* gDNA, preliminary studies based on the use of oligonucleotide sequences were carried out. Then, the sensing strategy was successfully applied for the detection of bacterial gDNA, demonstrating the applicability of the sensing approach for the detection of pathogen gDNA extracted from contaminated food. It is worth considering that DNA isolated from pathogen contaminated food samples would include bacterial DNA from contaminating microorganism and, in some cases, also host DNA extracted from the high number of somatic cells.[247,248] In this respect, the detection of bacterial gDNA in the presence of bovine gDNA was also investigated, in order to mimic a DNA sample extracted from contaminated food matrix and also to test the selectivity of the developed genosensor.

PNA and oligonucleotide sequences used for the experiments were chosen accordingly to literature data[249,250] and were then optimized on the basis of studies carried out by considering gene sequences reported in the Nucleotide BLAST (Basic Local Alignment Search Tool)[251] and thermodynamic calculations of hybridization reactions performed with "The DINAMelt Web Server".[252]

An appropriate probe design and a suitable surface architecture are essential prerequisites to develop a selective and specific DNA biosensor. Sequence analysis and thermodynamic calculations are directed at reducing cross-hybridization between homologous sequences and at reaching higher thermodynamic stability of the complex formed with the target sequence. The presence of secondary structures interferes with the DNA hybridization reaction for which the efficiency of the detection process

decreases. The effect of secondary structures on hybridization reactions can be predicted by ΔG. In particular, low ΔG values results in the promotion of secondary structures and in a limitation of the extent of the hybridization between complementary ssDNA.[61] ΔG values related to PNA:DNA hybrids are shown in **Figure 15**. ΔG value for *S. Aureus* DNA hybridization with PNA Ctr is also displayed.

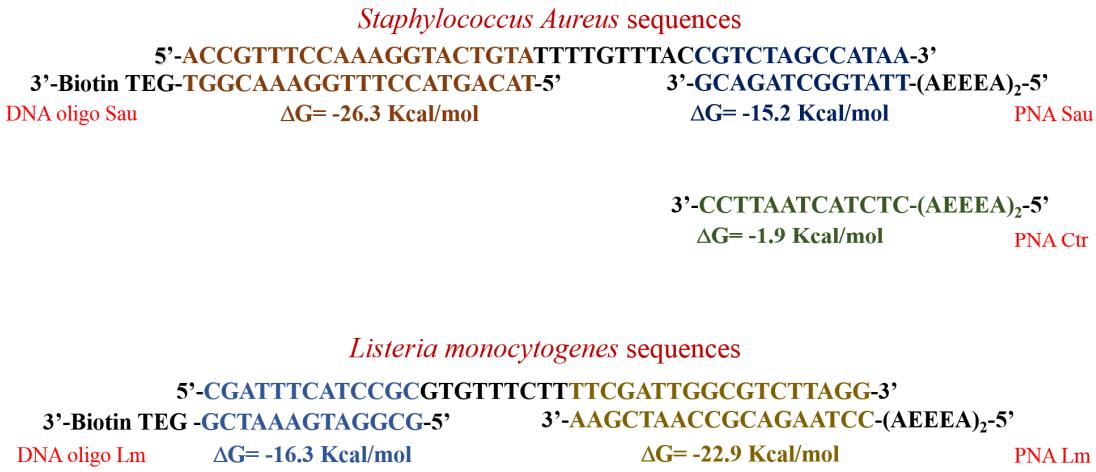

Figure 15. Hybridization reaction ΔG values of DNA target with PNA probes and oligonucleotides sequences.

ΔG values for the potential self-hybridization of the selected sequences are shown in **Figure 16**.

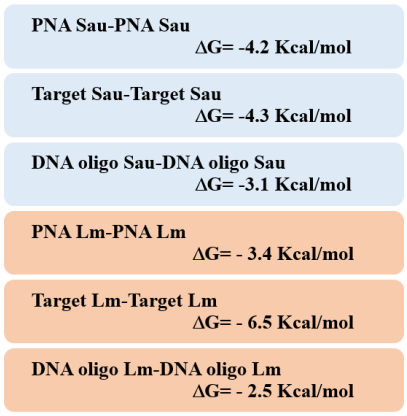

Figure 16. Hybridization reactions ΔG values of a sequence with itself.

DNA sequences immobilized on the surface influence the efficiency of DNA hybridization because of the electrostatic repulsion between the DNA strands

themselves. [253] Moreover, ionic strength, sequence composition and temperature affect surface hybridization.[254] PNA probes have been shown to hybridize to complementary DNA or RNA strands by normal Watson-Crick base pairing with higher affinity and specificity than normal oligonucleotide probes. In particular, PNAs offer many interesting features compared to DNA sequences for sensor-based hybridization applications:

-PNA/DNA and PNA/RNA complexes have enhanced thermal stability with respect to DNA/DNA and DNA/ RNA duplexes thanks to the lack of the electrostatic repulsion between the neutral PNA and charged DNA backbones;

-the high affinity of the PNA/DNA duplex reduces the limit of detection for DNA recognition;

- enhanced selectivity providing higher mismatch discrimination;

- enzymatic and chemical stability;

- hybridization is less susceptible to the presence of salts and PNA/DNA binding can be efficiently reached even under very low salt conditions. A similar independence from ionic strength makes the analytical procedures more robust, especially for complex matrices (e.g., foods).[255,256]

The uncharged nature of PNA probes gives important advantages to surface hybridization technologies such as SPR.[257] PNAs have been shown to contribute to the SPRI ultrasensitive detection of gDNA, allowing the fabrication of surfaces that efficiently immobilize gDNA fragments carrying the target sequence.

Optical features of AuNPs can be employed to monitor properties such as the concentration of the colloidal suspension, size of nanoparticles and their aggregation state.[258] AuNPs exhibit a strong absorption in the visible region, known as the surface

plasmon resonance (SPR) band. The increase in diameter of AuNPs increases the extinction coefficient and produces a red shift of the plasmon band.[259] Dynamic light scattering (DLS) is an useful analytical tool for evaluating the hydrodynamic radius, and size distribution. DLS can be also used to asses bioconjugation of AuNPs.

AuNPs are extraordinary light scatters at or near their surface plasmon resonance wavelength.[260] DLS techniques are 'hydrodynamic' techniques in that they directly measure hydrodynamic quantities (e.g. translational and/or rotational diffusion coefficients) which are related to sizes and shapes of nanostructures.[261] DLS data analysis yield the mean intensity-weighted size, commonly called Z-average diameter, and measure the broadness of the size distribution, polydispersity index or PDI. The latter parameter indicates the relative variance of the size polydispersity.[261]

Zeta (ζ-) potential is another important parameter that characterize nanoparticles.[262] ζ-potential is the electrostatic potential at the electrical double layer surrounding a nanoparticle in solution. Nanoparticles with a ζ-potential between −10 and +10 mV are considered approximately neutral, while nanoparticles with zeta potentials greater than +30 mV or less than −30 mV are strongly cationic or anionic, respectively.[263]

AuNPs synthesized for *S. Aureus* and *Listeria m.* detection exhibited a surface plasmon absorption band centered at 520 nm (**Figure 17**) and 517.8 nm (**Figure 18**), respectively. The band position was shifted to 524 nm (**Figure 17**) and 519.9 nm (**Figure 18**) after functionalization with streptavidin (AuNPs-SA) and to 528 nm (**Figure 17**) and 524.8 nm (**Figure 18**) after conjugation with the DNA oligo Sau (AuNPs-DNA oligo Sau) and DNA oligo Lm (AuNPs-DNA oligo Lm), respectively. The functionalization process didn't introduce a significant broadening of the UV-vis spectrum, thus suggesting the absence of aggregation processes. The change in the absorbance of the plasmon band that occurs after the AuNPs surface modification is

caused by the change in the concentration of the dispersion occurred during the workup of oligonucleotide-modified nanoparticles.

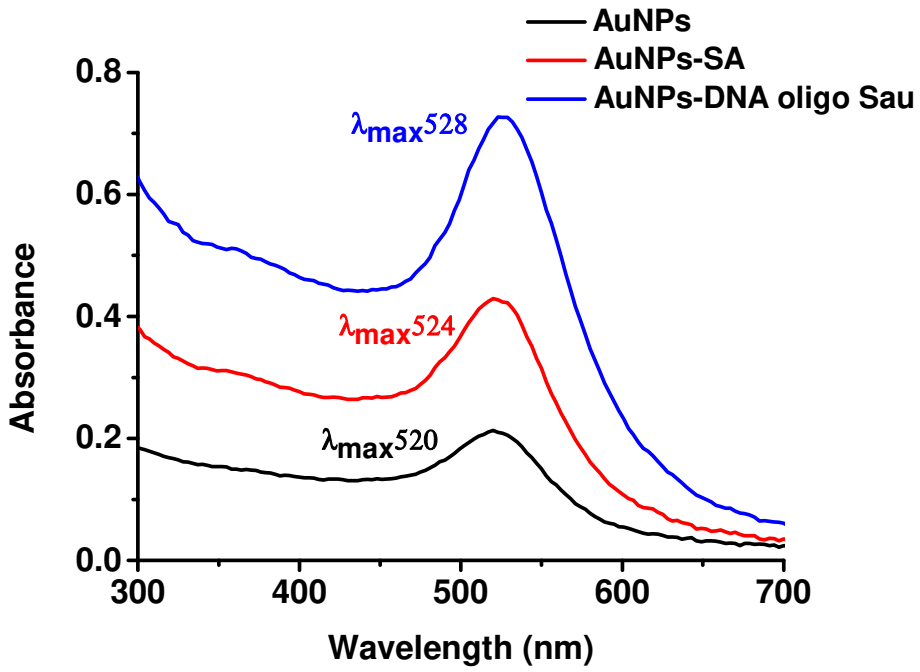

Figure 17. Absorption spectra of AuNPs functionalized with streptavidin (AuNPs-SA) and conjugated with DNA oligo Sau (AuNPs-DNA oligo Sau) for *S. Aureus* detection, acquired with NanodropTM 1000.

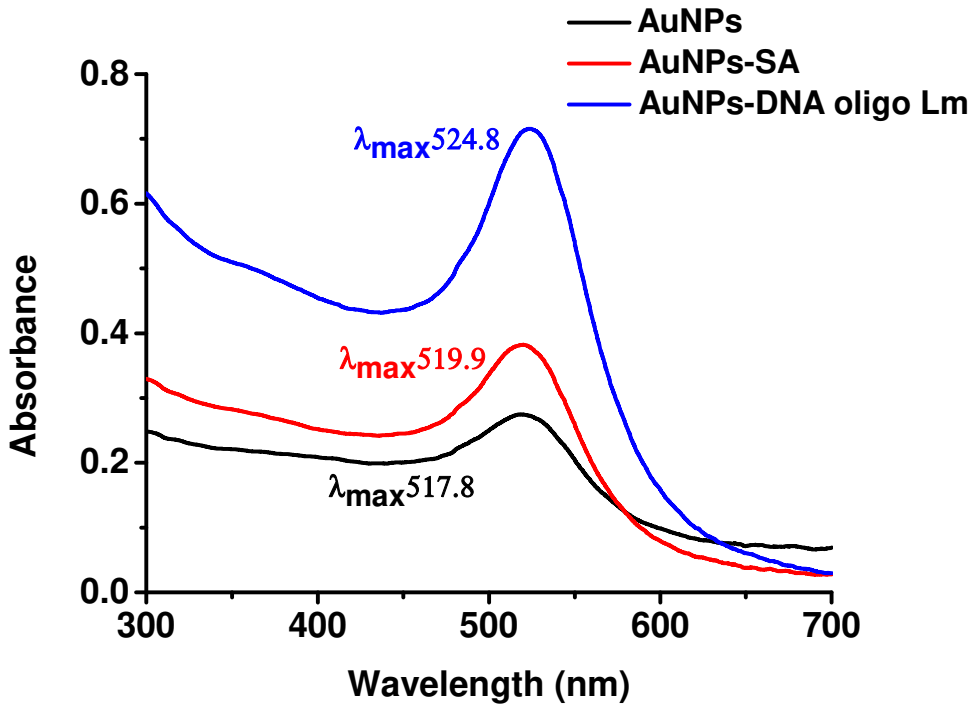

Figure 18. Absorption spectra of AuNPs functionalized with streptavidin (AuNPs-SA) and conjugated with DNA oligo Lm (AuNPs-DNA oligo Lm) for *Listeria m.* detection, acquired with Expedeon VersaWave.

DLS measurements (**Table 4** and **Table 5**) demonstrated that the synthesized AuNPs for *S. Aureus* and *Listeria m.* detection have a Z-average of 19.7 ± 0.4 nm (PDI =0.20) and 17.2 ± 0.3 nm (PDI = 0.16), respectively. The stability of AuNPs was evaluated by ζ-potential measurements. ζ-potential data (**Table 4** and **Table 5**) testifies the negatively charged surface of the AuNPs and their good stability in suspension. AuNPs were successfully coated with streptavidin as indicated by the Z-average increase and ζ-potential change (**Table 4** and **Table 5**). The latter demonstrate an increased of streptavidin-capped AuNPs compared with bare AuNPs. Also the successful conjugation of streptavidin-coated AuNPs with the biotinylated oligonucleotide is proved by the increase of Z-average. It is worth noticing that the decrease of ζ-potential measured after the functionalization with the biotinylated oligonucleotide is not a consequence of a destabilization of AuNPs-DNA oligo Sau

(**Table 4**) and AuNPs-DNA oligo Lm (**Table 5**) but reflects the shielding induced by the change of the buffer in which they are dispersed (PBS). The influence of the buffer is demonstrated by ζ-potentials of AuNPs-SA dispersed in H_2O and PBS reported in **Table 5**.

Table 4. Data from DLS and ζ-potential characterization of AuNPs functionalized with streptavidin (AuNPs-SA) and conjugated with DNA oligo Sau (AuNPs-DNA oligo Sau).

Sample	**Z aver. ± sd (nm)**	**PDI ± sd**	**ζ ± sd (mV)**
AuNPs	19.7 ± 0.4	0.20 ± 0.003	-42.3 ± 1.0[a]
AuNPs-SA	23.1 ± 0.4	0.40 ± 0.02	-49.3 ± 3.3[a]
AuNPs-DNA oligo Sau	44.8 ± 0.7	0.30 ± 0.03	-24.2 ± 1.1[b]

Note: a= in H_2O; b= in PBS.

Table 5. Data from DLS and ζ-potential characterization of AuNPs functionalized with streptavidin (AuNPs-SA) and conjugated with DNA oligo Sau (AuNPs-DNA oligo Lm).

Sample	**Z aver. ± sd (nm)**	**PDI ± sd**	**ζ ± sd (mV)**
AuNPs	17.2 ± 0.3	0.16 ± 0.017	-35.5 ± 1.9[a]
AuNPs-SA	30.6 ± 0.4	0.45 ± 0.076	-40.7 ± 2.9[a] -28.1 ± 1.5[b]
AuNPs-DNA oligo Lm	39.9 ± 0.4	0.35 ± 0.017	-27.5 ± 1.3[b]

Note: a= in H_2O; b= in PBS.

In order to perform preliminary studies with the oligonucleotide sequence related to *S. Aureus* DNA (Target Sau, **Table 3**), PNA Sau and Ctr probes were immobilized on gold sensor chips modified with DTSP. A dense surface immobilization of PNA probes affects the sensitivity of the detection of oligonucleotide.[264]

Figure 19 shows Δ%R over time obtained after the immobilization of PNA Sau and PNA Ctr probes (**Table 3**) on the gold SPRI surface. The experiments have been performed by using microfluidic devices with six parallel channels that allowed the parallel immobilization of PNA Sau and PNA Ctr probes.

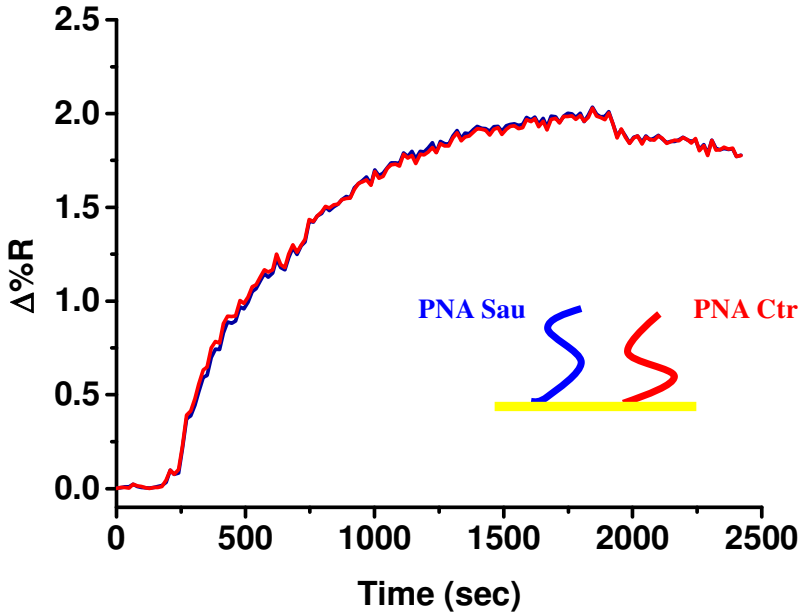

Figure 19. Representative time-dependent SPRI curves referring to the parallel immobilization of PNA Sau and PNA Ctr probes on the SPRI sensor surface.

The direct interaction of PNA probes with Target Sau (1 fM, 50 fM and 100 fM in concentration) produced no significant changes in the detected signal (**Figure 20**).

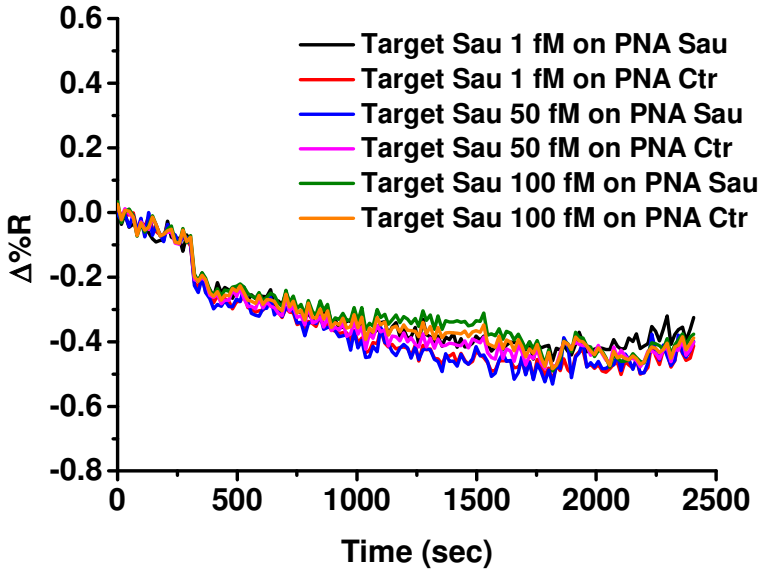

Figure 20. Time-dependent SPRI curves obtained after the direct hybridization of the Target Sau with the PNA probes immobilized on the sensor surface.

AuNPs-DNA oligo Sau, complementary to the final tract of the target sequence not involved in the hybridization with PNA probes, were used to produce a detectable signal, following the sandwich strategy described in **Figure 14**. By using this approach, AuNPs-DNA oligo Sau at concentration 0.5 nM were fluxed into the microchannels and significant increase of SPRI signals were attained, thus providing an indirect detection of the hybridization between the Target Sau and PNA probes immobilized on the surface. The specificity was checked by comparing the nanoparticle-enhanced SPRI response obtained from the specific PNA probe compared to the unrelated PNA sequence. **Figures 21, 22, 23** show representative SPRI responses generated after interaction of AuNPs-DNA oligo Sau with the Target Sau solutions having concentration 1fM, 50 fM and 100 fM, respectively.

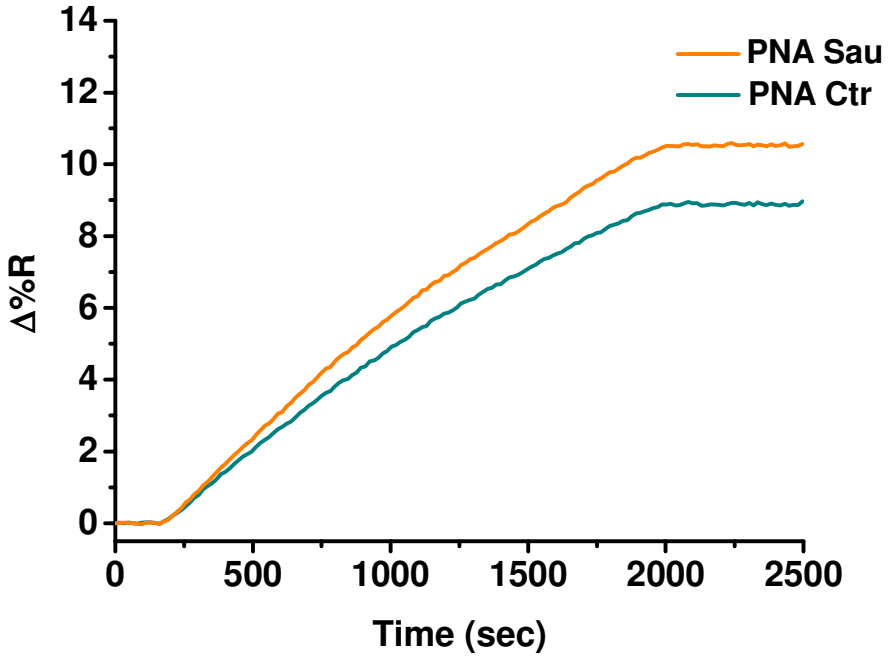

Figure 21. Time-dependent SPRI curves showing the nanoparticle-enhanced SPRI detection of Target Sau at concentration 1 fM.

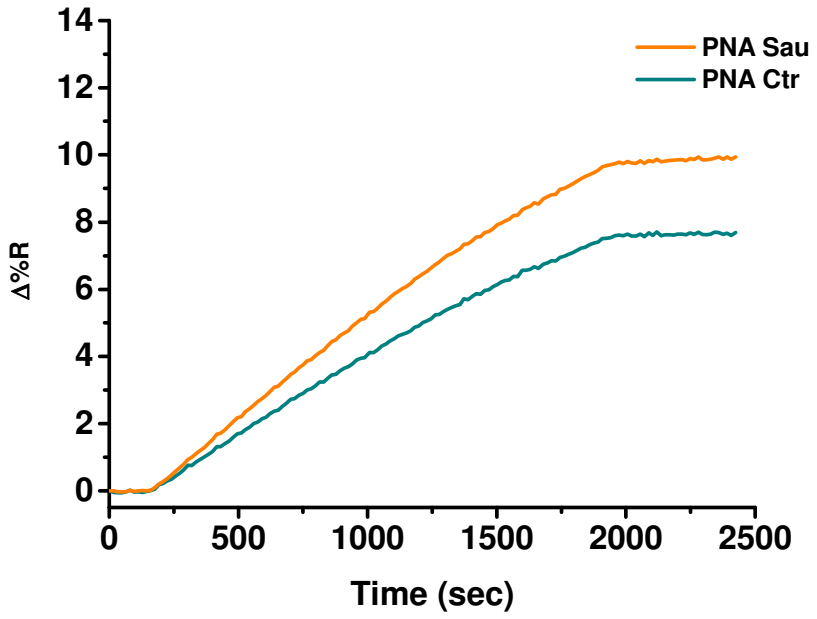

Figure 22. Time-dependent SPRI curves showing the nanoparticle-enhanced SPRI detection of Target Sau at concentration 50 fM.

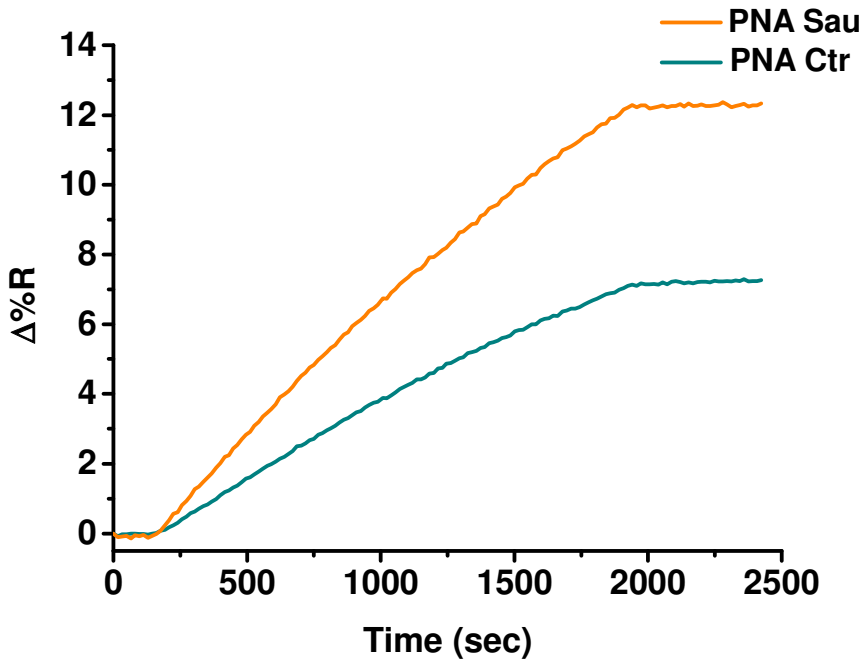

Figure 23. Time-dependent SPRI curves showing the nanoparticle-enhanced SPRI detection of Target Sau at concentration 100 fM.

Replicated independent experiments shows that SPRI responses are useful to discriminate between differently concentrated Target Sau solutions (1 fM, 50 fM and 100 fM). **Figure 24** shows data obtained from replicated experiments. Data are shown as the ratio between the Δ%R measured from the specific PNA Sau probe and the unrelated PNA Ctr probe after the nanoparticle-enhanced SPRI detection of Target Sau. Error bars represent mean confidence interval at 95% level.

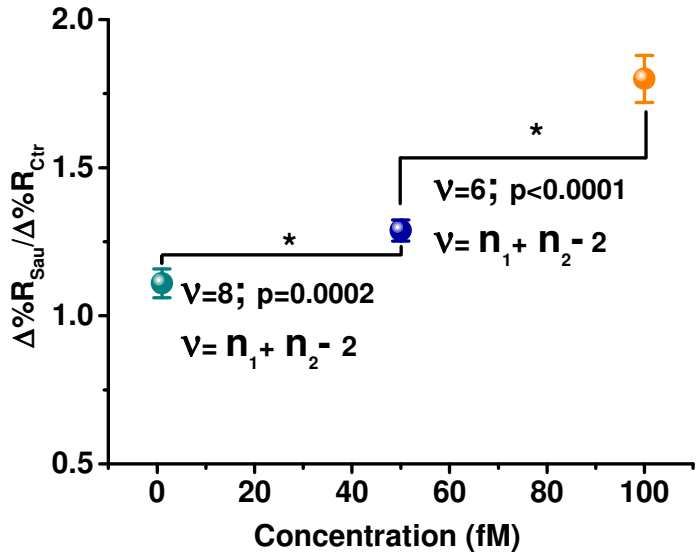

Figure 24. The mean of the ratios $\Delta\%R_{PNA\ Sau}/\Delta\%R_{PNA\ Ctr}$ as a function of concentration of Target Sau.

The mean $\Delta\%R_{PNA\ Sau}/\Delta\%R_{PNA\ Ctr}$ ratio ($\Delta\%R_{PNA\ Sau}/\Delta\%R_{PNA\ Ctr}$=1.11; SD=0.05; n=5 for target concentration 1 fM; $\Delta\%R_{PNA\ Sau}/\Delta\%R_{PNA\ Ctr}$=1.29; SD=0.04; n=5 for target concentration 50 fM; $\Delta\%R_{PNA\ Sau}/\Delta\%R_{PNA\ Ctr}$ =1.80; SD=0.08; n=3 for target concentration 50 fM) as a function of concentrations of the Target Sau solutions (1, 50 e 100 fM) were statistically different (t-test; 95% confidence interval).

SPRI data shows that the developed approach is useful to detect the selected DNA target sequence even at 1 fM concentration. The obtained results suggests that it would have been possible to use the same sandwich hybridization strategy for the detection of *S. Aureus* gDNA.

S. Aureus gDNA was expected to interact only with the PNA Sau, therefore different interactions were expected to be established between *S. Aureus* gDNA and PNA Sau or PNA Ctr.

The direct hybridization of PNA Sau probe with *S. Aureus* Strain Mu50 gDNA at concentration in the fM range produced no significant changes in the detected Δ%R (**Figure 25**).

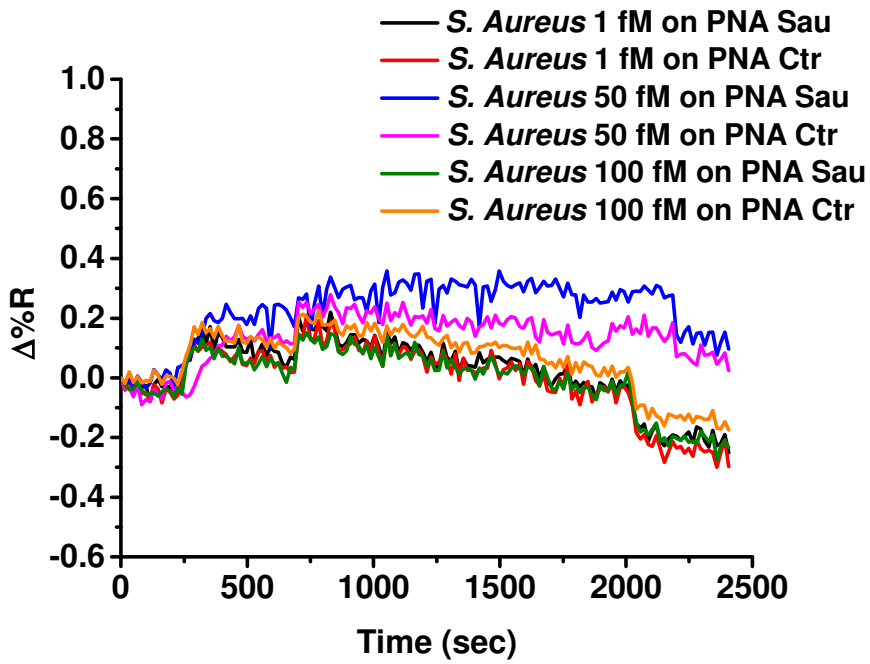

Figure 25. Time-dependent SPRI curves obtained after the direct hybridization of the *S. Aureus* gDNA with PNA probes immobilized on the sensor surface.

Also in this case, AuNPs-DNA oligo Sau were successfully employed to enhance the SPRI response by adopting the sandwich assay strategy depicted in **Figure 14**. In particular, 0.5 nM AuNPs-DNA oligo Sau were allowed to adsorb on the chip surface after the *S. Aureus* gDNA hybridization with PNA Sau and PNA Ctr probes, and a significant enhancement of the detected SPRI signal was achieved with a discrimination between signal generated by the PNA probes. The specificity was checked by comparing the nanoparticle-enhanced SPRI response detected from PNA Sau with that detected from PNA Ctr. **Figures 26, 27, 28** show representative SPRI responses obtained after interaction of AuNPs-DNA oligo Sau with the *S. Aureus* gDNA solutions 1 fM, 50 fM and 100 fM, respectively.

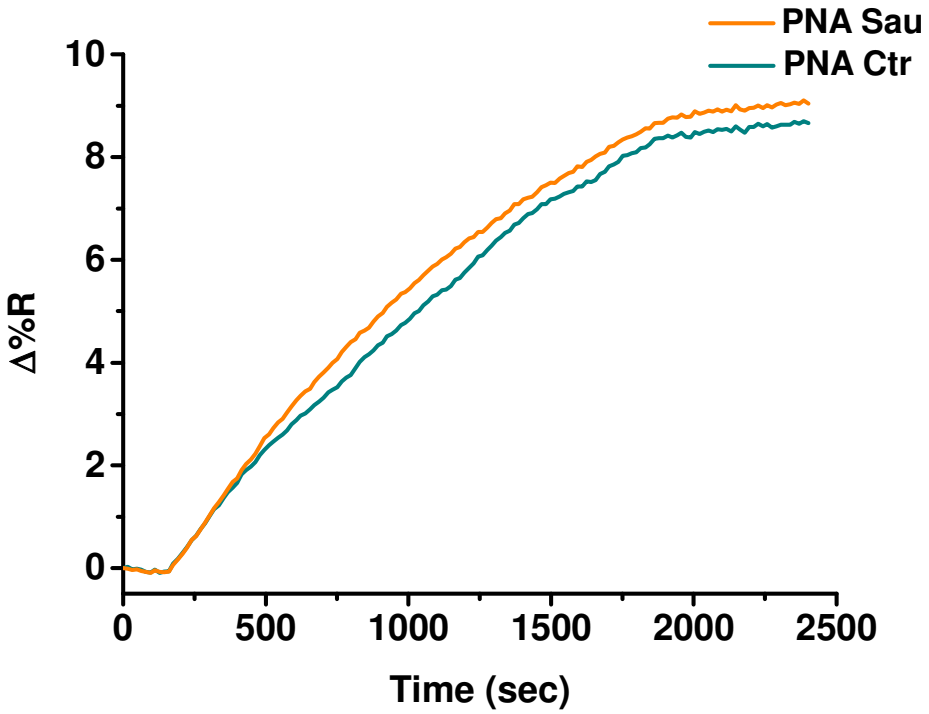

Figure 26. Time-dependent SPRI curves showing the nanoparticle-enhanced SPRI detection of *S. Aureus* gDNA at concentration 1 fM.

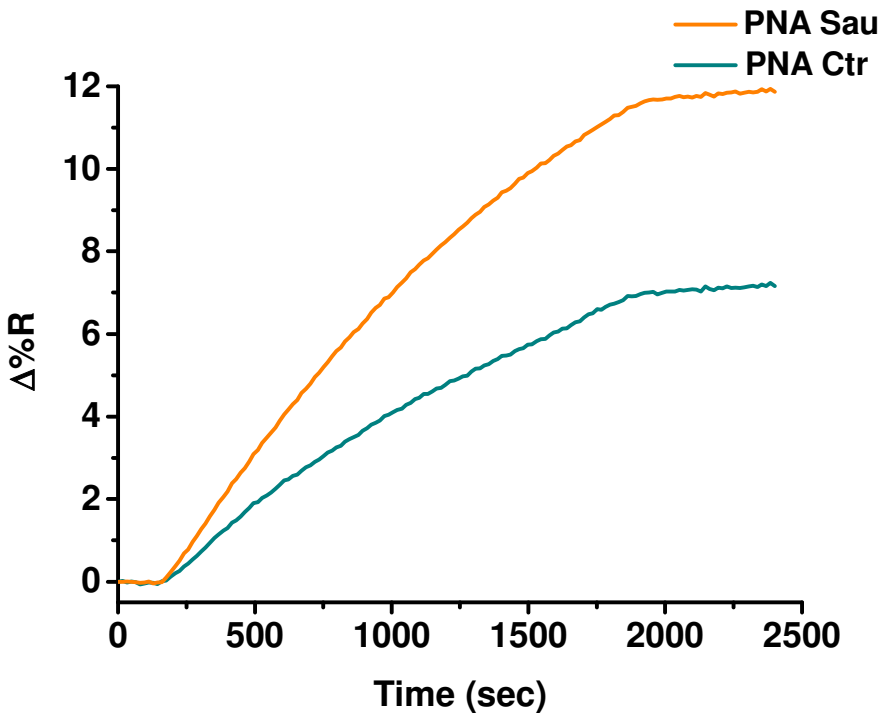

Figure 27. Time-dependent SPRI curves showing the nanoparticle-enhanced SPRI detection of *S. Aureus* gDNA at concentration 50 fM.

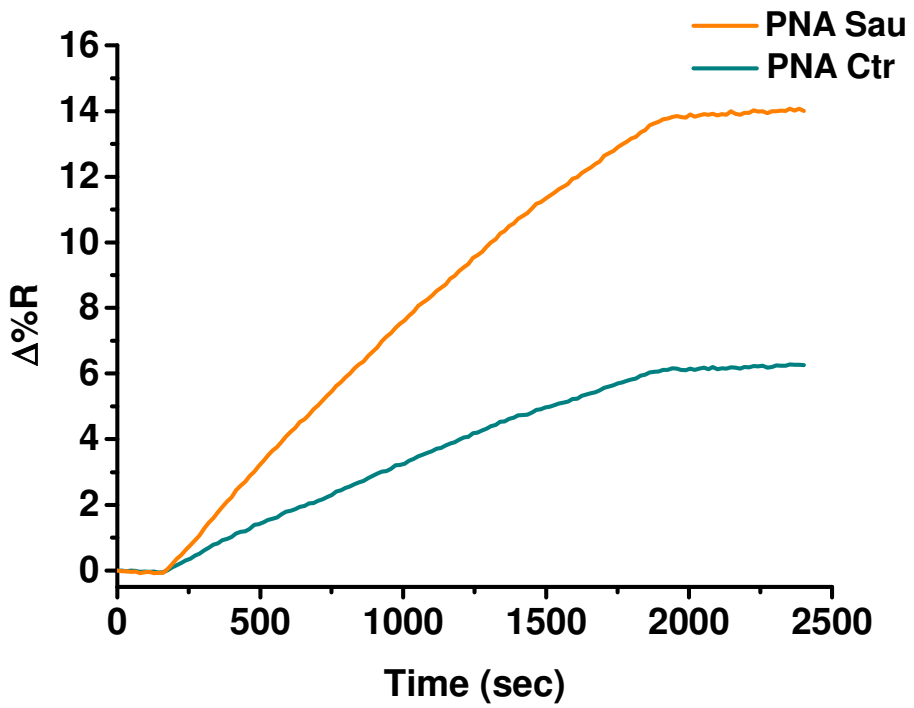

Figure 28. Time-dependent SPRI curves showing the nanoparticle-enhanced SPRI detection of *S. Aureus* gDNA at concentration 100 fM.

Replicated independent experiments showed that SPRI responses allowed us to discriminate between differently concentrated *S. Aureus* gDNA solutions (1 fM, 50 fM and 100 fM). In **Figure 29** data obtained from replicated experiments are summarized. Error bars represent mean confidence interval at 95% level.

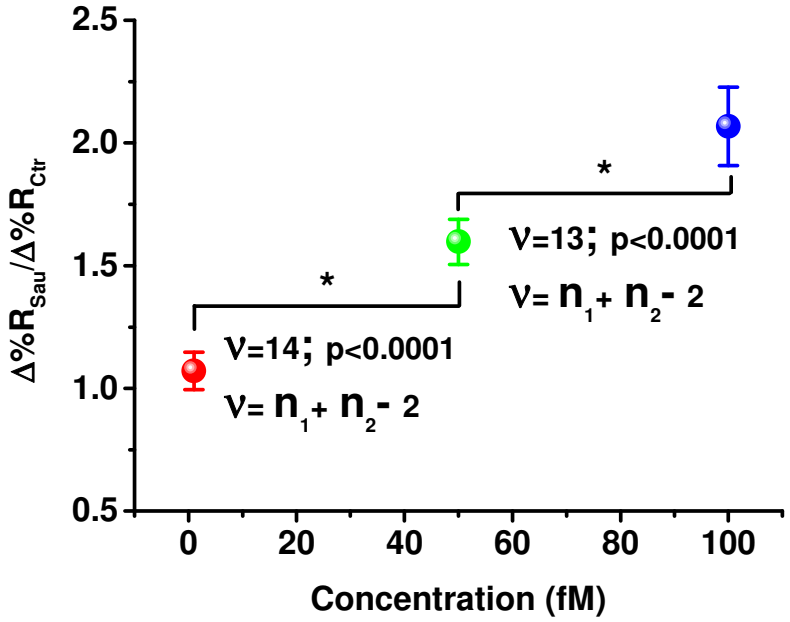

Figure 29. Mean of the ratio $\Delta\%R_{PNA\ Sau}$ /$\Delta\%R_{PNA\ Ctr}$ as a function of concentration of *S. Aureus* gDNA.

Means $\Delta\%R_{PNA\ Sau}$ /$\Delta\%R_{PNA\ Ctr}$ ratio ($\Delta\%R_{PNA\ Sau}/\Delta\%R_{PNA\ Ctr}$= 1.07; SD= 0.07; n=8 for gDNA concentration 1 fM; $\%R_{PNA\ Sau}/\Delta\%R_{PNA\ Ctr}$= 1.60; SD= 0.0; n=8 for gDNA concentration 50 fM; $\%R_{PNA\ Sau}/\Delta\%R_{PNA\ Ctr}$= 2.10; SD= 0.16; n=7 for gDNA concentration 100 fM) as a function of *S. Aureus* gDNA concentration (1 fM, 50 fM, 100 fM) were statistically different (t-test; 95% confidence interval).

The next point that was taken into account in SPRI *S. Aureus* genosensing development was the mixing of *S. Aureus* gDNA with bovine gDNA. Infact, as already discussed, DNAs extracted from milk includes both bacterial and bovine gDNA. Kits commercially available are designed in order to guarantee the large prevalence of bacterial gDNA.

The extraction of DNA is a multi-step process involving the cell lysis, the inactivation of cellular nucleases and the separation nucleic acids from other components of the cellular matrix.[265]

The quality of direct high-grade DNA isolation from the target pathogen in milk is depending from several factors:

-low pathogen DNA concentration in the food sample;

-low degree of cellular lysis;

- DNA binds to particulate material;

-the DNA may be degraded or sheared;

- sample processing method should efficiently lyses resistant bacterial cell walls without damaging target DNA. Such issue is particularly important for gram-positive bacteria such as *S. Aureus*.[266]

Each step in DNA isolation from food samples should be accurately evaluated in order to ensure an efficient pathogen DNA recovery. [267]

In order to assess the new SPRI performances in detecting gDNA mixtures of bacterial and bovine gDNA solutions were used. Mixtures were 5 ng/mL in concentration of total gDNA with different ratios between *S. Aureus* and bovine gDNAs (**Table 6).**

Table 6. *C*oncentrations and ratios of *Aureus* gDNA and Bovine gDNA in the analyzed mixtures.

S. Aureus gDNA/ Bovine gDNA ratio	*S. Aureus* gDNA-Bovine gDNA concentration	Total gDNA concentration
1/2	1.67 ng/mL-3.33 ng/mL	5 ng/mL
1/5	0.83 ng/mL-4.17 ng/mL	5 ng/mL
1/10	0.45 ng/mL-4.55 ng/mL	5 ng/mL

The Nucleotide Primer Blast[268] was used to check the simultaneous absence of sequences complementary to PNA Sau and DNA oligo Sau sequences (used to detect *S. Aureus* Strain Mu50) within the genome of the Bos Taurus sequence registered in

the National Center for Biotechnology Information (NCBI) database and no overlaps were found. In contrast, when the same search was performed against the *S. Aureus* Strain Mu50 genome sequence in the database the expected complementarity was found.

The study was carried out considering the PNA Sau sequence as both forward or reverse primer and the DNA oligo Sau as reverse or forward primer, respectively.

After PNA Sau and PNA Ctr probes immobilization on SPRI gold sensor surface, properly fragmented and denatured mixtures of bacterial and bovine gDNA were adsorbed on PNA modified-surfaces. As expected, no significant change in the detected signal was observed (**Figure 30**).

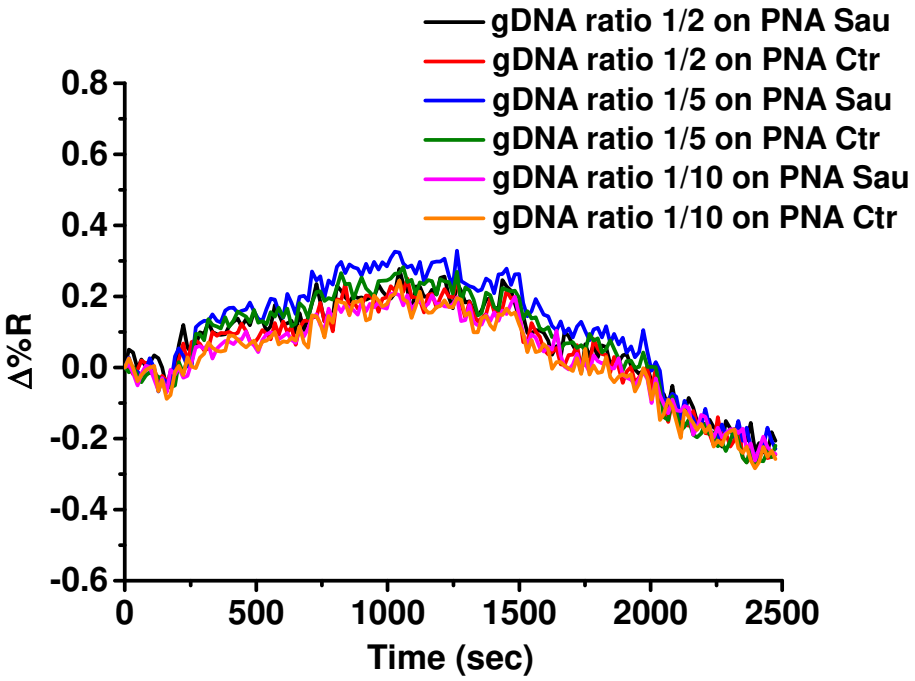

Figure 30. Time-dependent SPRI curves obtained after the direct hybridization of the mixtures of gDNA (total concentration 5 ng/mL) with PNA probes immobilized on the sensor surface.

Figures 31, **32** and **33** show time-dependent SPRI curves obtained after the AuNPs-DNA oligo Sau signal enhancement and showing the preferential

hybridization between PNA Sau and the bacterial gDNA component of the gDNA mixture.

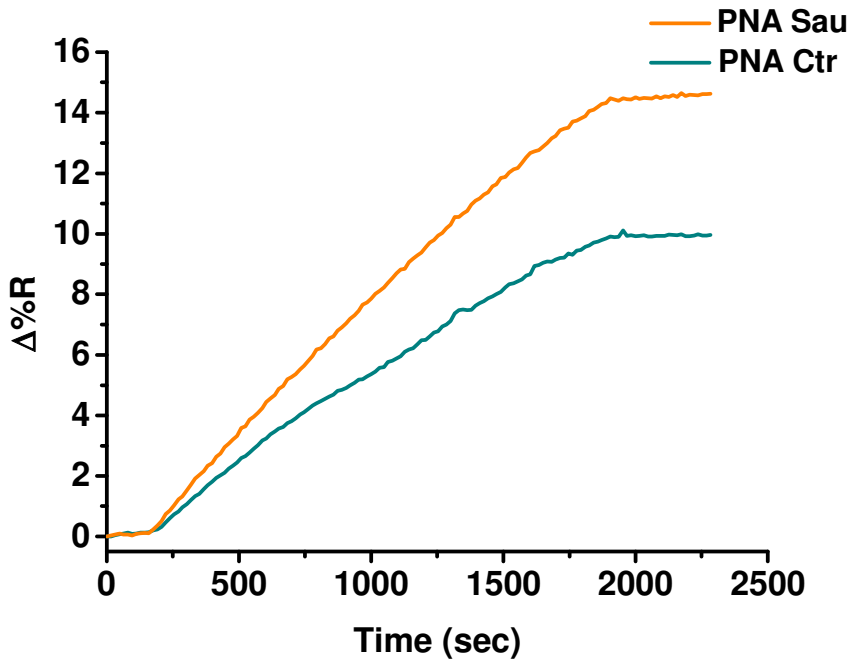

Figure 31. Time-dependent SPRI curves showing the nanoparticle-enhanced SPRI detection of *S. Aureus* in solution with bovine gDNA in ratio 1/2.

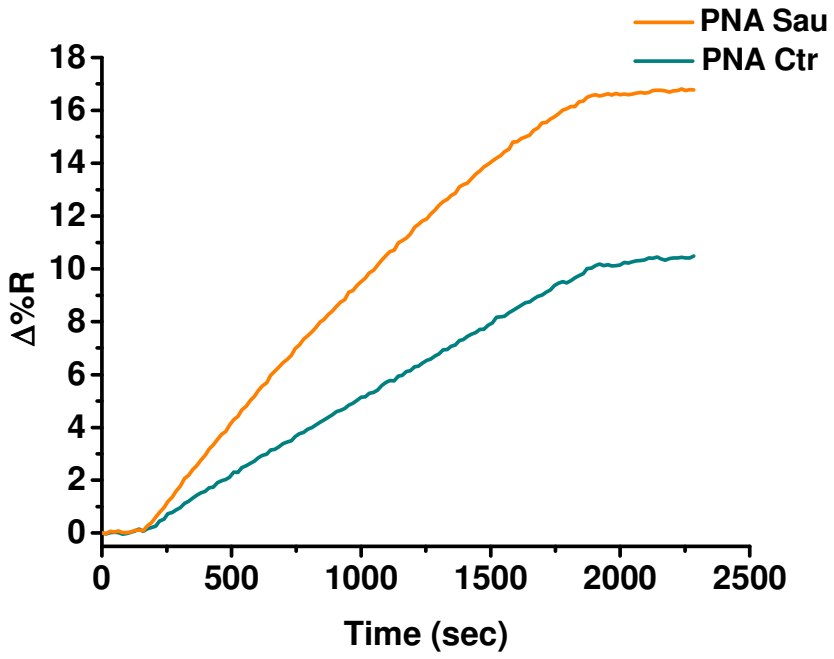

Figure 32. Time-dependent SPRI curves showing the nanoparticle-enhanced SPRI detection of *S. Aureus* in solution with bovine gDNA in ratio 1/5.

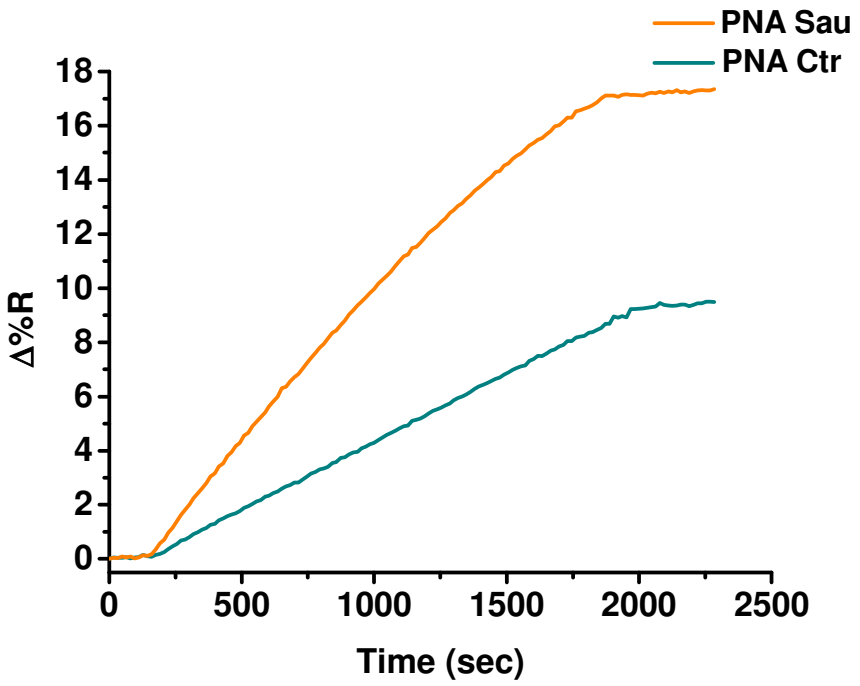

Figure 33. Time-dependent SPRI curves showing the nanoparticle-enhanced SPRI detection of *S. Aureus* in solution with bovine gDNA in ratio 1/10.

Replicated independent experiments shows that SPRI responses were useful to discriminate *S. Aureus* gDNA mixed in different ratios with bovine gDNA (**Figure 34**). In particular, mean $\Delta\%R_{PNA\ Sau}/\Delta\%R_{PNA\ Ctr}$ ratio values ($\%R_{PNA\ Sau}/\Delta\%R_{PNA\ Ctr}$= 1.32; SD= 0.08; n=5 for *S.Aureus* gDNA/Bovine gDNA ratio 1/2; $\%R_{PNA\ Sau}/\Delta\%R_{PNA\ Ctr}$= 1.65; SD= 0.08; n=5 for *S.Aureus* gDNA/Bovine gDNA ratio 1/5; $\Delta\%R_{PNA\ Sau}/\Delta\%R_{PNA\ Ctr}$= 2.07; SD= 0.02; n=5 for *S.Aureus* gDNA/Bovine gDNA ratio 1/10) as a function of *S.Aureus* gDNA/Bovine gDNA ratio (1/2, 1/5, 1/10) were statistically discriminated (t-test). Error bars represent mean confidence interval at 95% level.

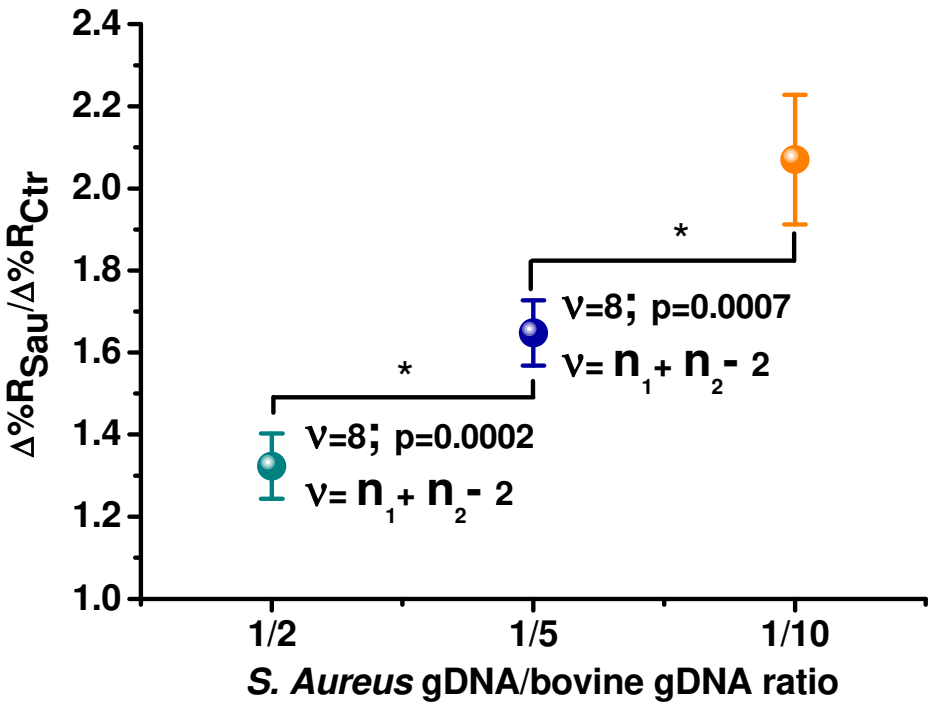

Figure 34. Mean of the $\Delta\%R_{PNA\ Sau}$ / $\Delta\%R_{PNA\ Ctr}$ ratios a function of *S. Aureus* gDNA/Bovine gDNA concentration ratio (1/10, 1/5, 1/2). Total gDNA concentration 5 ng/mL

SPRI data confirm the capability of the developed genosensor to discriminate between pathogen and bovine gDNA in differently concentrated mixed gDNA solutions, allowing the detection *of S. Aureus* gDNA in the mixture 0.45 ng/mL (237 aM) at concentration.

In order to further prove the versatility and applicability of the proposed sensing approach for the detection of gDNA from foodborne pathogen contaminated food, the same analytical approach was used to detect *Listeria m.* gDNA.

PNA Lm probes (**Table 3**) were immobilized on SPRI gold chip surface modified with DTSP (**Figure 35**), as outlined above.

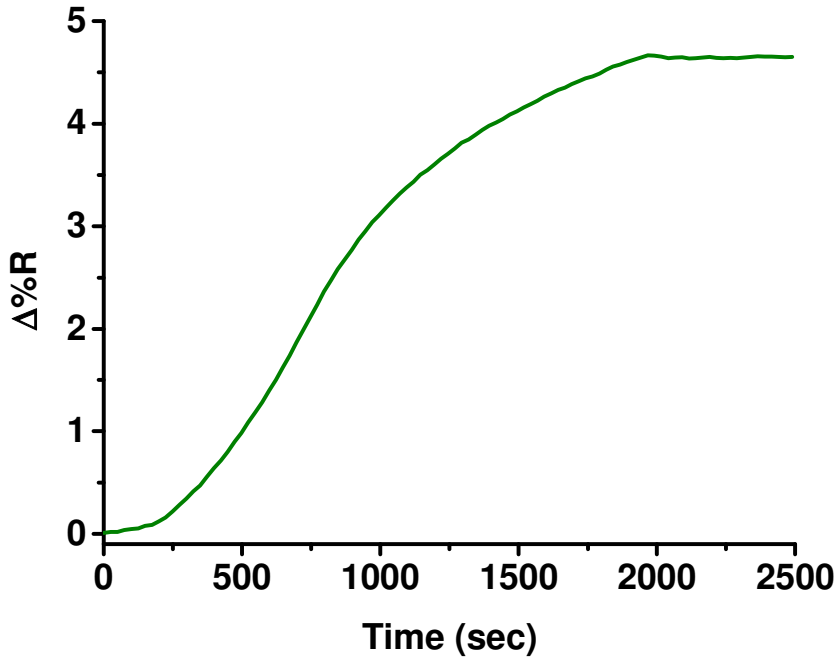

Figure 35. Representative time-dependent SPRI curve referring to the parallel immobilization of PNA Lm probe on the SPRI sensor surface.

Then, *Listeria m.* Strain EGDe gDNA and *S. Aureus* Strain Mu50 gDNA (concentrations 1, 10 and 100 aM) were allowed to flow on PNA Lm functionalized sensor chip. *S. Aureus* gDNA was expected not to interact with the immobilized PNA probes whose sequence was specifically designed to detect *Listeria m.* The detected SPRI responses were also in this occasion close to the instrumental noise (data not shown). AuNPs-enhanced SPRI signal allowed discrimination between differently concentrated *Listeria m.* gDNA solutions from *S. Aureus* gDNA solutions (1 aM, 10 aM and 100 aM) (**Figure 36**).

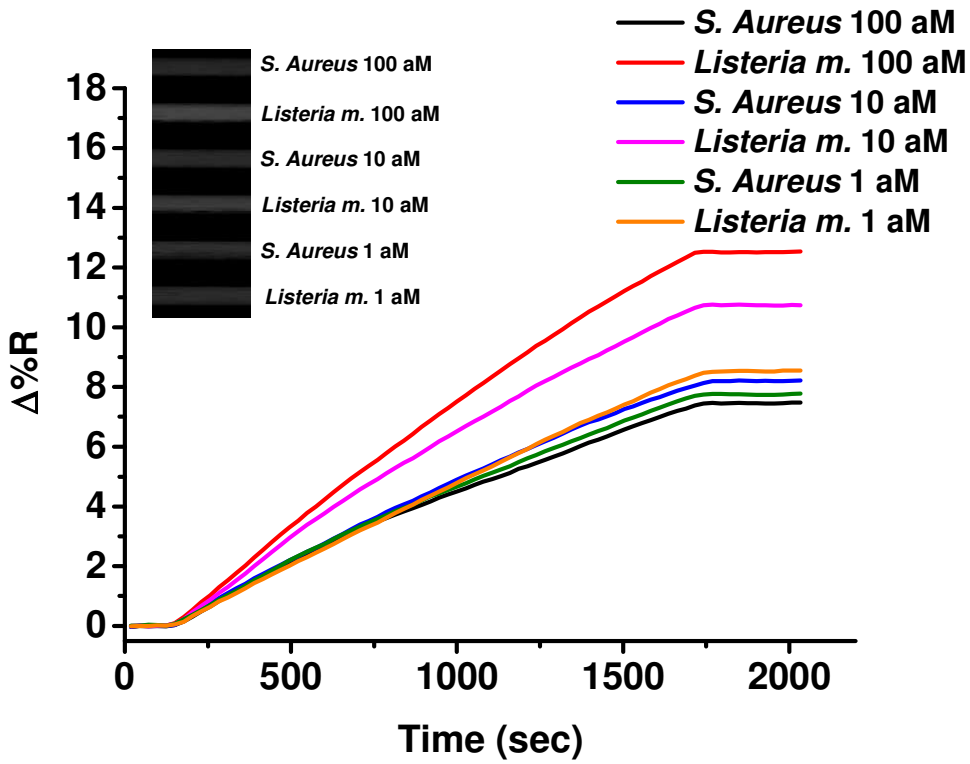

Figure 36. Representative time-dependent SPRI curves showing the nanoparticle-enhanced SPRI detection of 1, 10 and 100 aM *Listeria m.* gDNA solutions. A representative SPRI difference image of the gDNA parallel detection is also shown.

Data obtained from replicated experiments are shown in **Figure 37**. Data are shown as the ratio between the Δ%R detected after AuNPs-DNA oligo Lm-enhanced SPRI detection of *Listeria m.* gDNA/PNA Lm interaction ($\Delta\%R_{gDNA\ Lm}$) and the Δ%R measured after the *S. Aureus* gDNA/PNA Lm interaction ($\Delta\%R_{gDNA\ Sau}$). Mean $\Delta\%R_{gDNA\ Lm}/\Delta\%R_{gDNA\ Sau}$ ratio values ($\Delta\%R_{gDNA\ Lm}/\Delta\%R_{gDNA\ Sau}$ = 1.06; SD=0.03; n=4 for gDNA concentration 1 aM; $\Delta\%R_{gDNA\ Lm}/\Delta\%R_{gDNA\ Sau}$ = 1.37; SD= 0.06; n= 3 for gDNA concentration 10 aM; $\Delta\%R_{gDNA\ Lm}/\Delta\%R_{gDNA\ Sau}$ = 1.74; SD= 0.11; n= 3 for gDNA concentration 100 aM) as a function of the gDNA concentration were statistically different (t-test; 95% confidence interval).

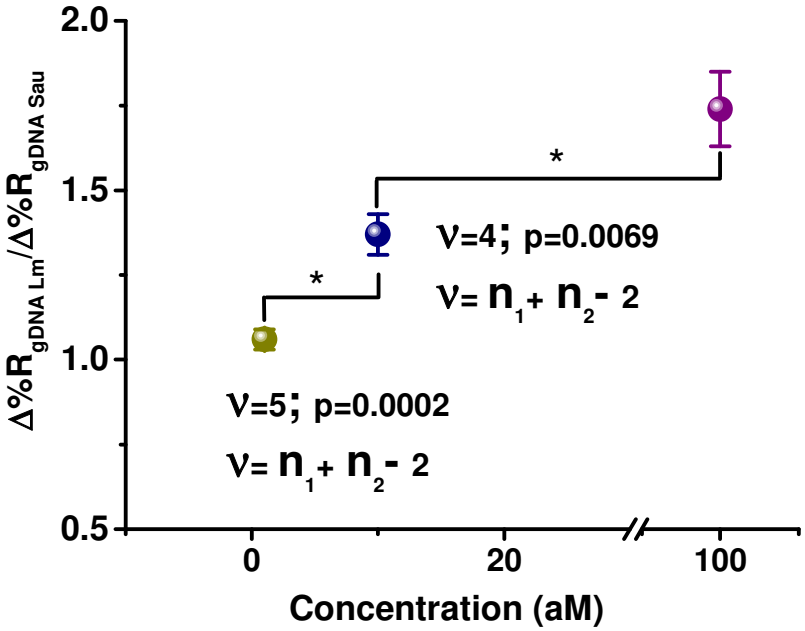

Figure 37. Mean of the ratio $\Delta\%R_{gDNA\ Lm}/\Delta\%R_{gDNA\ Sau}$ as a function of gDNA concentration (1 aM, 10 aM and 100 aM). Error bars represent mean confidence interval at 95% level.

10.2. SPRI-based immunosensors for the detection of staphylococcal enterotoxin A (SEA) in food

In order to develop SPRI immunosensors to be used for the detection of SEA, a sandwich strategy (**Figure 38**) was adopted for detection of SEA in PBS and a direct approach (**Figure 39**) was instead applied for SEA detection in milk samples.

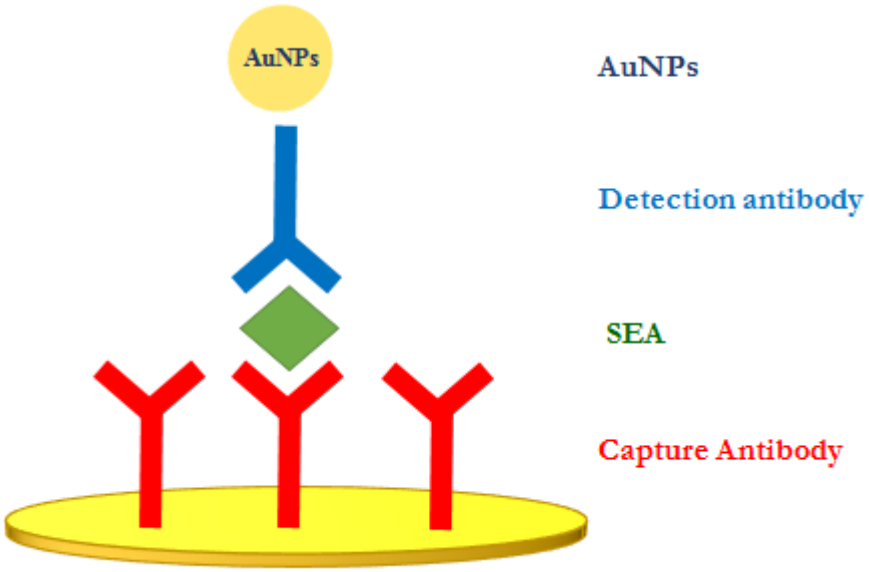

Figure 38. Pictorial description of the sandwich strategy used for the SPRI detection of the SEA in PBS.

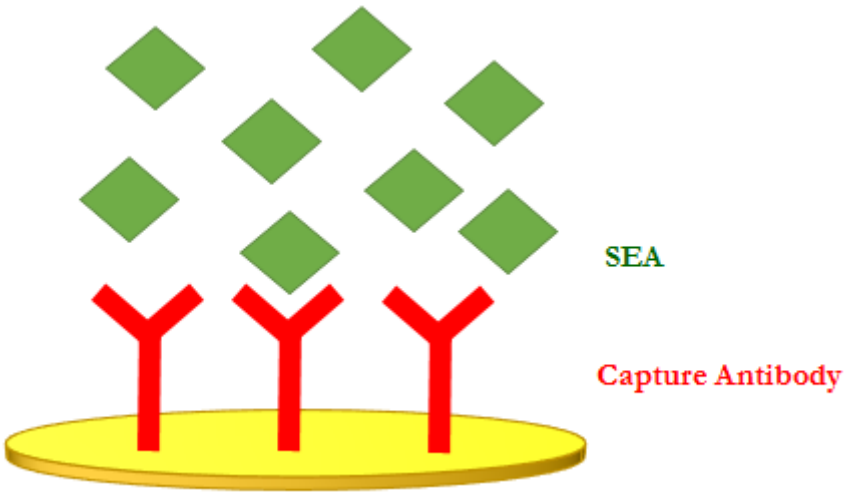

Figure 39. Pictorial description of the direct strategy used for the SPRI detection of the SEA in milk.

The assay strategy was based on the use of the following specific mouse anti *Staphylococcus aureus* Enterotoxin type A monoclonal antibodies:

- Clone F12 for the capture (Anti-SEA F12);
- Clone H5 for the detection (Anti-SEA H5);
- Clone H5 biotinylated for the detection (Anti-SEA H5B).

Different surface functionalization procedures of SPRI gold sensors have been tested in order to efficiently immobilize capture antibody. Immobilized antibodies should preserve the ability to bind analytes by assuring the highly sensitive detection and reproducible performances. It is well known that the geometry of the SPR sensor surface on which receptors are immobilized considerably affects the detection sensitivity and specificity. Not appropriate geometries negatively impact on the detection by concurring to non-specific adsorption of chemical compounds on the sensor surface.[269]

Thiol and dithiol SAMs on metals, and in particular on gold, have attracted great attention thanks to their easy preparation and their relatively high stability mediated by the strength of the S–Au bond and by van der Waals interactions.[270] Gold substrates functionalized with SAMs have been extensively employed for SPR detection.

In our case, SPRI gold sensors were functionalized with a mixture of methyl- and carboxy-thiol PEGylation reagents (Methyl-PEG4-Thiol and Carboxy-PEG12-Thiol) (**Figure 40**), *n*-dodecil mercaptano (NDM)/graphene oxide (GO) (NDM/GO) (**Figure 41**) or DTSP (**Figure 7**).

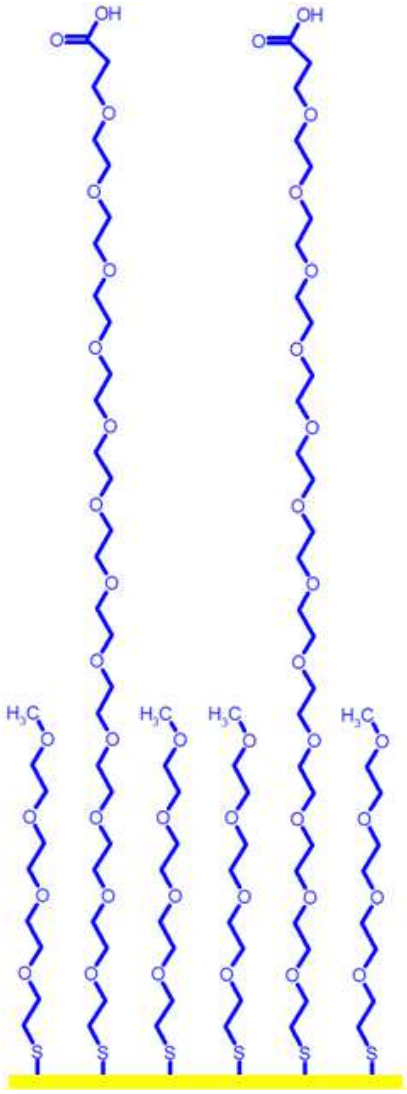

Figure 40. Surface modification with mixed Carboxy-PEG12-Thiol and Methyl-PEG4-Thiol.

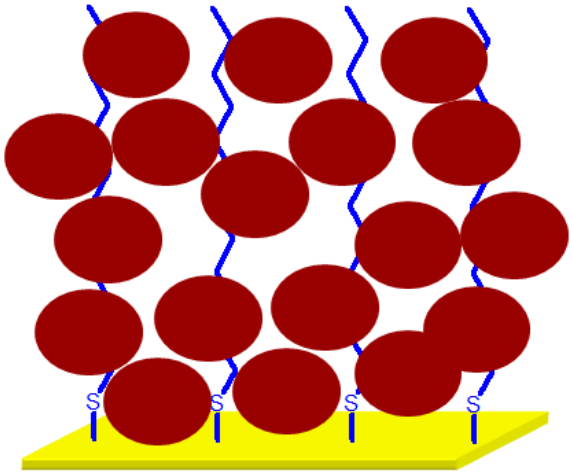

Figure 41. Surface modification with NDM/GO.

Carboxyl groups of Carboxy-PEG12-Thiol and GO were activated with EDC and NHS. After the activation, the modified substrate was used to study the immobilization of the antibody.

Figure 42 refers to the SPRI signal detected during the sensor surface modification with Carboxy-PEG12-Thiol and Methyl-PEG4-Thiol mixture (ratio 1/10) and the subsequent activation of surface carboxylic acid groups with EDC/NHS.

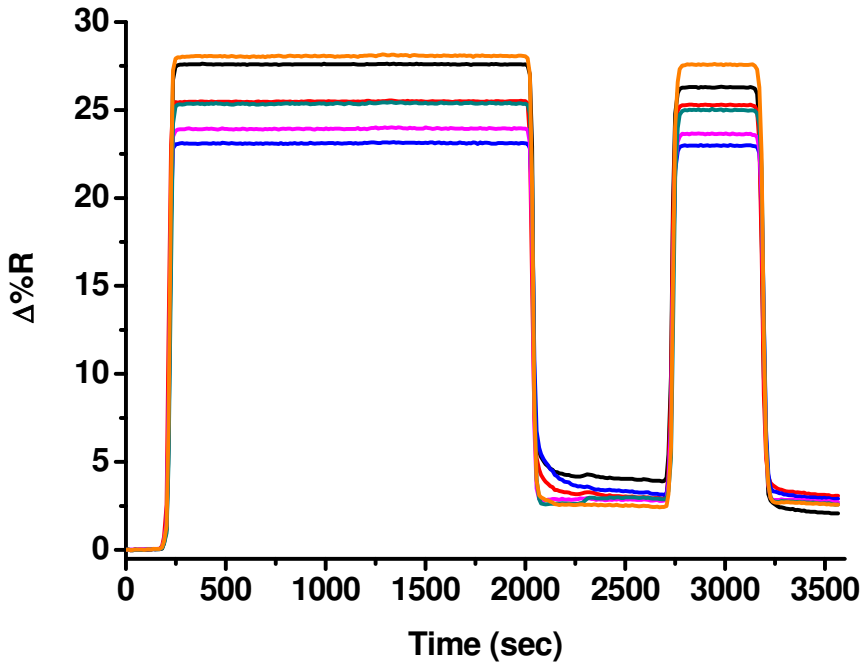

Figure 42. Time-dependent SPRI curves showing sensor surface functionalization with Carboxy-PEG12-Thiol and Methyl-PEG4-Thiol and subsequently activation of carboxylic groups with EDC/NHS.

Anti-SEA F12 (concentrations ranging from 0.05 to 40 µg/mL in PBS pH=7.4) was adsorbed on the functionalized surface and unreacted NHS ester groups were deactivated by using ethanolamine hydrochloride 1 M pH =8.5 (**Figure 43**).

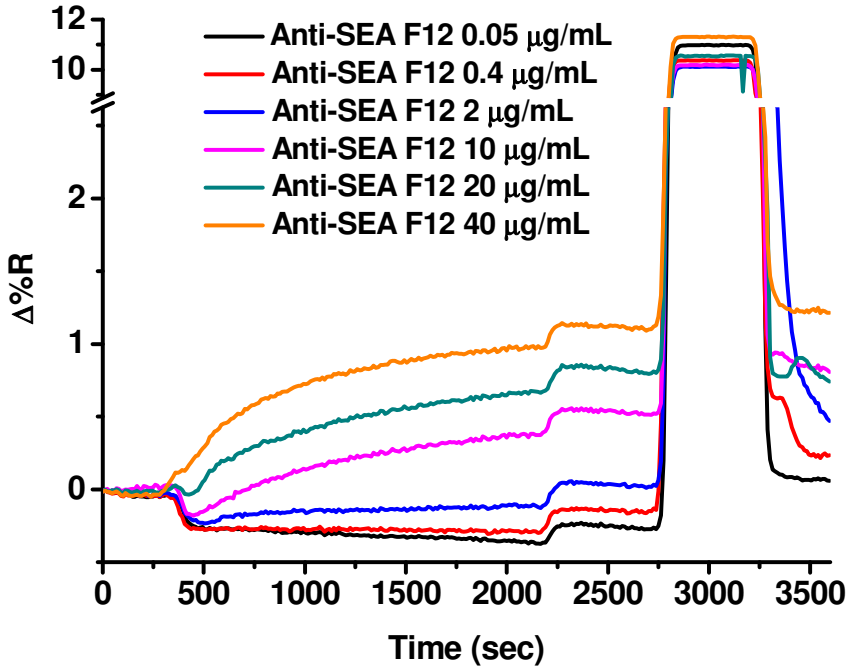

Figure 43. Time-dependent SPRI curves obtained after the immobilization of Anti-SEA F12 (solution concentrations ranging from 0.05 to 40 µg/mL in PBS pH=7.4) on SPRI surface modified with Carboxy-PEG12-Thiol and Methyl-PEG4-Thiol and deactivation of unreacted NHS groups.

Optimal conditions for Anti-SEA F12 immobilization were investigated by varying the antibody solution concentration (**Figure 43**) and 20 µg/mL was selected as the optimal concentration to be used for subsequent experiments.

Time-dependent SPRI curves obtained after the immobilization of Anti-SEA F12 (20 µg/mL) on NDM/GO-activated gold surface and the subsequent deactivation of unreacted groups NHS groups are displayed in **Figure 44**.

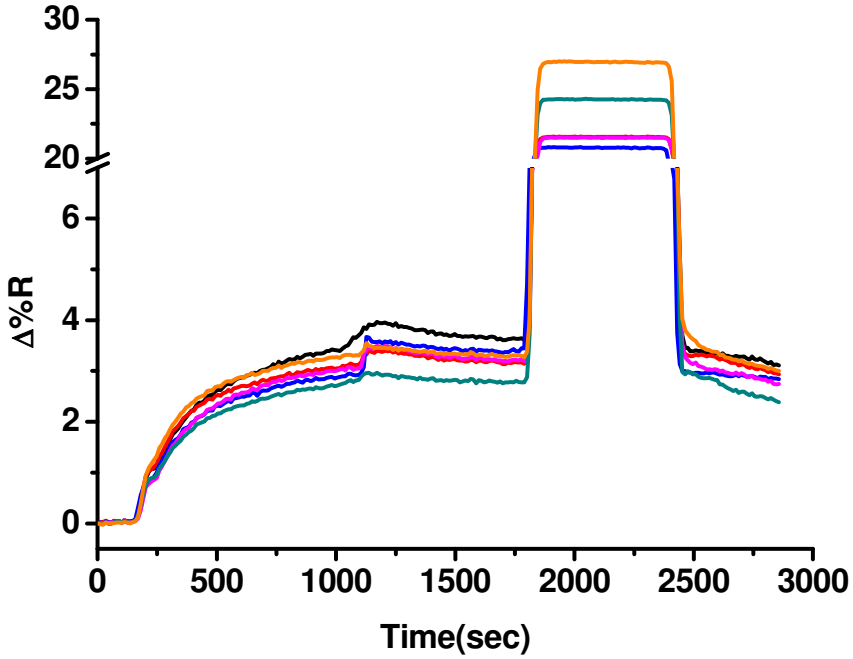

Figure 44. Time-dependent SPRI curves obtained after the immobilization of Anti-SEA F12 on NDM/GO-modified sensor surface and deactivation of unreacted NHS groups.

GO consists of a hexagonal ring-based carbon network having both sp2-hybridized carbon atoms and sp3-hybridized carbons bringing hydroxyl and epoxide functional groups on either side of the sheet, while the sheet edges are typically adorned by carboxyl and carbonyl groups.[271] In recent years, graphene oxide has attained remarkable interest in SPR biosensing.[272,273,274,275,276]

Moving to sensor substrates functionalized with the DTSP, the Anti-SEA F12 immobilization (20 μg/mL in PBS) generated an SPRI response higher than that generated when PEG or NDM/GO modified substrates were used (**Figure 45**).

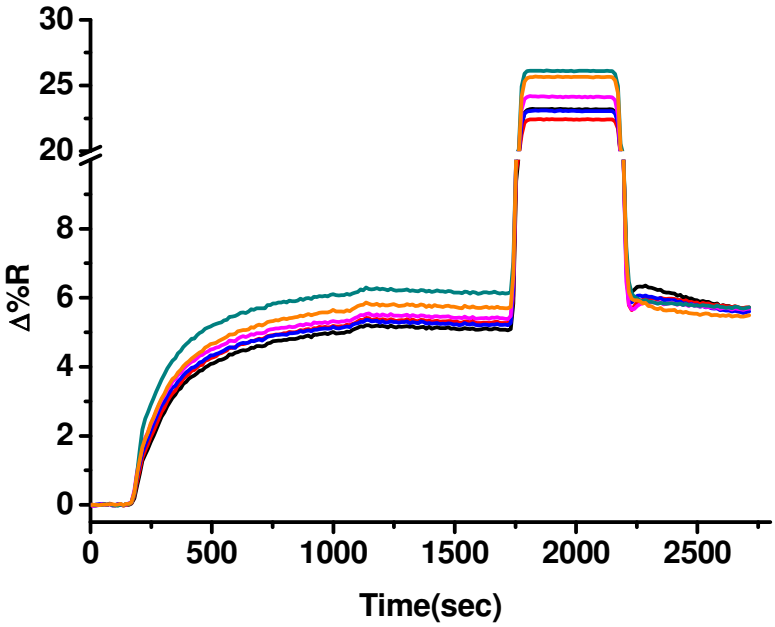

Figure 45. Time-dependent SPRI curves obtained after the immobilization of Anti-SEA F12 at concentration 20 μg/mL on DTSP-modified sensor surface and deactivation of unreacted NHS groups with EDC/NHS.

Consequently, the concentration of antibody used for immobilization on the sensor chips modified with DTSP was decreased to 8 μg/mL (in PBS) (**Figure 46**).

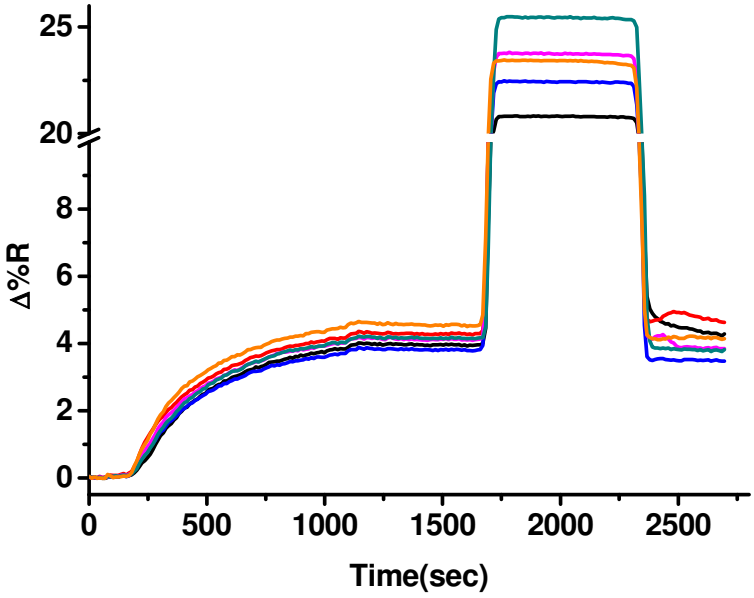

Figure 46. Time-dependent SPRI curves obtained after the immobilization of Anti-SEA F12 at concentration 8 μg/mL on DTSP-modified sensor surface and deactivation of unreacted NHS groups with EDC/NHS.

A sandwich detection strategy was then investigated by adsorbing SEA (concentrations 36 nM, 9 nM, 1.8 nM , 180 pM, 18 pM and 0 pM) on antibody immobilized on the sensor surface and by using AuNPs modified with the detection antibody Anti-SEA H5 to provide an enhanced SPRI detection.

Time-dependent SPRI curves obtained after the adsorption of AuNPs-Anti-SEA H5 (0.05 nM in PBS) are displayed in **Figure 47**.

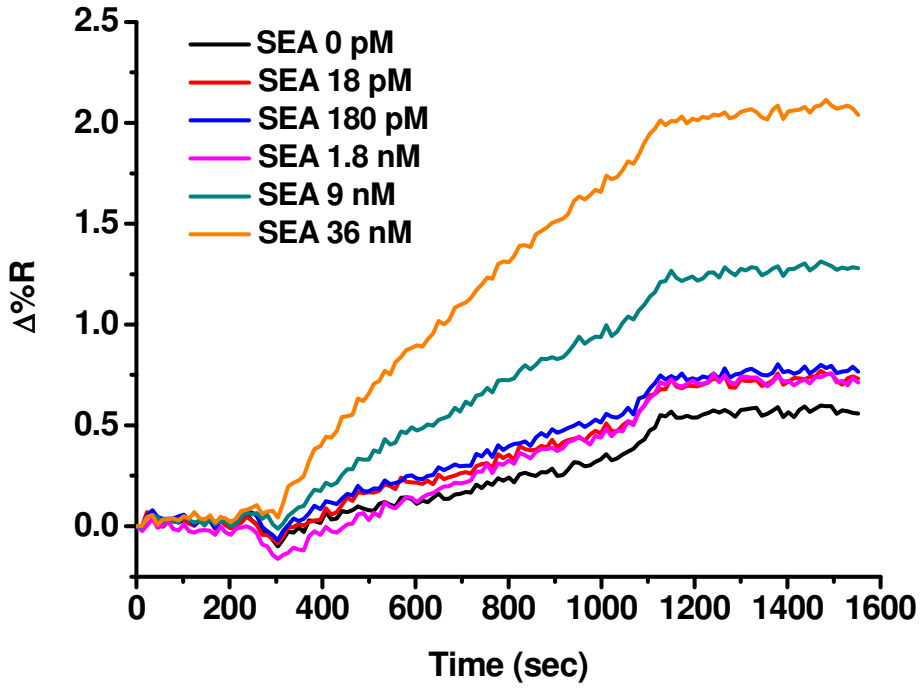

Figure 47. Time-dependent SPRI curves obtained after the adsorption of AuNPs-Anti-SEA H5 (0.05 nM) on differently concentrated SEA immobilized on the functionalized SPRI sensor chip.

The conjugation of Anti-SEA H5 with AuNPs allowed us to detect the SEA below 36 nM and to discriminate the differently concentrated SEA solutions down to 1.8 nM. SEA concentrations lower than 1.8 nM are not discriminated but are distinguished from buffer solution (SEA 0 pM).

The next issue that was taken into account was the improvement of SPRI immunosensor against the detection of SEA concentrations lower than 1.8 nM. In this

respect, detection antibodies, Anti-SEA H5 (not biotinylated) and Anti-SEA H5B (biotinylated), were allowed to interact with SEA-modified SPRI sensor surface and SPRI signals generated by SEA were compared. With this aim, Anti-SEA F12 was immobilized on the DTSP-modified sensor surface, as described above. After SEA (18 pM or 0.9 pM in PBS pH=7.4) interaction with Anti-SEA F12 immobilized on the sensor surface, detection antibodies Anti-SEA H5 or Anti-SEA H5B (10 µg/mL) were adsorbed and SPRI responses resulting from the interaction of the latter antibodies with immobilized SEA are shown in **Figure 48**.

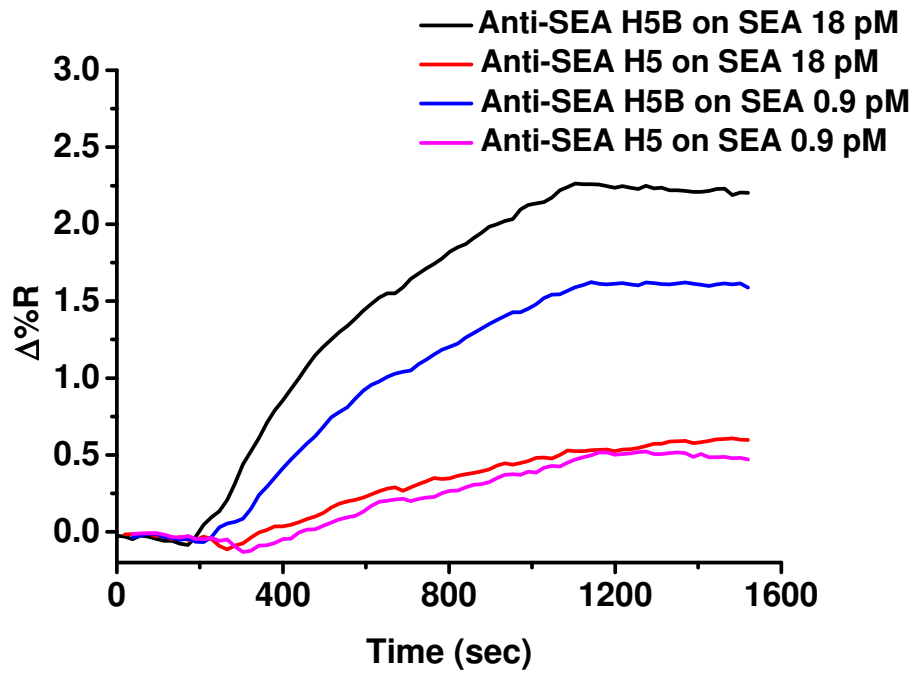

Figure 48. Time-dependent SPRI curves obtained after the interaction of Anti-SEA H5 and H5B (10 µg/mL in PBS) with the SEA on the sensor surface.

As can be seen in **Figure 48**, at the same concentration of SEA, Anti-SEA H5B antibody generates a larger change in Δ%R over time than the non biotinylated antibody (Anti-SEA H5). Furthermore, an increase of SEA concentration lead to an increased SPRI response.

In order to enhance detected SPRI responses, commercially available AuNPs conjugated with streptavidin (AuNPs-SA NP) were allowed to flow on the SPRI sensor surface (0.1 nM in concentration) (**Figure 49**).

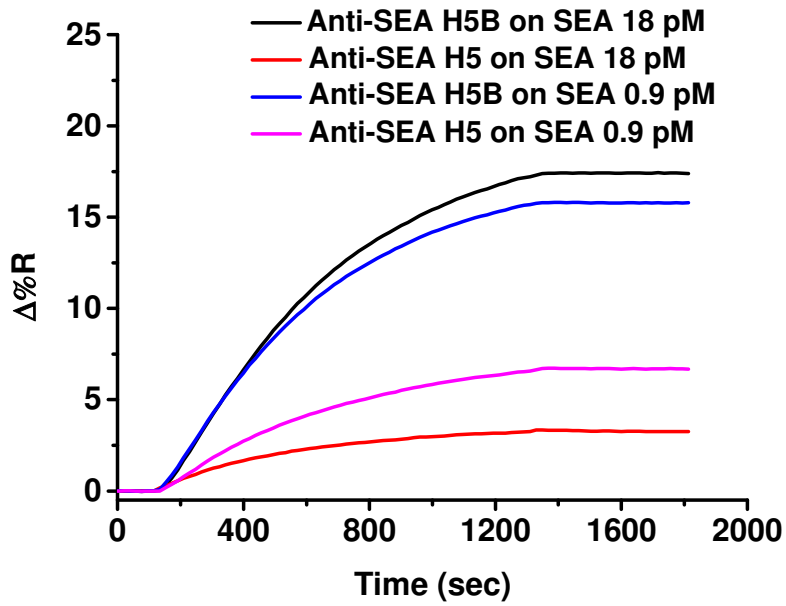

Figure 49. Time-dependent SPRI curves obtained after the flowing of AuNPs-SA NP on Anti-SEA H5 and Anti-SEA H5B.

As already pointed out, streptavidin strongly interacts with biotin, therefore AuNPs-SA NP are expected to better interact with biotinylated antibody compared to the not biotinylated one. Data obtained from replicated experiments are reported in **Figure 50**. Data are shown as the ratio between the Δ%R detected after AuNPs-SA NP interaction with Anti-SEA H5B ($\Delta\%R_{H5B}$) and the Δ%R measured after the AuNPs-SA NP interaction with Anti-SEA H5 ($\Delta\%R_{H5}$). Mean $\Delta\%R_{H5B}/\Delta\%R_{H5}$ ratio ($\Delta\%R_{H5B}/\Delta\%R_{H5}$ =2.24; SD=0.25; n=2 for gDNA concentration 0.9 pM; $\Delta\%R_{H5B}/\Delta\%R_{H5}$ = 5.46; SD=0.14; n=3 for SEA concentration 18 pM) as a function of SEA concentration were statistically different (t-test; 95% confidence interval).

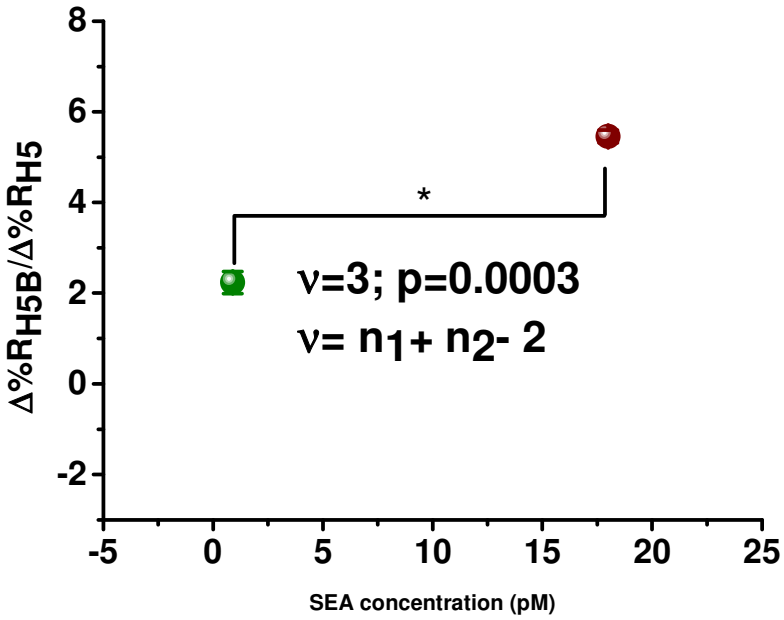

Figure 50. The mean Δ%RH5B / Δ%RH5 ratio as a function of the SEA concentration (18 pM and 0.9 pM in PBS pH=7.4). Means are statistically different (t-test; 95% confidence interval).

Lastly, a direct detection approach was used to detect SEA in milk (1.8 nM and 180 pM). The detection antibody Anti-SEA F12 was immobilized on DTSP-modified SPRI sensor surface. Then, unreacted NHS groups have been blocked with mPEG 5000 4 mM, used also to reduce non-specific adsorption of milk components on the sensor surface (**Figure 51**).

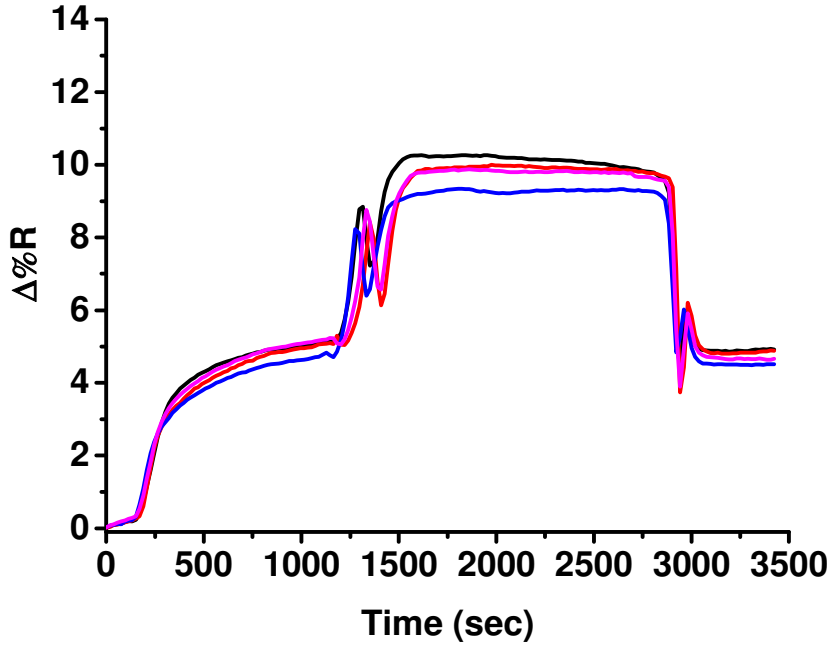

Figure 51. Time-dependent SPRI curves obtained after the immobilization of the Anti-SEA F12 (8 μg/mL) on DTSP-modified sensor surface and deactivation of unreacted NHS groups with mPEG 5000 4 mM.

In order to further reduce non-specific adsorption of milk components onto SPRI gold sensors surface, BSA (BSA in PBS, concentration 250 ng/mL) was adsorbed onto tubing and the sensor surface for 30 minutes.[52]

In **Figure 52** time-dependent SPRI curves obtained after the adsorption of milk with (SEA 180 pM and 1.8 nM) and without SEA (Blank SEA 180 pM and Blank SEA 1.8 nM) are displayed.

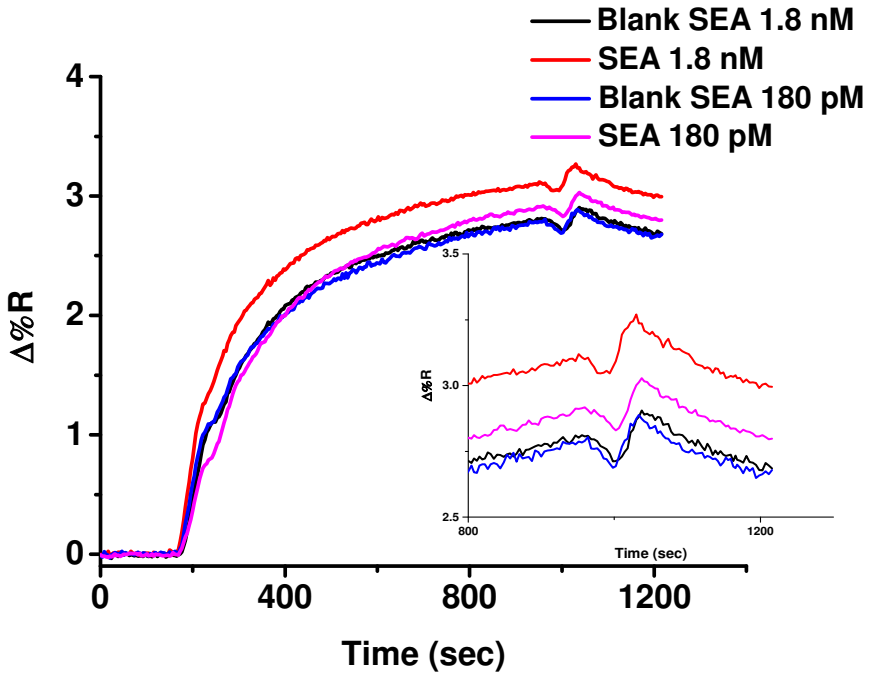

Figure 52. Time-dependent SPRI curves obtained after the adsorption of SEA and SEA-free milk solutions on the Anti-SEA F12 immobilized on the sensor surface. A zoom of the Δ%R over time is also shown in the insert.

Replicated independent experiments showed that SPRI responses were useful to discriminate between differently concentrated SEA solutions in milk (1.8 nM and 180 pM). In **Figure 53** data obtained from replicated experiments are displayed. Data are shown as the difference between the Δ%R detected after SPRI detection of SEA milk solutions ($\Delta\%R_{SEA}$) and the Δ%R measured after the SPRI detection of SEA-free milk solutions ($\Delta\%R_{Blank}$). The mean $\Delta\%R_{SEA}$ - $\Delta\%R_{Blank}$ ratio values ($\Delta\%R_{SEA}$-$\Delta\%R_{Blank}$ =0.10; SD =0.02=; n= 3 for SEA concentration 180 pM; $\Delta\%R_{SEA}$-$\Delta\%R_{Blank}$ =0.29; SD =0.02; n= 3 for SEA concentration 1.8 nM) as a function of SEA concentration were extremely statistically different (t-test; 95% confidence interval).

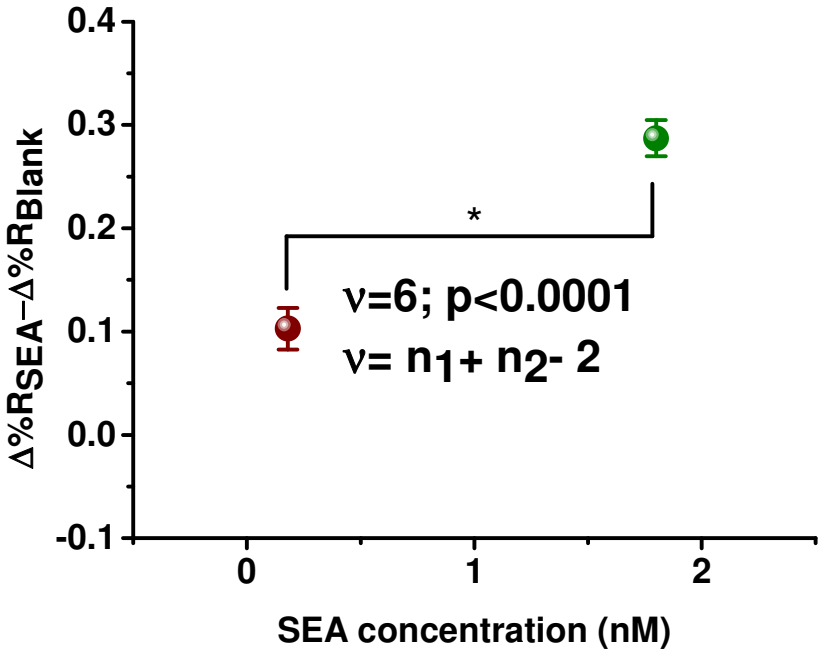

Figure 53. The mean $\Delta\%R_{SEA}$ - $\Delta\%R_{Blank}$ ratio values as a function of the SEA concentration (180 pM and 1.8 nM) were statistically different (t-test; 95% confidence interval).

The developed immunosensor allowed to detect SEA at concentration 0.9 pM in PBS and 180 pM in milk.

10.3. Antifouling surfaces development for SPRI biosensing

The fabrication of surface geometries of SPRI biosensors able to resist fouling from food components (e.g. lipids, proteins, saccharides, vitamins, minerals, and even synthetic low-molecular-weight additives) is a challenge when the detection of foodborne pathogens in food samples is going to be concerned.[277]

Coatings with fouling levels <1000 pg mm^{-2} for single or complex protein solutions are referred as to "antifouling".[211]

Different sensor surfaces functionalization strategies have been evaluated to minimize non-specific absorption of milk components on SPRI sensor surface. In particular, anti-fouling properties of Anti-*S. Aureus*-modified SPRI sensor surfaces have been tested against differently functionalized surfaces:

- SAM of MUA (**Figure 54**);

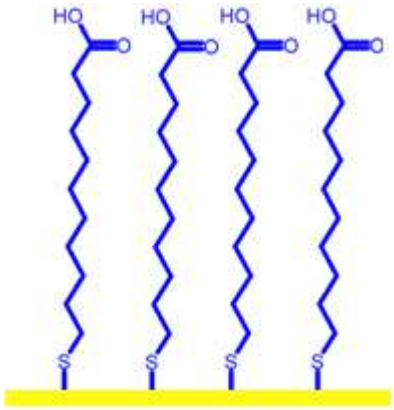

Figure 54. SPRI surface modification with MUA.

- mixed self-assembled monolayer of Carboxy-PEG12-Thiol and Methyl-PEG4-Thiol in ratio 1/10 (**Figure 40**).

In both cases, carboxyl groups have been activated with EDC and NHS before to study the immobilization of the Anti-*S. Aureus* (concentrations ranging between 2 µg/mL and 18 µg/mL in PBS). The behavior of surfaces obtained after the antibody immobilization against the non specific adsorption of milk components was then investigated.

Figure 55 displays the SPRI response detected after the immobilization of Anti-*S. Aureus* (18 µg/mL) on MUA-modified surfaces. The subsequent deactivation of unreacted NHS moieties with TRIZMA HCl 0.25 M is also displayed.

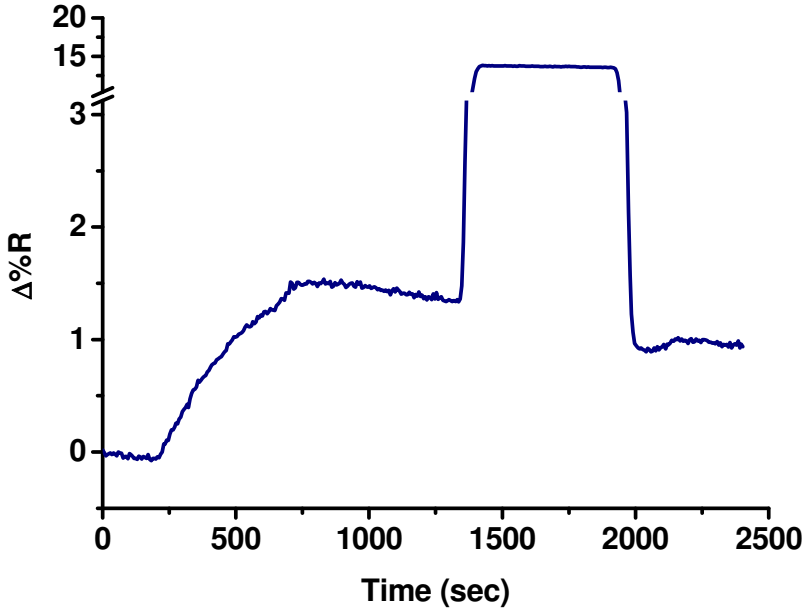

Figure 55. SPRI response obtained after the immobilization of Anti-*S. Aureus* (18 µg/mL) on MUA-modified sensor surface and deactivation of unreacted NHS groups with TRIZMA HCl 0.25 M.

Commercial skimmed milk, centrifuged for 45 min and again for 30 min and diluted in PBS 400x, was flowed on the sensor surface in order to evaluate surface resistance to non-specific interaction (**Figure 56**).

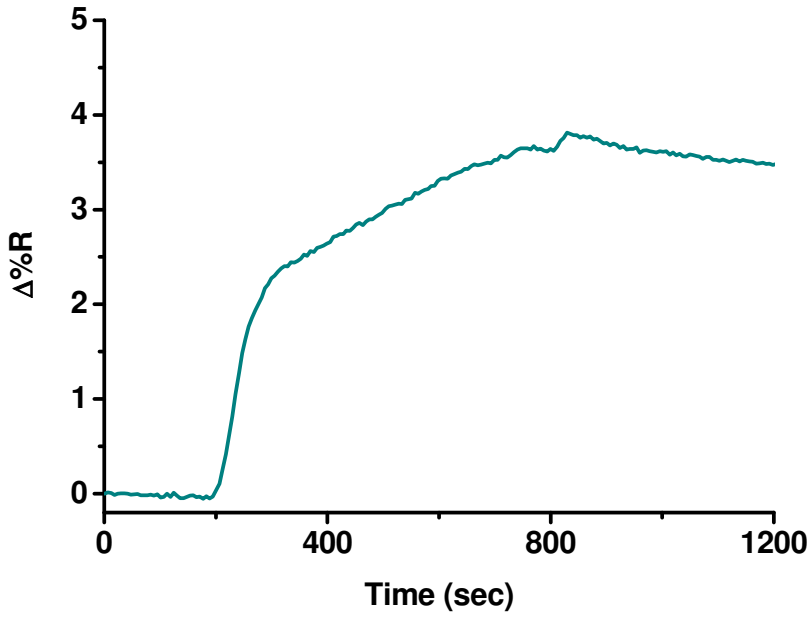

Figure 56. SPRI response obtained after the interaction of skimmed milk, centrifuged for 45 min and again for 30 min and diluted in PBS 400x, with Anti-*S. Aureus* (18 μg/mL) immobilized on MUA-modified sensor surface.

The non-specific absorption on the functionalized surface produces a relatively intense SPRI signal that must be minimized.

Mixed SAMs of alkanethiolates derived from tri(ethylene glycol)-terminated thiol and hexa(ethylene glycol)-carboxylic acid-terminated thiol have been described to effectively resist the non-specific adsorption of proteins.[278] In addition, it has been demonstrated that proteins are preferentially immobilized on SAMs formed by mixed thiols rather than on homogeneous SAM.[223,279,280,281] Mixed thiols SAMs also minimize steric hindrance between immobilized receptors and their binding counterparts.[282]

On this basis, Anti-*S. Aureus* has been immobilized on SPRI sensor surfaces modified with a mixture of methyl- and carboxy-thiol PEGylation reagents.

In **Figure 57** the sensor surface modification with a carboxy-PEG12-thiol and methyl-PEG4-thiol (ratio 1/10) mixed SAM and the subsequent activation of carboxylic acid groups with EDC/NHS is shown.

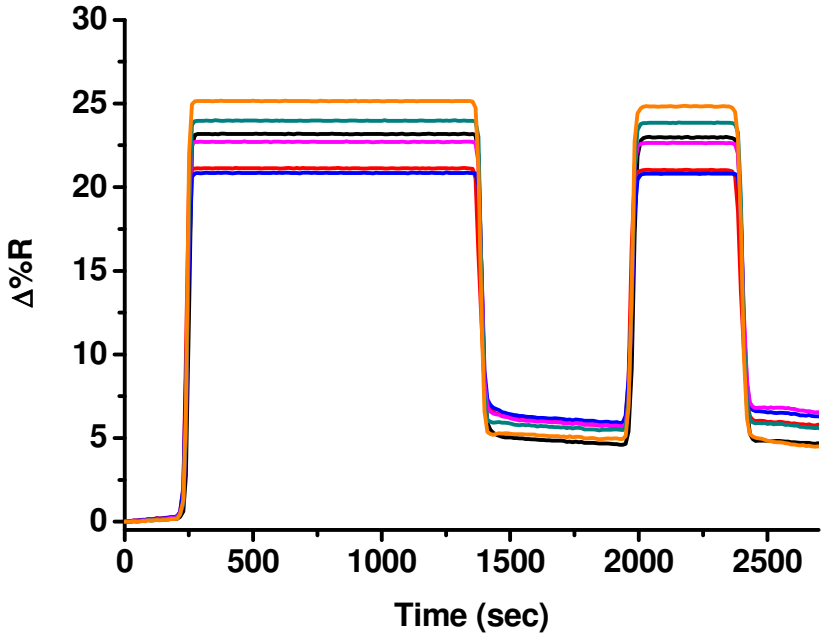

Figure 57. Time-dependent SPRI curves showing sensor surface functionalization with Carboxy-PEG12-Thiol and Methyl-PEG4-Thiol (ratio 1/10) and the subsequent activation of carboxylic groups with EDC/NHS.

Anti-*S. Aureus* solutions (2 µg/mL, 6 µg/mL and 18 µg/mL in PBS) were then adsorbed on the functionalized surface and unreacted NHS groups deactivated (TRIZMA HCl) (**Figure 58**).

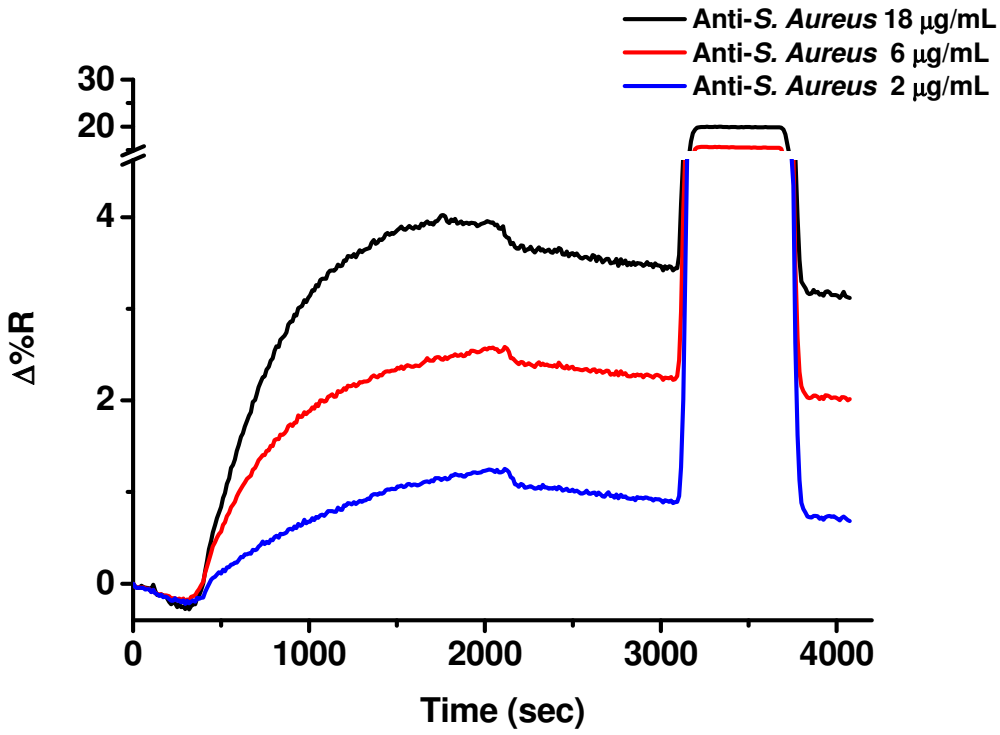

Figure 58. Time-dependent SPRI curves obtained after the immobilization of Anti-*S. Aureus* at concentrations 2, 6, 18 µg/mL on the sensor surface modified with Carboxy-PEG12-Thiol and Methyl-PEG4-Thiol and deactivation of unreacted groups NHS with TRIZMA HCl.

The interaction of antibodies with surfaces functionalized with the mixed SAM based on carboxy-PEG12-Thiol and methyl-PEG4-Thiol produced a more efficient immobilization (**Figure 58**) compared to MUA functionalized surfaces (**Figure 56**). After the antibody immobilization, milk samples (centrifuged for 45 min and again for 30 min and diluted in PBS 400x) were introduced to evaluate non-specific adsorption (**Figure 59**).

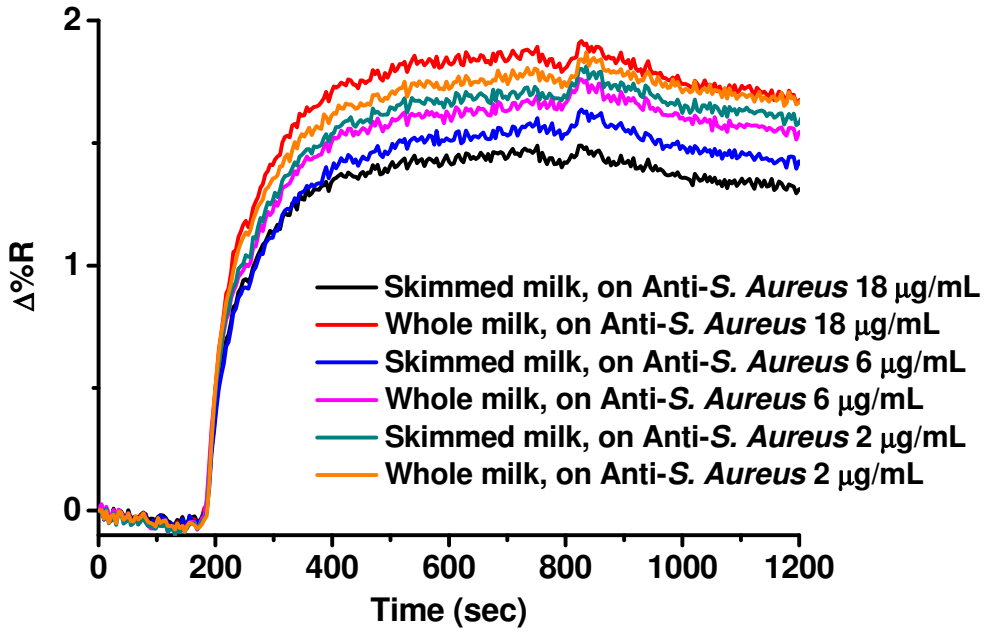

Figure 59. Time-dependent SPRI curves showing the interaction of skimmed milk and fresh whole milk with Anti-*S. Aureus* at concentrations 2, 6, 18 μg/mL immobilized on Carboxy-PEG12-Thiol and Methyl-PEG4-Thiol modified sensor surface. All milk samples tested have been centrifuged for 45 min and again for 30 min and diluted in PBS 400x before the analysis.

Figure 59 shows the detected effects of non-specific adsorption of milk components. The comparison of SPRI responses (Δ%R) obtained when the same milk sample interacted with mixed SAMs or MUA functionalized surface demonstrates the better efficiency of mixed monolayers in minimizing non-specific adsorptions (**Figure 60**) even though a relatively high level of non specific adsorption is registered for both cases.

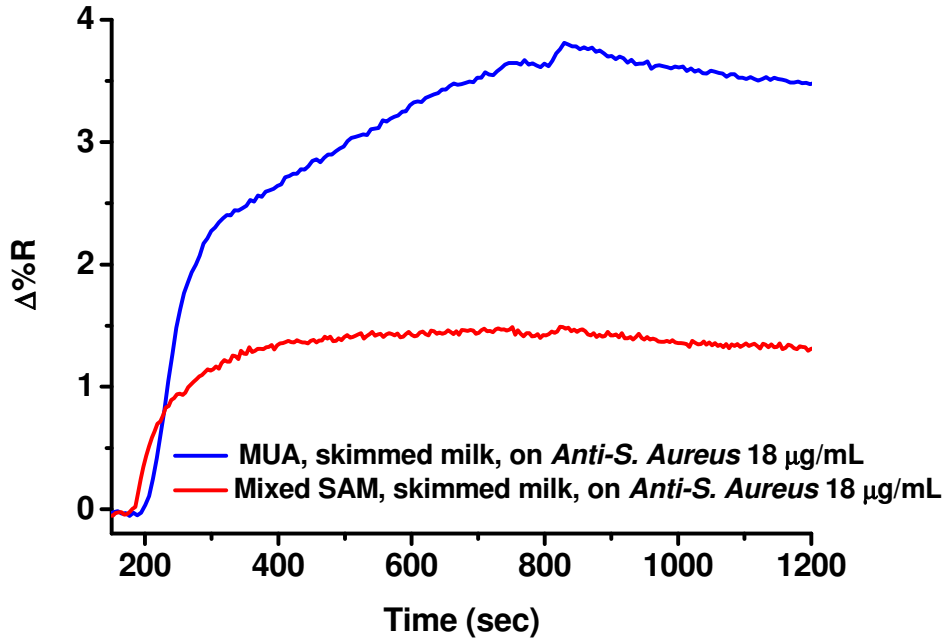

Figure 60. Representative time-dependent SPRI curves showing the better resistance to non-specific adsorption of mixed SAM of Carboxy-PEG12-Thiol and Methyl-PEG4-Thiol compared to MUA-SAM. All milk samples tested have been centrifuged for 45 min and again for 30 min and diluted in PBS 400x before the analysis.

The observed results are coherent with literature data on SAM resistance to non-specific adsorption of proteins.[224]

Data demonstrate that skimmed milk provided reduced non-specific adsorption compared to whole milk (**Figure 61**).

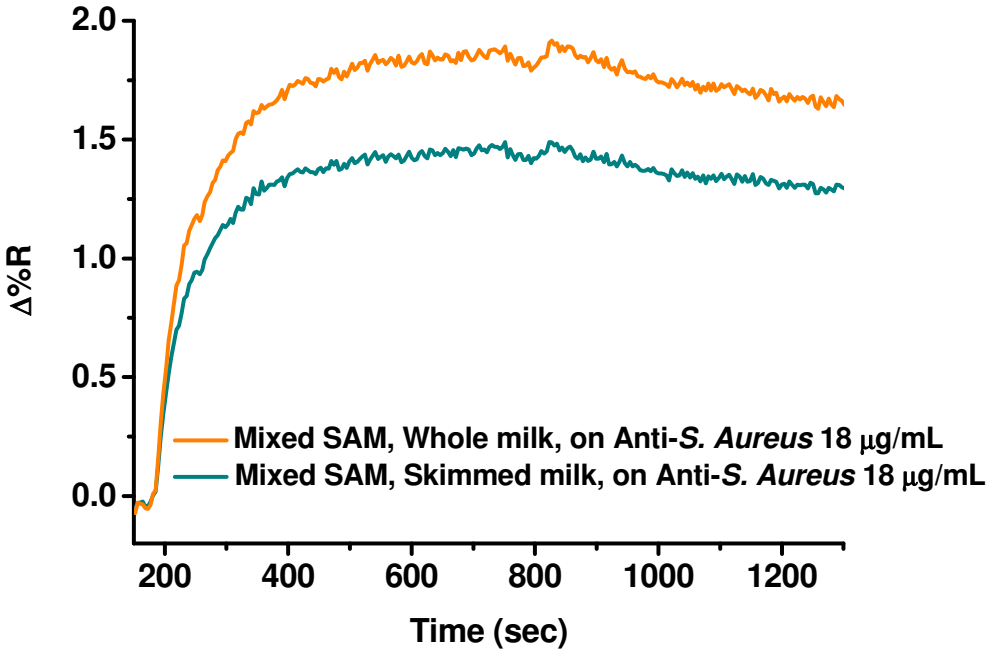

Figure 61. Time-dependent SPRI curves showing that skimmed milk provided reduced non-specific adsorption on mixed SAM compared to whole milk.

Both alkanethiols and dialkyl disulfides forms ordered monolayers on gold surfaces.[283] In addition, it is known that PEG offers good performances as anti-fouling material.[284] For those reasons, PEG disulfides have been also tested. In particular, the following systems have been tested:

- mPEG disulfide/NHS PEG disulfide 1/1 (total concentration 2 mM);
- mPEG disulfide/NHS PEG disulfide 10/1 (total concentration 2 mM);
- mPEG disulfide/NHS PEG disulfide 7/3 (total concentration 2 mM);
- mPEG disulfide (concentration 2 mM).

In **Figures 62, 63, 64** and **65,** SPRI data referring to the adsorption of milk on functionalized surfaces are displayed. Experiments were performed with the aim to evaluate adsorption from differently pre-treated milk samples.

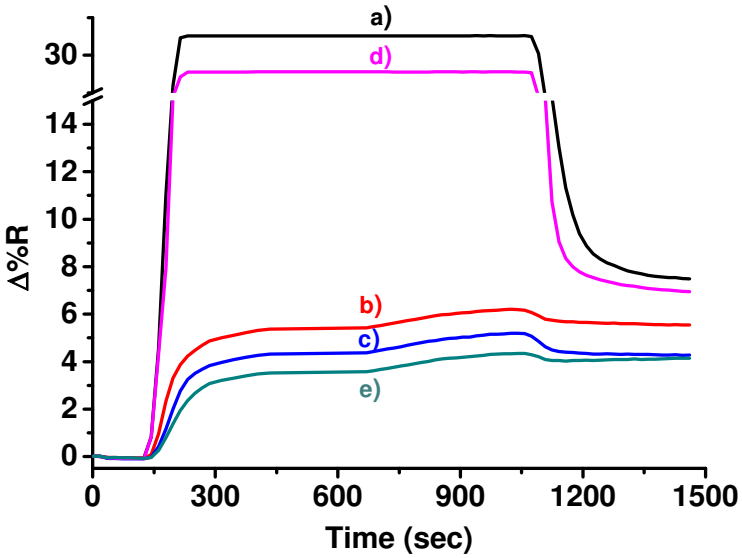

Figure 62. Time-independent SPRI curves recorded after the flowing of skimmed milk solutions on the SPRI sensor surface modified with mPEG disulfide/NHS PEG disulfide 1/1 (total concentration 2 mM). a) undiluted; b) diluted in PBS 400x; c) centrifuged for 45 min and diluted in PBS 400x; d) centrifuged for 45 min and again for 30 min; e) centrifuged for 45 min and again for 30 min and diluted in PBS 400x.

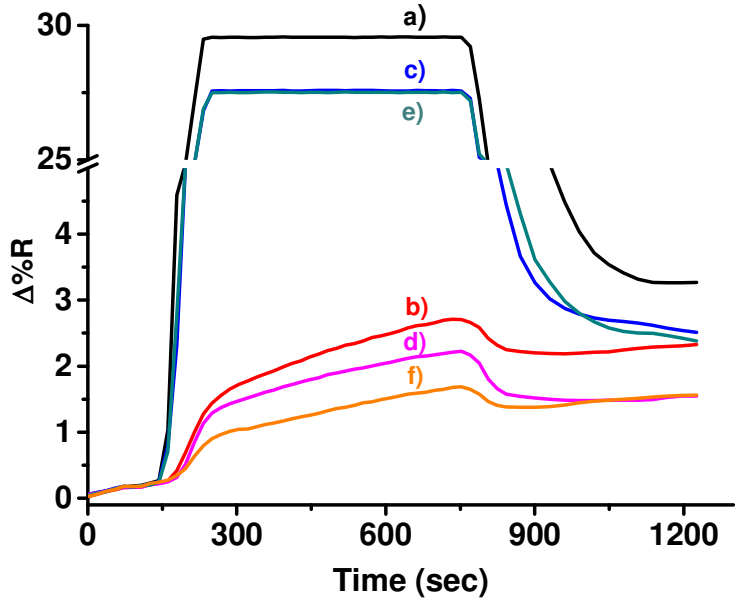

Figure 63. Time-independent SPRI curves obtained after the flowing of skimmed milk solutions on the SPRI sensor surface modified with mPEG disulfide/NHS PEG disulfide 10/1 (total concentration 2 mM). a) undiluted; b) diluted in PBS 400x; c) centrifuged for 45 min; d) centrifuged for 45 min and diluted in PBS 400x; e) centrifuged for 45 min and again for 30 min; f) centrifuged for 45 min and again for 30 min and diluted in PBS 400x.

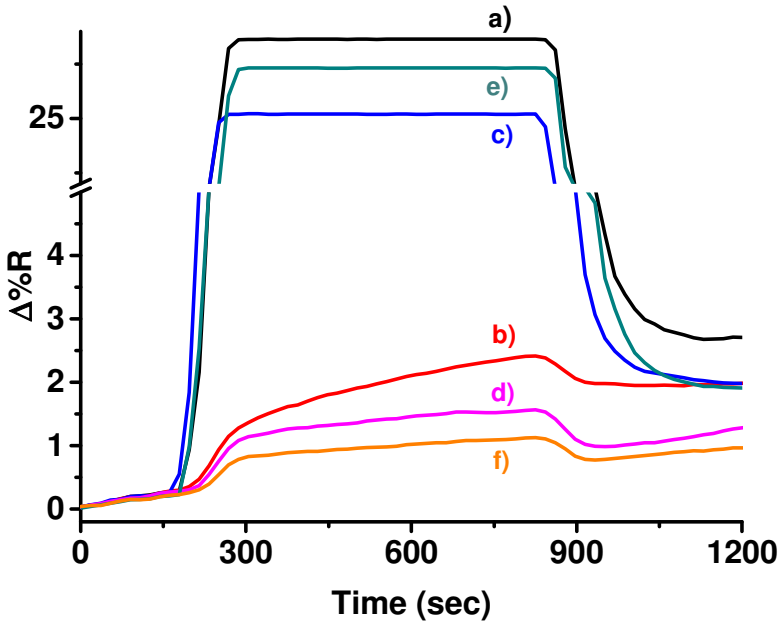

Figure 64. Time-independent SPRI curves obtained after the flowing of skimmed milk solutions on the SPRI sensor surface modified with mPEG disulfide/NHS PEG disulfide 7/3 (total concentration 2 mM). a) undiluted; b) diluted in PBS 400x; c) centrifuged for 45 min; d) centrifuged for 45 min and diluted in PBS 400x; e) centrifuged for 45 min and again for 30 min; f) centrifuged for 45 min and again for 30 min and diluted in PBS 400x.

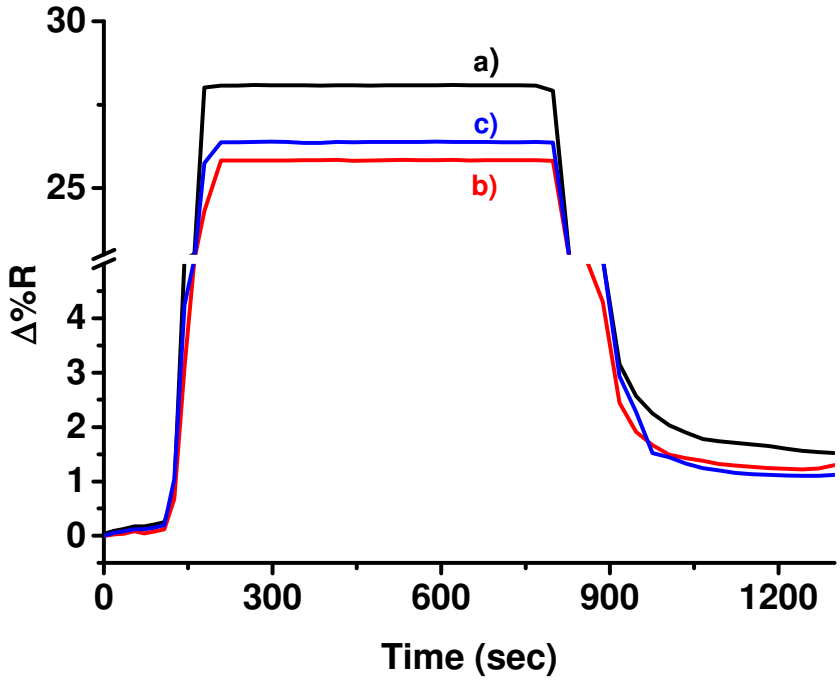

Figure 65. Time-independent SPRI curves obtained after the flowing of skimmed milk solutions on the SPRI sensor surface modified with mPEG disulfide 2 mM. a) undiluted; b) undiluted, centrifuged for 45 min; c) undiluted, centrifuged for 45 min and again for 30 min.

The comparison of SPRI responses (Δ%R) obtained when the same milk sample (e.g. undiluted skimmed milk) interacted with surfaces functionalized with mPEG disulfide/NHS PEG disulfide 1/1, mPEG disulfide/NHS PEG disulfide 10/1, mPEG disulfide/NHS PEG disulfide 7/3, respectively, shows a better resistance to non-specific adsorption of mPEG disulfide/NHS PEG disulfide 7/3-modified sensor surface ($\Delta\%R_{\text{mPEG disulfide/NHS PEG disulfide 7/3}} = 2.7$; $\Delta\%R_{\text{mPEG disulfide/NHS PEG disulfide 10/1}} = 3.3$; $\Delta\%R_{\text{mPEG disulfide/NHS PEG disulfide 1/1}} = 7.5$) compared to the other systems. As reference, the SPRI response for the adsorption on mPEG disulfide 2 mM is also shown ($\Delta\%_{\text{mPEG disulfide}} = 1.5$). In the latter case, the sensor surface lacks of reactive groups useful for the subsequent surface modifications (immobilization of antibodies).

The backfilling of high molecular weight PEG SAM with lower molecular weight PEG molecules represents an useful approach to enhance anti-fouling performances of

surfaces.[285] To test the efficiency of a similar procedure against milk samples, SPRI sensor chips have been functionalized with NHS PEG disulfide and then backfilled with mPEG disulfide according to the following concentration ratios:

- NHS PEG disulfide 0.2 mM, mPEG disulfide 1 mM (ratio 1/5);
- NHS PEG disulfide 1 mM, mPEG disulfide 4 mM (ratio 1/4);
- NHS PEG disulfide 0.5 mM, mPEG disulfide 4.5 mM (ratio 1/9).

Figures 66, **67** and **68** show time-dependent SPRI curves obtained after the adsorption of different milk samples on the modified surfaces.

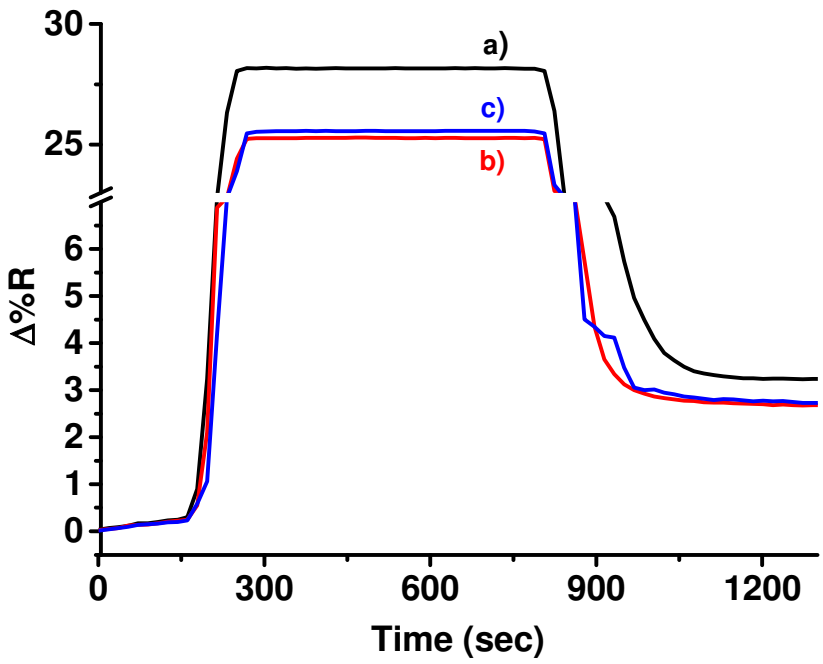

Figure 66. Time-independent SPRI curves obtained after the adsorption of skimmed milk samples on the SPRI sensor surface modified with NHS PEG disulfide 0.2 mM and backfilled with mPEG disulfide 1 mM. a) undiluted; b) undiluted, centrifuged for 45 min; c) undiluted, centrifuged for 45 min and again for 30 min.

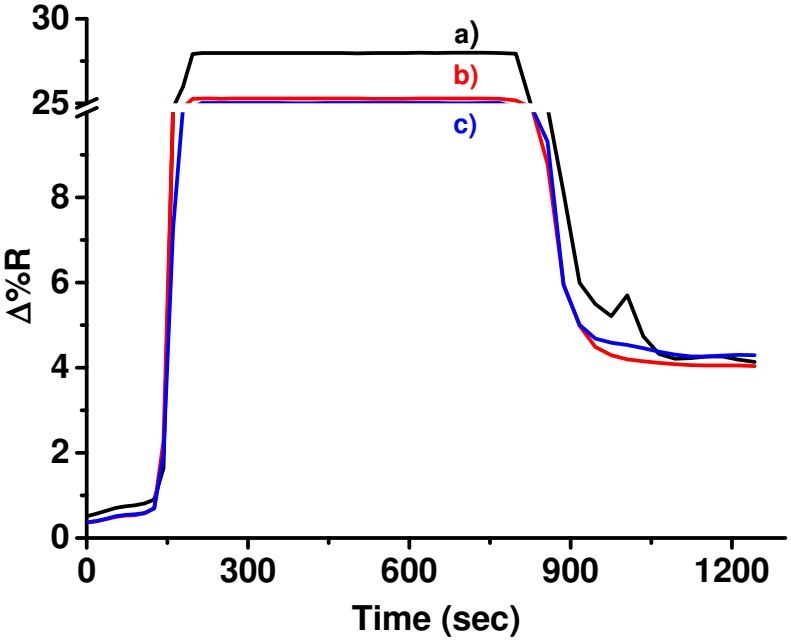

Figure 67. Time-independent SPRI curves obtained after the adsorption of skimmed milk samples on the SPRI sensor surface modified with NHS PEG disulfide 1 mM and backfilled with mPEG disulfide 4 mM. a) undiluted; b) undiluted, centrifuged for 45 min; c) undiluted, centrifuged for 45 min and again for 30 min.

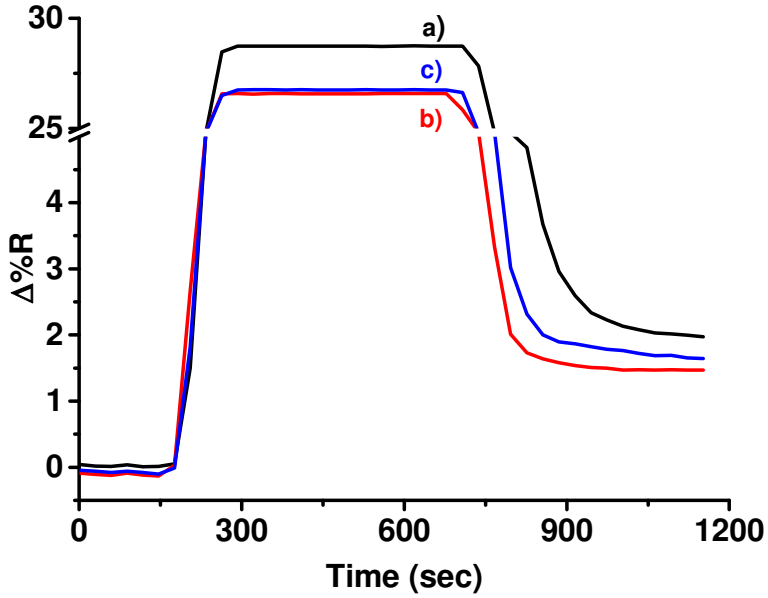

Figure 68. Time-independent SPRI curves obtained after the adsorption of skimmed milk samples on the SPRI sensor surface modified with NHS PEG disulfide 0.5 mM and backfilled with mPEG disulfide 4.5 mM. a) undiluted; b) undiluted, centrifuged for 45 min; c) undiluted, centrifuged for 45 min and again for 30 min.

Surfaces modified with NHS PEG disulfide 0.5 mM and backfilled with mPEG disulfide 4.5 mM provided the best anti-fouling capability ($\Delta\%R_{\text{NHS PEG disulfide 0.5 mM/backfilled with mPEG 4.5 mM}} = 2.0$; $\Delta\%R_{\text{NHS PEG disulfide 0.2 mM/backfilled with mPEG 1 mM}} = 3.2$; $\Delta\%R_{\text{NHS PEG disulfide 1 mM/backfilled with mPEG 4 mM}} = 4.1$. **Figure 68**). Moreover, the surface exposes reactive groups for the subsequent surface modifications.

Further improvements of anti-fouling properties of the functionalized surfaces have been obtained by combining PEG antifouling performances together with betaines. In this perspective, gold surfaces have been functionalized with NHS PEG disulfide subsequently modified an amine-PEG-azide (NH_2-PEG-N_3, structure not reported) linker. A "click chemistry" reaction has been performed to add an alkyne-carboxybetaine-based moiety after the hydrolysis and deactivation of unreacted NHS esters. For click chemistry reaction $CuBr(PPh_3)_3$ has been used as catalyst[286].

Click reactions are categorized into four classes, including cycloadditions, additions to carbon-carbon multiple bonds, nucleophilic substitutions and carbonyl chemistry of non-aldol type transformations. The copper-catalyzed azide-alkyne cycloaddition (CuAAC), commonly known as Cu-catalyzed click chemistry, fulfills criteria of the Sharpless theory on which click chemistry is based.[287] Different copper catalysts can be used for the CuAAC reaction whose general aim is to kept Cu^I concentration at its maximum to promote the reaction:

- Cu^{II} salts (usually $CuSO_4$) together with reducing agents (ue.g. sodium ascorbate);
- Cu^I compounds (such as CuBr or CuOAc), together with a base or an amine ligand and a reducing agent (sodium ascorbate) in order to inhibit aerobic oxidation to Cu^{II};
- Cu^0 whose surface produces the required Cu^I species.[288]

Recently, $CuBr(PPh_3)_3$ has been shown to perform as a catalyst. It works at room temperature, with 0.5 mol % [Cu] (or less) and with no additives. In addition, the formed triazole is pure and can be used with no further purification.[289]

Modified gold surfaces were then used to investigate the influence of betaine moieties on antifouling performances against milk samples (**Figure 69**).

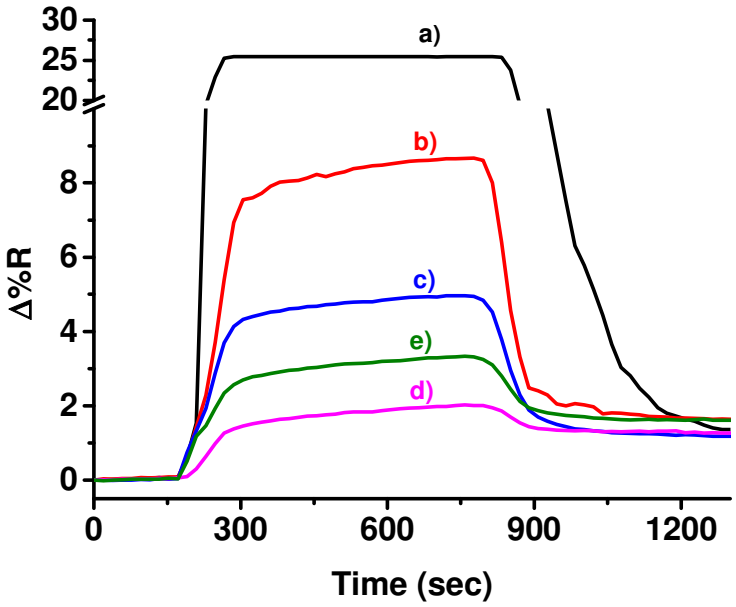

Figure 69. Time-independent SPRI curves obtained after the adsorption of skimmed milk on SPRI sensor surface modified with PEG-alkyne-carboxybetaine-based compound. a) undiluted; b) diluted in PBS 10x; c) diluted in PBS 20x; d) diluted in PBS 400x; e) diluted in PBS 50x.

By comparing SPRI responses (Δ%R) obtained when the same milk sample (skimmed milk, undiluted) was adsorbed on the modified surfaces, we can conclude that the PEG-alkyne-carboxybetaine-based compound-modified surface provided the best resistance to non-specific adsorption from milk samples ($\Delta\%R_{\text{PEG-alkyne-carboxybetaine-based compound}} = 1.4$).

11. CONCLUSIONS AND FUTURE PERSPECTIVES

During my PhD I investigated SPRI capabilities in detecting foodborne pathogens. In particular, I explored:

1) SPRI genosensors for the detection of *S. Aureus* and *Listeria m.* genomic DNAs;
2) SPRI immunosensors for the detection of SEA toxin;
3) SPRI biosensor surfaces able to resist fouling from milk where the investigated pathogens and toxins are usually found.

SPRI results shows that an ultrasensitive DNA sensor for pathogen genomic detection has been developed. The optimized specific sandwich sensing strategy allows to detect *S. Aureus* and *Listeria m.* genomic DNA at the fM-aM level, by using only 300 zeptomoles of the genomic DNA target. The method does not involve any genomic DNA amplification step and combines the high affinity and selectivity of PNA probes with gold nanoparticle-enhanced SPRI detection performances. Therefore the assay represents an alternative to conventional methods today used for pathogens detection.

SPRI data shows that the developed genosensor is able to discriminate pathogen gDNA from interfering gDNA, such as bovine gDNA, thus allowing the detection of aM concentrations of *S. Aureus* gDNA even if bovine gDNA is present in the analyzed sample. Such performances demonstrates that the method can be applied for the detection of bacterial gDNA extracted from contaminated milk.

The SPRI immunosensor developed for the detection of SEA allowed to detect SEA concentrations down to 0.9 pM in PBS by using specific monoclonal antibodies Anti-SEA and a sandwich detection approach. SPRI immunosensor developed for the detection of SEA in milk are able to detection SEA at 180 pM concentration.

SPRI sensor surface antifouling capability were also investigated, with particular attention to surface geometries useful to minimize non-specific binding events from milk samples.

Mixed carboxy-PEG12-thiol and methyl-PEG4-thiol SAMs reduced non-specific adsorption from milk samples better than MUA SAMs. Further experiments showed that NHS PEG disulfide modified surfaces backfilled with mPEG disulfide provided even better anti-fouling performances. Finally, the positive influence of carboxybetaine units on surface antifouling properties have been investigated by testing a new PEG-alkyne-carboxybetaine-based compound that manifested the best resistance to non-specific adsorption of milk components.

RESEARCH PRODUCTS

Oral Presentations:

Angela M. Aura, Roberta D'Agata, Giuseppe Spoto; *Detection of foodborne pathogens by optical biosensing*. ISA, Incontro di Spettroscopia Analitica, Matera, 29th May-1st **June 2016**.

Angela M. Aura, Roberta D'Agata, Noemi Bellassai, Cristina Valenti, Giuseppe Spoto; *Surface Plasmon Resonance Imaging detection of foodborne pathogens by using PNA Probes and gold nanoparticles*. XXV Congresso della Divisione di Chimica Analitica della Società Chimica Italiana, Trieste, 13rd-17th **September 2015**. ISBN: 978-88-907670-2-9.

Angela Margherita Aura, Roberta D'Agata, Cristina Valenti, Giuseppe Spoto; *Surface Plasmon Resonance Imaging genosensors to detect pathogens in food.* XXV Congresso Nazionale della Società Chimica Italiana, Rende (CS), 07th-12nd **September 2014**.

Poster presentations:

Angela M. Aura, Roberta D'Agata, Giuseppe Spoto; *Surface Plasmon Resonance Imaging Biosensing for the detection of Staphylococcus Aureus in food.* XXVI Congresso della Divisione di Chimica Analitica, Giardini Naxos (Me), 18th-22nd **September 2016**. ISBN: 978-88-86208-91-8.

Angela M. Aura, Roberta D'Agata, Giuseppe Spoto; *Surface Plasmon Resonance Imaging genosensing for the ultrasensitive detection of foodborne pathogens*. European Advanced Material Congress, Biosensors and Bioelectronics Symposium, Stockholm, Sweden, 23rd-25th **August 2016**. VBRI Press, DOI: 10.5185/eamc2016, ISBN: 978-91-88252-02-9.

Co-authored presentations:

Giuseppe Spoto, Alessandro Rapisarda, Giuseppe Grasso, Roberta D'Agata, Angela Aura, Maria Chiara Giuffrida, Marzia Calcagno, Cristina Valenti; *Atmospheric pressure MALDI-MS for the direct analysis of carbonaceous inks used in XVII century manuscripts*. Technart 2015, Catania, 27th-30th **April 2015**.

Cristina Valenti, Roberta D'Agata, Angela Margherita Aura, Giuseppe Spoto; *SPRI detection and discrimination of a SNP in the K-ras oncogene*. XXV Congresso Nazionale della Società Chimica Italiana, Rende (CS), 07th-12nd **September 2014**.

Roberta D'Agata, Alex Manicardi, Marzia Calcagno, Angela Margherita Aura, Roberto Corradini, Giuseppe Spoto, *High sensitive detection of MicroRNA-210 by using PNA probes and SPR Imaging*, ISA, Incontro di Spettroscopia Analitica, Ravenna, 5th-6th **June 2014**.

Roberta D'Agata, Alex Manicardi, Marzia Calcagno, Angela Margherita Aura, Roberto Corradini, Giuseppe Spoto; *Combined use of PNA probes and SPR Imaging for the sensitive detection of microRNA*, COST Action TD1003 - Bio-inspired nanotechnologies: from concepts to applications, Catania, 28th-30th **April 2014**.

Publications:

Pasquale Palladino, Angela M. Aura, Giuseppe Spoto; *Surface plasmon resonance for the label-free detection of Alzheimer's β-amyloid peptide aggregation.* Anal Bioanal Chem (**2016**) 408:849–854.

Valentina Giglio, Maurizio Viale, Massimiliano Monticone, Angela M. Aura, Giuseppe Spoto, Giovanni Natile, Francesco P. Intini and Graziella Vecchio; *Cyclodextrin polymers as carriers for the platinum-based anticancer agent LA-12*. RSC Adv (**2016**) 6:12461–12466.

Angela M. Aura, R. D'Agata, G. Spoto; *Surface Plasmon Resonance Imaging Genosensing of Staphylococcus Aureus and Listeria monocytogenes for Food Safety*. Manuscript submitted.

ACKNOWLEDGEMENTS

I would like to express my sincere appreciation to Prof. Giuseppe Spoto for his expert guidance, understanding and support. It was a pleasure collaborating with him.

I am grateful to Dr. Roberta D'Agata for her encouragement and generous advice.

I would like to extend my thanks to Prof. Giuseppe Spoto research group.

REFERENCES

[1] http://www.cfs.gov.hk/english/whatsnew/whatsnew_fst/whatsnew_fst_World_Health_Day_**2015**.html

[2] Newell DG; Koopmans M; Verhoef L; Duizer E; Aidara-Kane A; Sprong H; Opsteegh M; Langelaar M; Threfall J; Scheutz F; van der Giessenb J; Kruse H; *International Journal of Food Microbiology*, **2010**, 139, S3.

[3] http://www.who.int/topics/foodborne_diseases/en/

[4] Law JW-F; Ab Mutalib N-S; Chan K-G; Lee L-H; *Frontiers in Microbiology*, **2015**, 5, 1.

[5] Poltronieri P; Mezzolla V; Primiceri E; Maruccio, G; *Foods*, **2014**, 3, 511.

[6] Commission Regulation (EC) No 2073/2005 of 15 November **2005** on microbiological criteria for foodstuffs, Official Journal of the European Union.

[7] Centers for Disease Control and Prevention (CDC) (**2011**). *CDC Estimates of Foodborne Illness in the United States*. Available on line at: http://www.cdc.gov/foodborneburden/pdfs/factsheet_a_findings_updated4-13.pdf (Accessed15June**2014**).

[8] Scallan E; Hoekstra RM; Mahon BE; Jones TF; Griffin PM; *Epidemiology and Infection*, **2015**, 143, 2795.

[9] Majumdar T; Raychaudhuri U; Chakraborty R; *International Journal of Advanced Biotechnology and Research*, **2015**, 5, 96.

[10] Velusamy V; Arshak K; Korostynska O; Oliwa K; Adley C; *Biotechnology Advances*, **2010**, 28, 232.

[11] Verma MS; Rogowski JL; Jones L; Gu FX; *Biotechnology Advances*, **2015**, 33, 666.

[12] Zhao X; Lin C-W; Wang J, Hwan Oh D; *Journal of Microbiology and Biotechnology*, **2014**, 14, 297.

[13] Raba J; Fernández-Baldo MA; Pereira SV; Messina GA; Bertolino FA; Tosetti S; Sanz Ferramola MI; "Analytical biosensors for the pathogenic microorganisms determination" in Microbial Pathogens and Strategies for Combating Them: Science, Technology and Education, pp. 227-238, Formatex Research Center, **2013**.

[14] Brandão D; Liébana S; Pividori MS; *New Biotechnology*, **2015**, 32, 511

[15] Song L; Shan D; Zhao M; Pink BA; Minnehan KA; York L; Gardel M; Sullivan S; Phillips AF; Hayman RB; Walt DR; Duffy DC; *Analytical Chemistry*, **2013**, 85, 1932.

[16] De Medici D; Kuchta T; Knutsson R; Angelov A; Auricchio B; Barbanera M; Diaz-Amigo C; Fiore A; Kudirkiene E; Hohl A; Horvatek Tomic D; Gotcheva V; Popping B; Prukner-Radovcic E; Scaramaglia S; Siekel P; To KA; Wagner M; *Food Analytical Methods*, **2015**, 8, 255.

[17] Harvey RA, Nau Cornelissen C, Fisher BD, **2013**, Lippincott's IIIustrated reviews Microbiology Third Edition.

[18] Kärkkäinen, RM; Drasbek MR; McDowall I; Smith CJ; Young NWG; Bonwick GA; *International Journal of Food Science and Technology*, **2011**, 46, 445.

[19] Gehring AG ; Irwin PL ; Reed SA ; Tu SI ; *Journal of Rapid Methods & Automation in Microbiology*, **2006**, 14, 349.

[20] Magliulo M; Simoni P; Guardigli M; Michelini E; Luciani M; Lelli R; Roda A; *Journal of Agricultural and Food Chemistry*, **2007**; 55, 4933.

[21] Jechorek RP; Johnson RL; *Journal of AOAC INTERNATIONAL*, **2008**, 91, 164.

[22] Haghi AK; Carvajal-Millan E Editor, **2014**, Food Composition and Analysis Methods and Strategies, ISBN: 978-1-926895-85-7.

[23] Crowther JR (Ed.), **1995**, ELISA Theory and Practice. Humana Press Inc., USA, ISBN 0-89603-279-5.

[24] Bolton FJ; Fritz E; Poynton S; Jensen T; *Journal of AOAC INTERNATIONAL*, **2000**, 83, 299.

[25] Aschfalk A; Mülller W; *Canadian Journal of Microbiology*, **2002**, 48, 365.

[26] Kumar BK; Raghunath P; Devegowda D; Deekshit VK; Venugopal MN; Karunasagar I; Karunasagar I*; International Journal of Food Microbiology*, **2011**, 145, 244.

[27] Shen Z; Hou N; Jin M; Qiu Z; Wang J; Zhang B; Wang ; Wang J; Zhou D; *Gut Pathogens*, **2014**, 6, 14.

[28] Zhang G; *Meducator*, **2013**, 1, 15.

[29] Kumar S; Dilbaghi N; Barnela M; Bhanjana G; Kumar R; *BioNanoScience*, **2012**, 2, 196.

[30] Leonard P; Hearty S; Brennan J; Dunne L; Quinn J; Chakraborty T; O'Kennedy R*; Enzyme and Microbial Technology*, **2003**, 32, 3.

[31] Gehring AG; Tu SI; *Annual Review of Analytical Chemistry*, **2011**, 4, 151.

[32] Hall RH; *Microbes and Infection*, **2002**, 4, 425.

[33] Lazcka O; Del Campo FJ; Muñoz FX; *Biosensors and Bioelectronics*, **2007**, 22, 1205.

[34] Perumal V; Hashim U; *Journal of applied biomedicine*, **2014**, 12, 1.

[35] Bahadır EB; Sezgintürk MK; *Analytical Biochemistry*, **2015**, 478, 107.

[36] Pejcic B; De Marco R; Parkinson G; *Analys*t, **2006**, 131, 1079.

[37] Ahmed A; Rushworth JV; Hirst NA; Millner PA; *Clinical Microbiology Reviews*, **2014**, 27, 631.

[38] Velusamy V; Arshak K; Korostynska O; Oliwa K; Adley C; *Biotechnology Advances*, **2010**,

28, 232.

[39] Ricci F; Volpe G; Micheli L; Palleschi G; *Analytica Chimica Acta*, **2007**, 605, 111.

[40] Singh A; Poshtiban S; Evoy S; *Sensors*, **2013**, 13, 1763.

[41] Vo-Dinh T Editor, Nanotechnology in Biology and Medicine: Methods, Devices, and Applications, **2007**, ISBN 9780849329494.

[42] Chen SH; Wu VCH; Chuang YC; Lin CS; *Journal of Microbiological Methods*, **2008**, 73, 7.

[43] Lermo A; Campoy S; Barbe J; Hernandez S; Alegret S; Pividori M; *Biosensors and Bioelectronics*, **2007**, 22, 2010.

[44] Kim-Fatt L ; Kritsanaporn C ; Patsamon R; Werasak S; Yean-Yean C; World *Journal of Microbiology & Biotechnology*, **2012**, 28, 1699.

[45] Sharma H; Mutharasan R; *Sensors and Actuators B*, **2013**, 183, 535.

[46] Yoo SM; Lee SY; *Trends in Biotechnology*, **2016**, 34, 7.

[47] Borisov SM; Wolfbeis OS; *Chemical Reviews*, **2008**, 108, 423.

[48] Long F; Zhu A; Shi H; *Sensors*, **2013**, 13, 13928.

[49] Spoto G; Minunni M; *Journal of Physical Chemistry Letters*, **2012**, 3, 2682.

[50] Taylor AD; Ladd J; Homola J; Jiang S; Principles of Bacterial Detection: Biosensors, Recognition Receptors and Microsystems, **2008**, pp 83-108.

[51] Rasooly A; *Journal of Food Protection*, **2001**, 64, 37.

[52] Homola J; Dostalek J; Chen S; Rasooly A; Jiang S; Yee SS; *International Journal of Food Microbiology*, **2002**, 75, 61-69.

[53] Barlen B; Mazumdar SD; Lezrich O; Kämpfer P; Keusgen M; *Sensors*, **2007**, 7, 1427.

[54] Mazumdar SD; Hartmann M; Kämpfer P; Keusgen M; *Biosensors and Bioelectronics*, **2007**, 22, 2040.

[55] Taylor AD; Ladd J; Yu QM; Chen SF; Homola J; Jiang SY; *Biosensors and Bioelectronics*, **2006**, 22, 752.

[56] Nanduri V; Bhunia AK; Tu S-I; Paoli GC; Brewster JD; *Biosensors and Bioelectronics*, **2007**, 23, 248.

[57] Subramanian A; Irudayaraj J; Ryan T; *Biosensors and Bioelectronics*, **2006**, 21, 998.

[58] Waswa J; Irudayaraj J; DebRoy C; *LWT- Food Science and Technology*, **2007**, 40, 187.

[59] Yakes BJ; Deeds J; White K; Degrasse SL; *Journal of Agricultural and Food Chemistry*, **2011**, 59, 839.

[60] Wood RW; *Philosophical Magazine Series 6*, **1912**, 23, 310.

[61] D'Agata R; Spoto G; *Detection of Non-Amplified Genomic DNA Soft and Biological Matter*, **2012**, Chapter 9, pp 235-261.

[62] Born M; Wolf E; *Pergamon Press, Oxford*, **1980**.

[63] D'Agata R; Spoto G; *Analytical and Bioanalytical Chemistry*, **2013**, 405, 573.

[64] Rich RL; Myszka DG; *Current Opinion in Biotechnology*, **2000**, 11, 54.

[65] D'Agata R; Grasso G; Iacono G; Spoto G; Vecchio G; *Organic & Biomolecular Chemistry*, **2006**, 4, 610.

[66] Lyon LA; Musick MD; Natan MJ; *Analytical Chemistry*, **1998**, 70, 5177.

[67] Frutos AG; Weibel SC; Corn RM; *Analytical Chemistry*, **1999**, 71, 3935.

[68] Hickel W; Kamp D; Knoll W; *Nature*, **1989**, 339, 186.

[69] Rothenhäusler B; Knoll W; *Nature*, **1988**,332, 615.

[70] Brockman JM; Nelson BP; Corn RM; *Annual Review of Physical Chemistry*, **2000**, 51, 41.

[71] D'Agata R; Grasso G; Spoto G; *The Open Spectroscopy Journal*, **2008**, 2, 1.

[72] Homola, J.; *Analytical and Bioanalytical Chemistry*, **2003**, 377, 528.

[73] Shankaran DR; Gobi KVA; Miura N; *Sensors and Actuators B*, **2007**, 121, 158.

[74] Homola J; Hegnerova H; Vala M; *Proceedings of SPIE*, **2009**, 7167, 716705.

[75] Saha K; Agasti SS; Kim C; Li X; Rotello VM; *Chemical Reviews*, **2012**, 112, 2739.

[76] Zeng S; Yong K-T; Roy I; Dinh X-Q; Yu X; Luan F; *Plasmonics*, **2011**, 6, 491.

[77] Liu X; Dai Q; Coutts J; Austin L; Knowles G; Huo Q; *Nanotechnology*, **2008**, 2, 256.

[78] Nune SK; Gunda P; Thallapally PV; Lin Y-Y; Forrest ML; Berkland CJ; *Expert Opinion on Drug Delivery*, **2009**, 6, 1175.

[79] Thakor AS; Jokerst J; Zaveleta C; Massoud TF; Gambhir SS; *Nano Letters*, **2011**, 11, 4029.

[80] Zanoli LM; D'Agata R; Spoto G; *Analytical and Bioanalytical Chemistry*, **2012**, 402, 1759.

[81] Jana NR; Gearheart L; Murphy CJ; *Chemistry of Materials*, **2001**, 13, 2313.

[82] Dong S-A; Zhou S-P; *Materials Science and Engineering B*, **2007**, 140, 153.

[83] Yusof NSM; Ashokkumar M; *Chemphyschem*, **2015**, 16, 775-81.

[84] Bastús NG; Comenge J; Puntes V; *Langmuir*, **2011**, 27, 11098.

[85] Hanžić N; Jurkin T; Maksimović A; Gotić M; *Radiation Physics and Chemistry*, **2015**, 106, 77.

[86] Turkevich J; Stevenson PC; Hillier J; *Discussions of the Faraday Society*, **1951**, 11, 55.

[87] Turkevich J; *Gold Bulletin*, **1985**, 18, 86.

[88] Frens G; *Nature Physical Science*, **1973**, 241, 20.

[89] Tantra R; Nanomaterial Syntheses in Nanomaterial Characterization: An Introduction, **2016**, ISBN: 978-1-118-75359-0.

[90] Brewer SH; Glomm WR; Johnson MC; Knag MK; Franzen S; *Langmuir*, **2005**, 21, 9303.

[91] Dumur F; Guerlin A; Dumas E; Bertin D; Gigmes D; Mayer CR; *Gold Bulletin*, **2011**, 44, 119.

[92] Kumar D; Meenan BJ; Mutreja I; D'sa R; Dixon D; *International Journal of Nanoscience*, **2012**, 11, 1250023.

[93] Ahmed SR; Oh S; Baba R; Zhou H; Hwang S; Lee J; Park EY; *Nanoscale Research Letters*, **2016**, 11, 65.

[94] DeLong RK; Reynolds CM; Malcolm Y; Schaeffer A; Severs T; Wanekaya A; *Nanotechnology, Science and Applications*, **2010**, 3, 53.

[95] Zhao W; Lin L; Hsing I-M; *Bioconjugate Chemistry*, **2009**, 20, 1218.

[96] Rosi NL; Giljohann DA; Thaxton CS; Lytton-Jean AKR; Han MS; Mirkin CA; *Science*, **2006**, 312, 1027.

[97] Patel PC; Giljohann DA; Daniel WL; Zheng D; Prigodich AE; Mirkin CA; *Bioconjugate Chemistry*, **2010**, 21, 2250.

[98] Han G; Ghosh P; Rotello VM; *Nanomedicine*, **2007**, 2, 113.

[99] Dhar S; Daniel WL; Giljohann DA; Mirkin CA; Lippard SJ; *Journal of the American Chemical Society*, **2009**, 131, 14652.

[100] Seferos DS; Giljohann DA; Hill HD; Prigodich AE; Mirkin CA; *Journal of the American Chemical Society*, **2007**, 129, 15477.

[101] Nicholls FJ; Rotz MW; Ghuman H; MacRenaris KW; Meade TJ; Modo M; Biomaterials, **2016**, 77, 291.

[102] Park S; Taton TA; Mirkin CA; *Science*, **2002**, 295, 1503.

[103] Bui MP; Baek TJ; Seong GH; *Analytical and Bioanalytical Chemistry*, **2007**, 388, 1185.

[104] Lee J-S; Han MS; Mirkin CA; *Angewandte Chemie*, **2007**, 119, 4065.

[105] Xue X; Wang F; Liu X; *Journal of the American Chemical Society*, **2008**, 130, 3244.

[106] Thaxton CS; Georganopoulou DG; Mirkin CA; *Clinica Chimica Acta*, **2006**, 363, 120.

[107] Cao YC, Jin R, Mirkin CA; *Science*, **2002**, 297, 1536.

[108] Baeissa A; Dave N; Smith BD; Liu J; *ACS Applied Materials & Interfaces*, **2010**, 2, 3594.

[109] D'Agata R; Corradini R; Ferretti C; Zanoli L; Gatti M; Marchelli R; Spoto G; *Biosensors and Bioelectronics*, **2010**, 25, 2095.

[110] He L; Musick MD; Nicewater SR; Salinas FG; Benkovic SJ; Natan MJ; Keating CD; *Journal of the American Chemical Society*, **2000**, 122, 9071.

[111] Wang Y; Alocilja EC; *Journal of Biological Engineering*, **2015**, 9, 16.

[112] Pissuwan D; Cortie CH; Valenzuela SM; Cortie MB; *Trends in Biotechnology*, **2010**, 28, 4.

[113] Watanabe K; Kuwata N; Sakamoto H; Amano Y; Satomura T; Suye S; *Biosensors and Bioelectronics*, **2015**, 67, 419.

[114] Lai H-Z; Wang S-G; Wu C-Y; Chen, Y-C; *Analytical Chemistry*, **2015**, 87, 2114.

[115] Shi J; Chan C; Pang Y; Ye W; Tian F; Lyu J; Zhang Y; Yang M; Biosensors and Bioelectronics, **2015**, 67, 595.

[116] Niu K; Zheng X; Huang C; Xu K; Zhi Y; Shen H; Jia N; *Journal of Nanoscience and Nanotechnology*, **2014**, 14, 5151.

[117] Li F; Zhao Q; Wang C; Lu X; Li X-F; Le XC; *Analytical Chemistry*, **2010**, 82, 3399.

[118] Lin YH; Chen SH; Chuang YC; Lu YC; Shen TY; Chang CA; Lin CS; *Biosensors and Bioelectronics*, **2008**, 23, 1832.

[119] Mao X; Yang L; Su X-L; Li Y; *Biosensors and Bioelectronics*, **2006**, 21, 1178.

[120] Guo X; Lin C-S; Chen S-H; Ye R; Wu VCH; *Biosensors and Bioelectronics*, **2012**, 38, 177.

[121] Masdor NA; Altintas Z; Tothill IE; *Biosensors and Bioelectronics*, **2016**, 78, 328.

[122] Huang X; Xu Z; Mao Y; Ji Y; Xu H; Xiong Y; Li Y; *Biosensors and Bioelectronics*, **2015**, 66, 184.

[123] Liu Z; Zhu J; Yang C; Li X; *Analytical Methods*, **2015**, 7, 8159.

[124] Fu Z; Zhou X; Xing D; *Sens Actuators B: Chemical*, **2013**, 182, 633–41.

[125] Verma MS; Rogowski JL; Jones L; Gu FX*; Biotechnology Advances*, **2015**, 33, 666.

[126] Poltronieri P; de Blasi MD; D'Urso OF; *Plant, Soil and Environment*, **2009**, 9, 363.

[127] Guo X; Lin C-S; Chen S-H; Ye R; Wu VCH; *Biosensors and Bioelectronics*, **2012**, 38, 177.

[128] Sung YJ; Suk H-J; Sung HJ; Li T; Poo H; Kim M-G; *Biosensors and Bioelectronics*, **2013**, 43, 432.

[129] Fang SB, Tseng WY, Lee HC, Tsai CK, Huang JT, Hou SY, *Journal of Microbiological Methods*, **2009**, 77, 225.

[130] Tong SYC; Davis JS; Eichenberger E; Holland TL; Fowler VG; *Clinical Microbiology Reviews*, **2015**, 28, 603.

[131] Baird-Parker T; Staphylococcus aureus. In: Lund B, Baird-Parker T, Gould G, editors. The Microbiological Safety and Quality of Food. Gaithersburg: Aspen Publishers., **2000**, pp 1317-1330.

[132] Medveďová A; Valík L; Chapter 4 in Agricultural and Biological Sciences "Structure and Function of Food Engineering", edited by Ayman Amer Eissa, **2012**, ISBN 978-953-51-0695-1.

[133] Pinchuk IV; Beswick EJ; Reyes VE; *Toxins*, **2010**, 2, 2177.

[134] Schelin J; Wallin-Carlquist N; Cohn MT; Lindqvist R; Barker GC; Rådström P; *Virulence*, **2011**, 2, 580.

[135] Sergeev N; Volokhov D; Chizhikov V; Rasooly A; *Journal of Clinical Microbiology*, **2004**, 42, 2134.

[136] Kadariya J; Smith TC; Thapaliya D; *BioMed Research International*, **2014**, Article ID 827965, http://dx.doi.org/10.1155/2014/827965.

[137]http://www.fda.gov/downloads/Food/FoodSafety/FoodborneIllness/FoodborneIllnessFoodbornePathogensNaturalToxins/BadBugBook/UCM297627.pdf

[138] Salmain M; Ghasemi M; Boujday S; Pradier C-M; *Sensors and Actuators B*, **2012**, 173, 148.

[139] Medina MB; *Journal of Rapid Methods and Automation in Microbiology*, **2006**, 14, 119.

[140] Karaseva N; Ermolaeva T; *Microchimica Acta*, **2015**, 182, 1329.

[141] Jay JM; Modern Food Microbiology, 6th Ed, Aspen Publishers, Gaithersburg, MD; **2000**; pp. 441–459.

[142] Rasooly R; Do PM; Friedman M; *Journal of Agricultural and Food Chemistry*, **2010**, 58, 5421.

[143] Ortega E; Abriouel H; Lucas R; Gálvez A; *Toxins*, **2010**, 2, 2117.

[144] Argudín MA; Mendoza MC; Rodicio MR; *Toxins*, **2010**, 2, 1751.

[145] Al-Bahry SN; Mahmoud IY; Al-Musharafi SK; Sivakumar N; *International Journal of Chemical Engineering and Applications*, **2014**, 5, 388.

[146] Porto de Oliveira LP; Santana Soares e Barros L; Silva VC; Gonçalves Cirqueira M; *Journal of Food Processing & Technology*, **2011**, 2, 128.

[147] Oliver SP; Jayarao BM: Almeida RA; *Foodborne pathogens and disease*, **2005**, 2, 2.

[148] Tortora GJ; Funke BR; Case CL; Microbiologia, Porto Alegre, Artemed, **2005**.

[149] Zschöck M; Kloppert B; Wolter W; Hamann HP; Lämmler Ch; *Veterinary Microbiology*, **2005**; 108, 243.

[150] http://www.foodsafety.govt.nz/elibrary/industry/factors-staphylococcal-enterotoxin-dairy.pdf

[151] Schmid D; Fretz R; Winter P; Mann M; Höger G; Stöger A; Ruppitsch W; Ladstätter J; Mayer N; de Martin A; Allerberger F; *Wiener klinische Wochenschrift*, **2009**, 121, 125.

[152] Jørgensen HJ; Mathisen T; Løvseth A; Omoe K; Qvale KS; Loncarevic S; *FEMS Microbiology Letters*, **2005**, 252, 267.

[153] Simeão do Carmoa L; Souza Diasb R; Roberto Linardic V; José de Senad M; Aparecida dos Santose D; Eduardo de Fariaf M; Castro Penaf E; Jettg M; Guilherme Heneineh L; *Food Microbiology*, **2002**, 19, 9.

[154] Le Loir Y; Baron F; Gautier M; *Genetics and molecular research*, **2003**, 2, 63.

[155] Asao T; Kumeda Y; Kawai T; Shibata T ; Oda H; Haruki K; Nakazawa H; Kozaki S; *Epidemiology & Infection*, **2003**, 130, 33.

[156] Ostyn A; De Buyser ML; Guillier F; Groult J; Félix B; Salah S; Delmas G; Hennekinne JA; *Eurosurveillance*, **2010**, 15, 19528.

[157] Gutiérrez D; Delgado S; Vázquez-Sánchez D; Martínez B; Cabo ML; Rodríguez A; Herrera JJ; García P; *Applied and Environmental Microbiology*, **2012**, 78, 8547.

[158] Kim B-R; Bae Y-M; Hwang J-H; Lee S-Y; *Food Science and Biotechnology*, **2016**, 25, 643.

[159] Kroning IS; Iglesias MA; Sehn CP; Gandra TKV; Mata MM; da Silva WP; *Food Microbiology*, **2016**, 58, 105.

[160] Lammie SL; Hughes JM; *Annual Review of Food Science and Technology*, **2016**, 7, 13.1.

[161] European Food Safety Authority, European Centre for Disease Prevention and Control; The European Union Summary Report on Trends and Sources of Zoonoses, Zoonotic Agents and Food borne Outbreaks in 2009; *EFSA Journal* **2011**; 9(3):2090.

[162] http://www.cdc.gov/mrsa/

[163] Gordon RJ; Lowy FD; *Clinical Infectious Diseases*, **2008**, 46 (Suppl 5), S350.

[164] Grema HA; Geidam YA; Gadzama GB; Ameh JA; Suleiman A; *Advances in Animal and Veterinary Science*s, **2015**, 3, 79.

[165] Visciano P; Pomilio F; Tofalo R; Sacchini L; Saletti MA; Tieri E; Schirone M; Suzzi G; *Food Control*, **2014**, 46, 532.

[166] Jones TF; Kellum ME; Porter SS; Bell M; Schaffner W; *Emerging Infectious Diseases*, **2002**, 8, 82.

[167] Traversa A; Gariano GR; Gallina S; Bianchi DM; Orusa R; Domenis L; Cavallerio P; Fossati L; Serra R; Decastelli L; *Food Microbiology*, **2015**, 52, 154.

[168] Normanno G; Corrente M; La Salandra G; Dambrosio A; Quaglia NC; Parisi A; Greco G; Bellacicco AL; Virgilio S; Celano GV; *International Journal of Food Microbiology*, **2007**, 117, 219.

[169] Crago B; Ferrato C; Drews SJ; Svenson LW; Tyrrell G; Louie M; *Food Microbiology*, **2012**, 32, 202.

[170] de Boer E; Zwartkruis-Nahuis JT; Wit B; Huijsdens XW; de Neeling AJ; Bosch T; van Oosterom RA; Vila A; Heuvelink AE; *International Journal of Food Microbiology*, **2009**, 134, 52.

[171] Boost MV; Wong A; Ho J; O'Donoghue M; *Foodborne Pathogens and Disease*, **2013**, 10, 705.

[172] Costa WL; Ferreira Jdos S; Carvalho JS; Cerqueira ES; Oliveira LC; Almeida RC; *Journal of Food Science*, **2015**, 80, M147.

[173] Kwon NH, Park KT; Moon JS; Jung WK; Kim SH; Kim JM; Hong SK; Koo HC; Joo YS; Park YH; *Journal of Antimicrobial Chemotherapy*, **2005**, 56, 624.

[174] Carfora V; Caprioli A; Marri N; Sagrafoli D; Boselli C; Giacinti G; Giangolini G; Sorbara L; Dottarelli S; Battisti A; Amatiste S; *International Dairy Journal*, **2015**, 42, 12.

[175] Jamali H; Paydar M; Radmehr B; Ismail S; Dadrasnia A; *Food Control*, **2015**, 54, 383.

[176] Cortimiglia C; Bianchini V; Franco A; Caprioli A; Battisti A; Colombo L; Stradiotto K; Vezzoli F; Luini M; *Journal of Dairy Science*, **2015**, 98, 2307.

[177] Fessler AT; Kadlec K; Hassel M; Hauschild T; Eidam C; Ehricht R; Monecke S; Schwarz S; *Applied and Environmental Microbiology*, **2011**, 77, 7151.

[178] Kitai S; Shimizu A; Kawano J; Sato E; Nakano C; Uji T; Kitagawa H; *Journal of Veterinary Medical Science*, **2005**, 67, 107.

[179] O'Brien AM; Hanson BM; Farina SA; Wu JY; Simmering JE; Brett MF; Kurlick ME; Wallinga DB; Smith TC; *PLoS ONE*, **2012**, 7, e30092.

[180] Riva A; Borghi E; Cirasola D; Colmegna S; Borgo F; Amato E; Pontello MM; Morace G; *Journal of Food Protection*, **2015**, 78, 1142.

[181] Karoonuthaisiri N; Charlermroj R; Teerapornpuntakit J; Kumpoosiri M; Himananto O; Grant IR; Gajanandana O; Elliott CT; *Food Control*, **2015**, 47, 462.

[182] Allen KJ; Wałecka-Zacharska E; Chen JC; Katarzyna K-P; Devlieghere F; Van Meervenne E; Osek J; Wieczorek K; Bania J; *Food Microbiology*, **2016**, 54, 178.

[183] Low JC; Donachie W; *Veterinary Journal*, **1997**, 153, 9.

[184] Tu Z; Chen Q; Li Y; Xiong Y; Xu Y; Hu N; Tao Y; *Analytical Biochemistry*, **2016**, 493, 1.

[185] http://www.cdc.gov/listeria/sources.html

[186] Antal EA; Dietrichs E; Løberg EM; Melby KK; Maehlen J; *Scandinavian Journal of Infectious Diseases*, **2005**, 37, 190.

[187] Hof H; *Expert Opinion on Pharmacotherapy*, **2004**, 5, 1727.

[188] Camejo A; Buchrieser C; Couve E; Carvalho F; Reis O; Ferreira P; Sousa S; Cossart P; Cabanes D; *PLoS Pathogens*, **2009**, 5, e1000449.

[189] Churchill RLT; Lee H; Hall JC; *Journal of Microbiological Methods*, **2006**, 64, 141.

[190] Schnupf P; Portnoy DA; *Microbes and Infection*, **2007**, 9, 1176.

[191] Dal Peraro M; van der Goot FG; *Nature Reviews Microbiology*, **2016**, 14, 77.

[192] Seveau S; *Subcellular Biochemistry*, **2014**, 80, 161.

[193] Sharma H; Mutharasan R; *Analytical Chemistry*, **2013**, 85, 3222.

[194] Piercey MJ; Hingston PA; Hansen LT; Piercey MJ; Hingston PA; Hansen LT; *International Journal of Food Microbiology*, **2016**, 223, 63.

[195] Nguyen UT; Harvey H; Hogan AJ; Afonso ACF; Wright GD; Burrows LL; *Antimicrobial Agents and Chemotherapy*, **2014**, 58, 6508.

[196] Auvolat A; Besse NG; *Food Microbiology*, **2016**, 53, 135.

[197] Bellio A; Astegiano S; Traversa A; Bianchi DM; Gallina S; Vitale N; Zuccon F; Decastelli L; *International Dairy Journal*, **2016**, 57, 15.

[198] *EFSA Journal*, **2015**, 13, 3991.

[199] *EFSA Journal*, **2015**, 13, 4329.

[200] http://www.cdc.gov/listeria/outbreaks/frozen-vegetables-05-16/index.html

[201] http://www.cdc.gov/listeria/outbreaks/raw-milk-03-16/index.html

[202] http://www.cdc.gov/listeria/outbreaks/bagged-salads-01-16/index.html

[203] http://www.cdc.gov/listeria/outbreaks/soft-cheeses-09-15/index.html

[204] http://www.cdc.gov/listeria/outbreaks/ice-cream-03-15/index.html

[205] http://www.cdc.gov/listeria/outbreaks/caramel-apples-12-14/index.html
http://www.cdc.gov/listeria/outbreaks/caramel-apples-12-14/index.html

[206] http://www.cdc.gov/listeria/outbreaks/cheese-02-14/index.html

[207] Commission regulation (EC) No 2073/2005 of 15 November 2005 on microbiological criteria for foodstuffs, *Official Journal of the European Union*, **2005**.

[208] s-Krajnik MK; Lim HSY; Zheng Q; Turner M; Yuk H-G; *Food Control*, **2016**, 60, 237.

[209] Carpentier B; Cerf O; *International Journal of Food Microbiology*, **2011**, 145, 1.

[210] Conter M; Paludi D; Zanardi E; Ghidini S; Vergara A; Ianieri A*; International Journal of Food Microbiology*, **2009**, 128, 497.

[211] Vaisocherová H; Brynda E; Homola J; *Analytical and Bioanalytical Chemistry*, **2015**, 407, 3927.

[212] Liu X; Huang R; Su R; Qi W; Wang L; He Z; *ACS Applied Materials & Interfaces*, **2014**, 6, 13034.

[213] Choi S; Yang Y; Chae J; *Biosensors and Bioelectronics*, **2008**, 24, 893.

[214] Chen S; Li L; Zhao C; Zheng J; *Polymer*, **2010**, 51, 5283.

[215] Zhang R; Liu Y; He M; Su Y; Zhao X; Elimelech M; Jiang Z; *Chemical Society Reviews*, **2016**, DOI: 10.1039/C5CS00579E.

[216] Zhang H; Chiao M; *Journal of Medical and Biological Engineering*, **2015**, 35, 143.

[217] Liu B; Liu X; Shi S; Huang R; Su R; Qi W; He Z; *Acta Biomaterialia*, **2016**, 40, 100.

[218] Chapman RG; Ostuni E; Takayama S; Holmlin RE; Yan L; Whitesides GM; J*ournal of the American Chemical Society*, **2000**, 122, 8303.

[219] Ostuni E; Chapman RG; Holmlin RE; Takayama S; Whitesides GM; *Langmuir*, **2001**, 17, 5605.

[220] Venault A; Huang W-Y; Hsiao S-W; Chinnathambi A; Alharbi SA; Chen H; Zheng J; Chang Y; *Langmuir*, **2016**, 32, 4113.

[221] Subramanian A; Irudayaraj J; Ryan T; *Sensors and Actuators B*, **2006**, 114, 192.

[222] Prime KL; Whitesides GM; *Science*, **1991**, 252, 1164.

[223] Frederix F; Bonroy K; Laureyn W; Reekmans G; Campitelli A; Dehaen W; Maes G; *Langmuir*, **2003**, 19, 4351.

[224] Deng L; Mrksich M; Whitesides GM; *Journal of the American Chemical Society*, **1996**, 118, 5136.

[225] Christopher Love J; Estroff LA; Kriebel JK; Nuzzo RG; Whitesides GM; *Chemical Reviews*, **2005**, 105, 1103.

[226] Riedel T; Riedelová-Reicheltová Z; Májek P; Rodriguez-Emmenegger C; Houska M; Dyr JE; Brynda E; *Langmuir*, **2013**, 29, 3388.

[227] Lowe S; O'Brien-Simpson nm; Connal LA; *Polymer Chemistry*, **2015**, 6, 198.

[228] Lokanathan AR; Zhang S; Regina VR; Cole MA; Ogaki R; Dong M; Besenbacher F; Meyer RL; Kingshott P; *Biointerphases*, **2011**, 6, 180.

[229] Luk Y-Y; Kato M; Mrksich M; *Langmuir*, **2000**, 16, 9604.

[230] Li L; Chen S; Jiang S; *Journal of Biomaterials Science, Polymer Edition*, **2007**, 18, 1415.

[231] Lin P; Ding L; Lin C-W; Gu F; *Langmuir*, **2014**, 30, 6497.

[232] Mi L; Jiang S; *Angewandte Chemie International Edition*, **2014**, 53, 1746.

[233] Schlenoff JB; *Langmuir*, **2014**, 30, 9625.

[234] Sin M-S; Chen S-H; Chang Y; *Polymer Journal*, **2014**, 46, 436.

[235] He M; Gao K; Zhou L, Jiao z, Wu M, Cao j, You X, Cai Z; Su Y; Jiang Z; *Acta Biomaterialia*, **2016**, 40, 142.

[236] Rodriguez-Emmenegger C; Schmidt BVKJ; Sedlakova Z; Šubr V; Alles AB; Brynda E; Barner-Kowollik C; *Macromolecular Rapid Communications*, **2011**, 32, 958.

[237] Grasso G; Fragai M; Rizzarelli E; Spoto G; Yeo KJ; *Journal of Mass Spectrometry*, **2006**, 41, 1561.

[238] http://www.ncbi.nlm.nih.gov/nuccore/47208328?report=graph

[239] http://www.cdc.gov/mrsa/

[240] Kuroda M; Ohta T; Uchiyama I; Baba T; Yuzawa H; Kobayashi I; Cui L; Oguchi A; Aoki K; Nagai Y; Lian J; Ito T; Kanamori M; Matsumaru H; Maruyama A; Murakami H; Hosoyama A; Mizutani-Ui Y; Takahashi NK; Sawano T; Inoue R; Kaito C; Sekimizu K; Hirakawa H; Kuhara S; Goto S; Yabuzaki J; Kanehisa M; Yamashita A; Oshima K; Furuya K; Yoshino C; Shiba T; Hattori M; Ogasawara N; Hayashi H; Hiramatsu K; *The Lancet*, **2001**, 357, 1225.

[241] Oliveri V; D'Agata R; Giglio V; Spoto G; Vecchio G; *Supramolecular Chemistry*, **2013**, 25, 465.

[242] Green NM; *Methods in Enzymology*, **1990**, 184, 51.

[243] Liu X; Dai Q; Austin L; Coutts J; Knowles G; Zou J; Chen H; Huo Q; *Journal of the American Chemical Society*, **2008**, 130, 2780.

[244] Hu W; Chen H; Zhang H; He G; Li X; Zhang X; Liu H; Li CM; *Journal of Colloid and Interface Science*, *2014*, 431,71.

[245] Sanvicens N; Pastells C; Pascual N; Marco M-P; *TrAC Trends in Analytical Chemistry*, **2009**, 28, 1243.

[246] Nielsen PE; Egholm M; Berg RH; Buchardt O; *Science*, **1991**, *254*, 1497.

[247] Hayman B; Hirst R; *Veterinary Microbiology*, **2003**, 91, 91.

[248] Parayre S; Falentin H; Madec M-N; Sivieri K; Le Dizes A-S; Sohier D; Lortal S; Journal of *Microbiological Methods*, **2007**, 69, 431.

[249] Sergeev N; Volokhov D; Chizhikov V; Rasooly A; *Journal of Clinical Microbiology*, **2004**, 42, 2134.

[250] Day JB; Basavanna U; Journal of Applied Microbiology, 2015, 118, 233.

[251] http://blast.ncbi.nlm.nih.gov/Blast.cgi

[252] http://mfold.rna.albany.edu/?q=DINAMelt/Two-state-melting

[253] Ravan H; Kashanian S; Sanadgol N; Badoei-Dalfard A; Karami Z; Analytical Biochemistry, 2014, 444, 41.

[254] Gao Y; Wolf LK; Georgiadis RM; Nucleic Acids Research, 2006, 34, 3370.

[255] Sforza S; Corradini R; Tedeschi T; Marchelli R; Chemical Society Reviews, **2011**, 40, 221.

[256] Park H; Germini A; Sforza S; Corradini R; Marchelli R; Knoll W; *Biointerphases*, **2007**, 2, 80.

[257] D'Agata R; Spoto G; *Artificial DNA: PNA & XNA*, **2012**, 3, 45.

[258] Haiss W; Thanh NTK; Aveyard J; Fernig DG; *Analytical Chemistry*, **2007**, 79, 4215.

[259] Huang X; El-Sayed MA; *Journal of Advanced Research*, **2010**, 1, 13.

[260] Jans H; Liu X; Austin L; Maes G; Huo Q; *Analytical Chemistry*, **2009**, 81, 9425.

[261] Pecora R; *Journal of Nanoparticle Research*, **2000**, 2, 123.

[262] Doane TL; Chuang C-H; Hill RJ; Burda C; Burda C; *Accounts of Chemical research*, **2012**, 45, 317.

[263] Scott E McNeil (editor), Methods in Molecular Biology 697, Humana Press, Springer, **2011**.

[264] D'Agata R; Breveglieri G; Zanoli LM; Borgatti M; Spoto G; Gambari R; *Analytical Chemistry*, **2011**, 83, 8711

[265] Tan SC; Yiap BC; Journal of Biomedicine and Biotechnology, 2009, Article ID 574398, 10 pages, 2009. doi:10.1155/2009/574398.

[266] Cremonesi P; Castiglioni B; Malferrari G; Biunno I; Vimercati C; Moroni P; Morandi S; Luzzana M; *Journal of Dairy Science*, **2006**, 89, 163.

[267] Detection, Identification, and Analysis of Foodborne Pathogens in Microarray Detection and Characterization of Bacterial Foodborne Pathogens, Part of the series SpringerBriefs in Food, Health, and Nutrition, Guillermo López-Campos, Joaquín V. Martínez-Suárez, Mónica Aguado-Urda, Victoria López-Alonso

[268] http://www.ncbi.nlm.nih.gov/tools/primer-blast/

[269] Subramanian A; Irudayaraj J; Ryan T; *Sensors and Actuators B*, **2006**, 114, 192.

[270] Vericat C; Vela ME; Benitez G; Carro P; Salvarezza RC; *Chemical Society Reviews*, **2010**, 39, 1805.

[271] Chiu, N-F; Huang T-Y; Lai H-C; Graphene Oxide Based Surface Plasmon Resonance Biosensors; Nanotechnology and Nanomaterials, "Advances in Graphene Science", Mahmood Aliofkhazraei, ISBN 978-953-51-1182-5

[272] Wu Q; Song D; Zhang D; Zhang H; Ding Y; Yu Y; Sun Y; *Microchimica Acta*, **2015**, 182, 1739.

[273] Chiu N-F; Huang T-Y; *Sensors and Actuators B: Chemical*, **2014**, 197, 35.

[274] Ryu Y; Moon S; Oh T; Kim Y; Lee T; Kim DH; Kim D; *Applied Optics*, **2014**, 53, 1419.

[275] Zhang H; Sun Y; Gao S; Zhang J; Zhang H; Song D; *Small*, **2013**, 9, 2537.

[276] Zhang J; Sun Y; Xu B; Zhang H; Gao Y; Zhang H; Song D; *Biosensors and Bioelectronics*, **2013**, 45, 230.

[277] Vaisocherová-Lísalová H; Víšová I; Ermini ML; Špringer T; Song XC; Mrázek J; Lamačová J; Lynn Jr NS; Šedivák P; Homola J; *Biosensors and Bioelectronics*, **2016**, 80, 84.

[278] Lahiri J; Isaacs L; Tien J; Whitesides GM; *Analytical Chemistry*, **1999,** 71, 777.

[279] Choi SH; Lee JW; Sim SJ; *Biosensors and Bioelectronics*, **2005**, 21, 378.

[280] Lee JW; Sim SJ; Cho SM; Lee J; *Biosensors and Bioelectronics*, **2005**, 20, 1422.

[281] Bonroy K; Frederix F; Reekmans G; Dewolf E; DePalma R; Borghs G; Declerck P; Goddeeris B; *Journal of Immunological Methods*, **2006**, 312, 167.

[282] Tsai W-C; Li I-C; *Sensors and Actuators B*, **2009**, 136, 8

[283] Bain CD; Biebuyck HA; Whiteside GM; *Langmuir*, **1989**, 5, 723.

[284] Sieger C; Biesalski M; Haag R; Chemistry - A European Journal, **2004**, 10, 2831.

[285] Lokanathan AR; Zhang S; Regina VR; Cole MA; Ogaki R; Dong M; Besenbacher F; Meyer RL; Kingshott P; *Biointerphases*, **2011**, 6, 180.

[286] Gujadhur R; Venkataraman D; Kintigh JT; *Tetrahedron Letters*, **2001**, 42, 4791.

[287] Tiwari VK; Mishra BB; Mishra KB; Mishra N; Singh AS; Chen X; *Chemical Reviews*, **2016**, 116, 3086.

[288] Liang L; Astruc D; *Coordination Chemistry Reviews*, **2011**, 255, 2933.

[289] Lal S; Díez-González S; *The Journal of Organic Chemistry*, **2011**, 76, 2367.

.